Development of rapid and robust assays to test the functions of human PTEN Variants of Unknown Significance in *Drosophila melanogaster*

by

Landiso Sibusiso Madonsela

B.Sc., Simon Fraser University, 2017

Thesis Submitted in Partial Fulfillment of the
Requirements for the Degree of
Master of Science
in the
Department of Molecular Biology and Biochemistry
Faculty of Science

SIMON FRASER UNIVERSITY
Spring 2020

Approval

Name:	**Landiso Sibusiso Madonsela**
Degree:	**Master of Science**
Title:	**Development of rapid and robust assays to test the functions of human PTEN Variants of Unknown Significance in *Drosophila melanogaster***
Examining Committee:	**Chair: Lisa Craig** Professor
	Esther Verheyen Senior Supervisor Professor
	Nicholas Harden Supervisor Professor
	Sharon Gorski Supervisor Professor
	Harald Hutter Internal Examiner Professor Biological Sciences
Date Defended/Approved:	April 17, 2020

Abstract

Large-scale sequencing projects and sequencing of patient samples can reveal mutations or polymorphisms in many genes, but the functional consequences are not always apparent especially for single amino acid substitutions. My research project focussed on addressing the discrepancy between the amount of sequenced gene variants and the knowledge about their functionality in development and disease. We developed Drosophila genetic assays for rapid, inexpensive functionalization of human PTEN variants with unknown significance (VUS) in order to learn if individual mutations play a role in development of disease. We assayed the ability of PTEN variants to suppress phenotypes observed when the oncogenic phosphoinositide 3-kinase (PI3K) signalling pathway is activated in the developing Drosophila wing. Our assay was validated with a few previously studied variants followed by characterizing 100+ human PTEN VUS. Ultimately, knowing which PTEN variants are non-functional or functional is crucial for targeted therapeutic and personalized treatment of PI3K-dependent diseases and cancers.

Keywords: PTEN; Drosophila PI3K; Variants of unknown significance (VUS); loss of function (LOF); gain of function (GOF)

Dedication

To my Mother and Father for their continued support and encouragement

Acknowledgements

First and foremost, I would like to express my greatest gratitude to my senior supervisor Dr. Esther Verheyen for her continuous support, guidance and immense knowledge. I will always be grateful for the opportunity to be a part of her lab since my undergraduate career.

Secondly, I also thank my committee members Dr. Nicholas Harden and Dr. Sharon Gorski for their immense knowledge and helpful feedback and suggestions during my annual committee meetings.

I would like to that Dr. Lisa Craig for being the chair at my defense and Dr. Harald Hutter who was the internal examiner at my defense. Thank, you both for your questions and helpful feedback.

I would like to thank the Dr. Doug Allan's Lab at the University of British Columbia, for providing the transgenic flies expressing PTEN variant that were vital for the completion of my project.

I am also grateful to my colleagues in the Verheyen Laboratory: Dr. Gritta Tettweiler (Ph.D), Dr. Don Sinclair (PhD), Kenny Wong, Stephen Kinsey, Jenny Liao, Nivi Ramkumar and Gerry Shipman. I am indebted to all of them for their friendship and support. I would also like to thank Katja MacCharles for her assistance in the latter stages my project, analysing images and developing PH3 counting protocol. I am also grateful to my other former undergraduate volunteers Jana Caine and Esztar Pal for their contribution to my research project.

Finally, I would like to thank my parents, family and friends for their continued support and encouragement throughout my studies.

Table of Contents

List of Figures

List of Tables

List of Acronyms

PI3K	Phosphoinositide 3-Kinase
PTEN	Human Phosphatase and Tensin homolog deleted on chromosome 10
PIP2	Phosphatidylinositol (4,5)-trisphosphate
PIP3	Phosphatidylinositol (3,4,5)-trisphosphate
Akt	Serine/threonine-specific protein kinase also known as Protein kinase B (PKB)
omb	Optomotor-blind
UAS	Upstream Activating Sequence
Socs36E	Suppressor of cytokine signaling at 36E
VUS	Variants of Unknown significance
dPI3K$^{[act]}$ or *Dp110-CAAX*	Drosophila Phosphoinositide 3-kinase [activated]
Wnt	Wingless/Integrated
Wg	Wingless
dll	Distal-less
eve	Even-skipped
Diap1	Drosophila inhibitor of apoptosis
Arm	Armadillo
Yki	Yorkie
Var	Variant
N[nucl]	Cleaved Notch domain or Nuclear Notch
JAK	Janus kinase
STAT	Signal-transducer and activator of transcription
STAT92E	Drosophila STAT protein at 92E (aka *marelle*)
Tcf	T-cell factor
drp49	Drosophila ribosomal protein 49
PH3	Phospho-Histone 3, indicates cell proliferation
TUNEL	Terminal deoxynucleotidyl transferase-mediated dUTP nick-end labeling, detects cell death

Chapter 1. Introduction

1.1. Signal Transduction

In multicellular organisms, cells receive and respond to signals from neighboring cells in their microenvironment which is important for development, tissue repair and normal tissue homeostasis. This process of integrating responses to cues and initiating a cellular response is termed signal transduction. Signal transduction, or signalling, is fundamental for organismal development. When the proper signalling within cells is disrupted it may result in many diseases including cancer characterized by an increase in cell growth and proliferation. In the modern era of molecular medicine, much effort has been placed on dissecting the signaling pathways and molecular mechanisms that control the development of an organism. Researchers aim to understand the mechanisms that control normal development with hopes that this knowledge will help prevent and treat the pathologies that arise when these mechanisms go awry (Lento et al., 2012). Most of the signalling pathways that are critical for development are often conserved between vertebrate and invertebrate, unicellular and multicellular organisms, with homologous genes found to be expressed in response to activation of similar pathways.

In this thesis I will be discussing the Phosphatidyl Inositol 3-Kinase (PI3K) signalling pathway which results in wing overgrowth when hyper-activated in Drosophila. The tumor suppressor PTEN (Phosphatase and Tensin homolog deleted on chromosome 10) is a well-established negative regulator of the PI3K signalling pathway. I will be demonstrating how I used genetic interaction studies in Drosophila to determine the functions of PTEN variants identified in human patients. I will first describe how we can use Drosophila to dissect signaling pathways and then provide details about the molecules involved in the study.

1.2. Drosophila as model organism

The fruit fly *Drosophila melanogaster* (Drosophila) was introduced as a model organism at the beginning of the 20th century by Thomas Hunt Morgan (Roberts, 2006). In fact, Drosophila has been used productively as a model organism for over a century to study a diverse range of biological processes including genetic mapping of traits, embryonic development, learning, behavior, as well as aging (Jennings, 2011). Drosophila is still a good model organism because of (i) well-established genetic manipulations, (ii) its short-life span and (iii) high survival rates under laboratory conditions (Blochlinger et al., 1987; Brook & Cohen, 1996). Furthermore, about 50% of fly protein sequences have mammalian analogues and about 60 to 75% of the genes responsible for human diseases have homologs in flies (Reiter et al., 2001; Ugur et al., 2016). These advantages allowed us to mimic the biology of tumors in a simple model organism like Drosophila and rapidly characterize the function of conserved oncogenes and of tumor suppressor genes in a whole animal (Walker et al., 2004).

Tissue and organ growth are often studied using larval imaginal discs, which comprise primarily a columnar epithelium. Imaginal discs are sac-like epithelial structures, found inside the larva of insects that undergo metamorphosis, that during pupation transform into the external structures of the head, thorax, limbs and genitalia (Aldaz et al., 2010) (Fig. 1.1). The developing wing imaginal disc was chosen for these assays as it is an ideal tissue in which to study cell proliferation, growth and death in order to characterize PTEN variants at the larval stage.

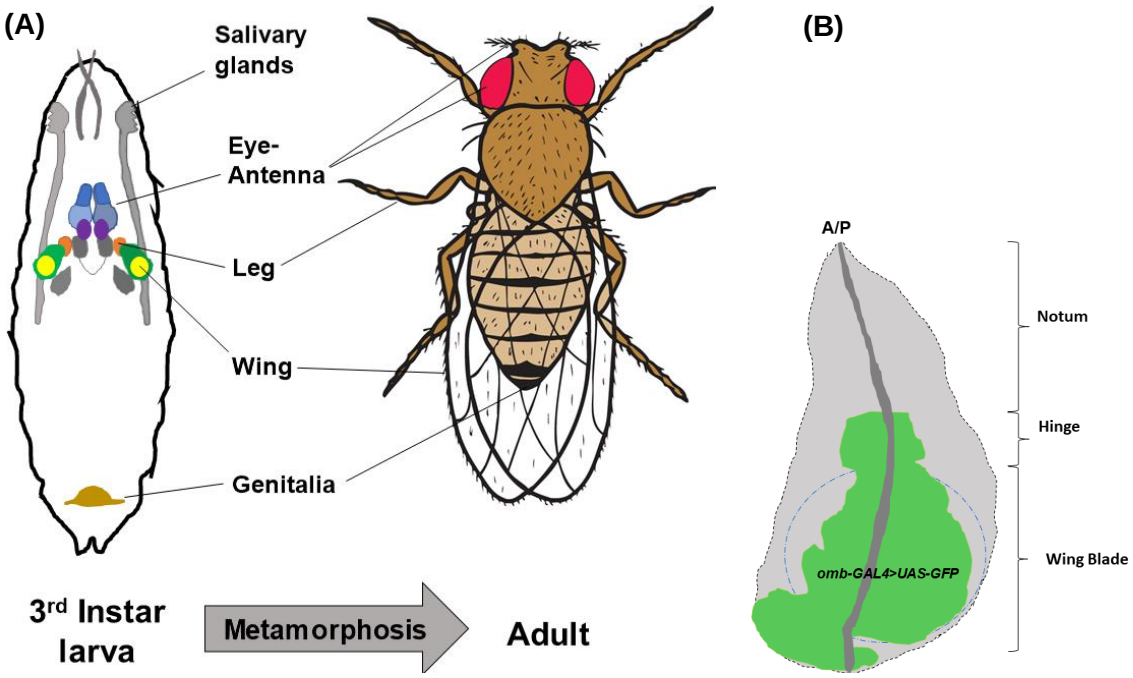

Figure 1.1. Drosophila Development, a well-established and powerful genetic model organism.

(A) Localization of the imaginal discs inside the third instar larva and the adult structures they eventually form after undergoing metamorphosis. Of interest is the wing imaginal disc (green), in which the pouch (yellow oval) forms the adult wing blade structure. This structure has been extensively studied as a model for tissue growth and development (Figure adapted from Aldaz et al., 2010). B) A simplified illustration of the wing imaginal disc with labels showing what sections eventually form the adult wing and notum structures after metamorphosis. The anterior-posterior boundary (grey strip), wing pouch (blue dashed circle) and *optomotor blind* expression domain (green) are shown.

1.3. The GAL4-UAS system used to express genes of interest in Drosophila

A powerful genetic tool often used in Drosophila research is the GAL4-UAS system. The GAL4-UAS system is adapted from yeast (*Saccharomyces cerevisiae*) and was designed to achieve selective expression of any cloned gene of interest in a wide variety of cell- or tissue-specific patterns (Brand & Perrimon, 1993; Duffy, 2002). Often UAS-driven transgenes are expressed together with a reporter protein such as green fluorescent protein (GFP) which enables the visualization of those cells that are expressing gene of interest (Edoff et al., 2007). The GAL4 system is highly flexible and useful tool for controlling ectopic expression of gene of interest both spatially and temporally.

The GAL4 protein is a yeast transcription factor that has been well studies for 30 years (Southall et al., 2008). It was discovered that the activity of GAL4 is not species-specific and can be used to express genes of interest in Drosophila, plants and mammalian cells (Southall et al., 2008). GAL4 binds a 17-nucleotide sequence, termed upstream activation sequence (UAS) that can be cloned upstream of a basal promoter and coding region of a gene of interest. The gene of interest will not be expressed in the absence of GAL4. Expression of GAL4 alone has few, if any, deleterious effects but there have been some studies showing that very high levels of GAL4 can lead to neuronal cell death in the adult Drosophila brain (Rezával et al., 2007). There are currently thousands of fly lines expressing different GAL4 drivers that are specific to different tissues e.g. eye discs, leg disc or wing disc etc. Therefore, one can choose different GAL4 drivers to express his/her UAS-transgene of interest and study its function in Drosophila.

The expression of GAL4 can be controlled in a spatial and temporal manner, thereby dictating where the UAS-transgene is expressed. This is achieved by crossing a GAL4 driver line to another fly line expressing a particular UAS-transgene.

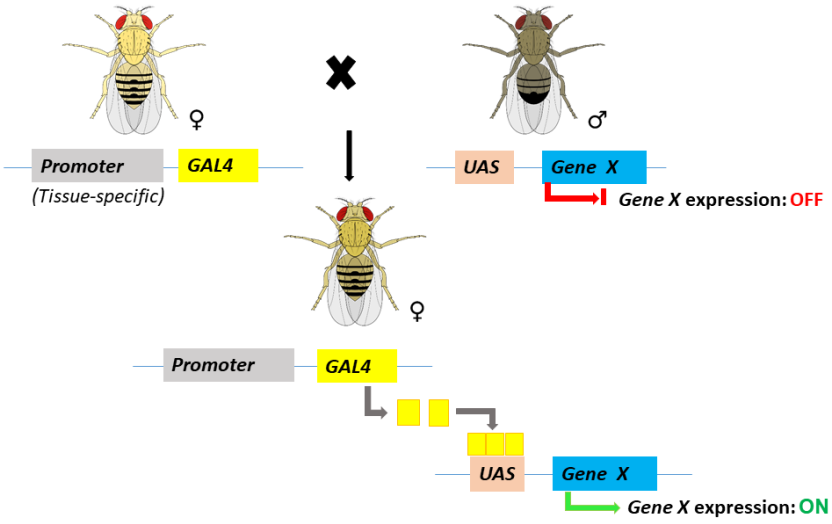

Figure 1.2. Targeted ectopic gene expression using the GAL4-UAS system.
The GAL4 gene, a transcriptional activator introduced into the Drosophila genome under the control of a specific endogenous promoter. Drosophila expressing the GAL4 protein in specific tissues are crossed to fly lines carrying a gene of interest, denoted by gene X in the figure, subcloned downstream of the GAL4 binding site (the UAS). The desired progeny will be expressing the desired gene of interest in the specific tissues. (Adapted from Brand and Perrimon 1993).

1.4. The PI3K-AKT/PTEN signalling is evolutionary conserved in vertebrates and invertebrates

The Phosphoinositide 3-kinase (PI3K)/AKT signaling pathway is a key regulator of normal cellular processes. PI3K is activated following ligand binding to a range of receptors such as integrin receptors, receptor tyrosine kinases and cytokine receptors (reviewed in Liu et al., 2009). Activated PI3K phosphorylates the membrane phospholipid phosphatidylinositol (4,5) biphosphate or PI(4,5)P2 to phosphatidylinositol (3,4,5) trisphosphates or PI-(3,4,5)P3. PIP3 acts as a second messenger by binding to and activating pleckstrin homology (PH) domain–containing proteins, including the Ser/Thr kinase Akt/PKB (protein kinase B) (Maehama and Dixon, 1998). The activation of Akt by PIP3 production triggers signaling through a multitude of Akt phosphorylation targets that control multiple cellular processes involved in cell survival, growth, proliferation, metabolism, motility and apoptosis (Luo et al., 2003).

Phosphorylated Akt activates downstream targets, mammalian Target of Rapamycin (mTORC1 or dTORC) which in turn up regulates protein synthesis in cells (Guertin & Sabatini, 2007). Phosphorylated Akt also phosphorylates glycogen synthase kinase 3 (GSK3), which in turn increases Myc and cyclin D1 activity and subsequently increases cell proliferation (Cross et al., 1995; Diehl et al., 1998; Sears et al., 2000). Studies have shown that expression of PTEN significantly decreases cell proliferation by inducing cell cycle arrest in G1 phase, in serum sensitive human glioblastoma cells (Furnari et al., 1998; Li & Sun, 1998). Furthermore, PTEN was reported to inhibits cell migration, spreading, and focal adhesions (Tamura et al., 1998). Aberrant activation of the PI3K/AKT pathway promotes the survival and proliferation of tumor cells in many human cancers (Huang & Hung, 2009; Porta et al., 2014).

Akt can also be activated through several signaling pathways independent of PI3K signalling. These include Akt activation by the platelet derived growth factor receptor (PDGF-R) and epidermal growth factor (EGF) (IGF-I) (Beniston, 2011; Chan et al., 1999). However, Akt1 (isoform 1) and Drosophila Akt is phosphorylated by phosphoinositide-dependent kinase-1 (PDK1) on Ser473 and on Thr308 by phosphoinositide-dependent kinase-2 (PDK2) (Persad et al., 2001). Thus, phosphorylation of Akt at Serine 473 and Threonine308 is specifically PI3-kinase dependent.

Previous studies also showed that activated Akt can phosphorylate a number of substrates to inhibit apoptosis. Akt phosphorylates and inactivates the forkhead box (FOXO) family of transcription factors, blocking their ability to induce pro-apoptotic regulators such as Bad and Fas ligand, and others (Morris et al., 2005). Akt also phosphorylates and inactivate caspase-9, as well as IκB; the latter resulting in the activation of NF-κB, which inhibits apoptosis (Khwaja, 1999; Kurokawa & Kornbluth, 2009). Akt phosphorylates and activates the E3 ubiquitin-protein ligase MDM2 (mouse double minute 2 homolog). As a result, phosphorylated MDM2 inhibit p53′s transcription functions, initiates p53 destruction thereby disabling p53-dependent apoptotic pathways (Haupt et al., 2003).

.

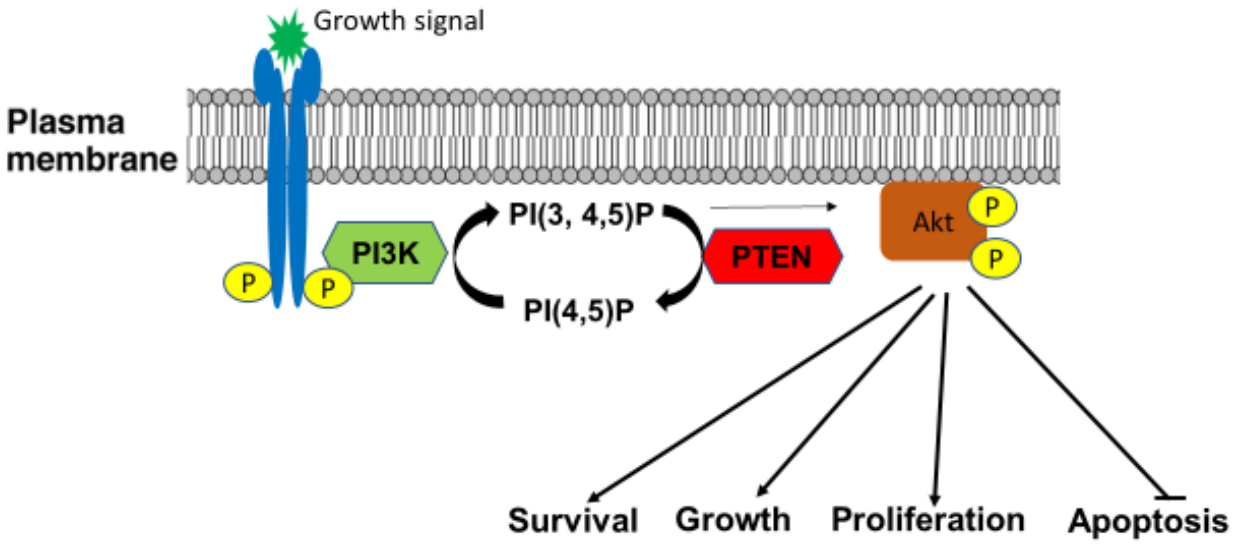

Figure 1.3. Schematic for the PI3K-Akt-PTEN signaling pathway is conserved between Drosophila and Humans.

Ligand or growth signal (green) binging to membrane receptors e.g. Receptor Tyrosine Kinases or RTKs (blue) recruits PI3-Kinase, following activation and phosphorylation (yellow). Activated PI3K phosphorylates PIP2 to PIP3, which activates AKT thereby activating the entire AKT signaling cascade which regulates cell survival, growth, proliferation and apoptosis. PTEN antagonizes PI3K by dephosphorylating PI(3,4,5) P3 to PI(4,5) P2 thereby inhibiting Akt activation. The Drosophila homolog of PI3K is Dp110. PI3K, Phosphoinositide 3-kinase; AKT, protein kinase B; PTEN, phosphatase and tensin homolog.

The tumor suppressor Phosphatase and Tensin homolog (PTEN) - dual lipid and protein phosphatase – is an established negative regulator of phosphoinositide 3-kinase (PI3K)-Akt signaling pathway (Li et al., 1997). PTEN is also known as MMAC1 (mutated in multiple advanced cancers) (Steck et al., 1997) and TEP1 (TGFβ-regulated and epithelial cell–enriched) (Li & Sun, 1997). PTEN negatively regulates PI3K signaling by dephosphorylating the membrane lipid PI-(3, 4, 5) P3, converting it back to PI (4, 5) P2 resulting in reduced cell growth, cell proliferation, cell survival, protein synthesis and inhibition of apoptosis (Maehama and Dixon, 1998).

The PI3K-Akt/PTEN antagonistic relationship is conserved across species. Drosophila PTEN has been shown to rescue enlarged eye phenotypes induced by over expressing Drosophila PI3-Kinase (*dPI3K*), Insulin receptor (*Inr*) and *chico* (Drosophila homolog of Insulin Receptor Substrate proteins 1-4 or IRS1-4) (Huang et al., 1999; Leevers et al., 1996). In fact, Drosophila PI3K (Dp110) was shown to cause lethality (flies did not enclose) at 25 °C abut this lethality was rescued when PTEN was co-expressed with Drosophila PI3K (Huang et al., 1999)

The C. elegans gene *daf-18* encodes a distant PTEN homolog which has the conserved phosphatase domain but contains a larger non-homologous C-terminal region. Nonetheless, *daf-18* mutants can suppress the mutant phenotypes of *daf-2*, the C. elegans insulin-like receptor, and *age-1*, the C. elegans PI3K (Gil et al., 1999; Ogg et al., 1998; Rouault et al., 1999)**.**

Similarly, Zebrafish mutants lacking functional PTEN are embryonically lethal. Zebrafish have two *pten* genes (*Pten^{a} and Pten^{b}*) and *pten* double homozygous mutant Zebrafish embryos develop a severe pleiotropic phenotype around 4 days post fertilization (4dpf), which can be largely rescued by re-introduction of *pten* mRNA at the one-cell stage (Stumpf & den Hertog, 2016).

In summary, the PI3K/PTEN antagonistic relationship is conserved between vertebrate and invertebrate model organisms but more importantly between Drosophila and humans. The PI3k-Akt signalling pathway plays a role in cell survival, growth and proliferation while also blocking apoptosis. The most established negative regulator of the PI3K-Akt pathway is the tumor suppressor PTEN. The structure and regulation of PTEN will be discussed next.

1.5. PTEN Structure

The structure of human PTEN (isoform 1, the most common isoform) has 403 amino acids long. The N terminus (amino acid residues 1-14) contains the PIP2 binding domain (PDB). The phosphatase domain (amino acid residues 15-185) is the catalytically active domain. The C2 domain (amino acid residues 186-351) is involved in membrane localization and binding to phospholipid bilayer. The C tail (amino acid residues 352-403) contains the PDZ domain (401-403) which is essential for protein-protein interactions (Hopkins et al., 2014; Naderali et al, 2018) (Fig. 1.4).

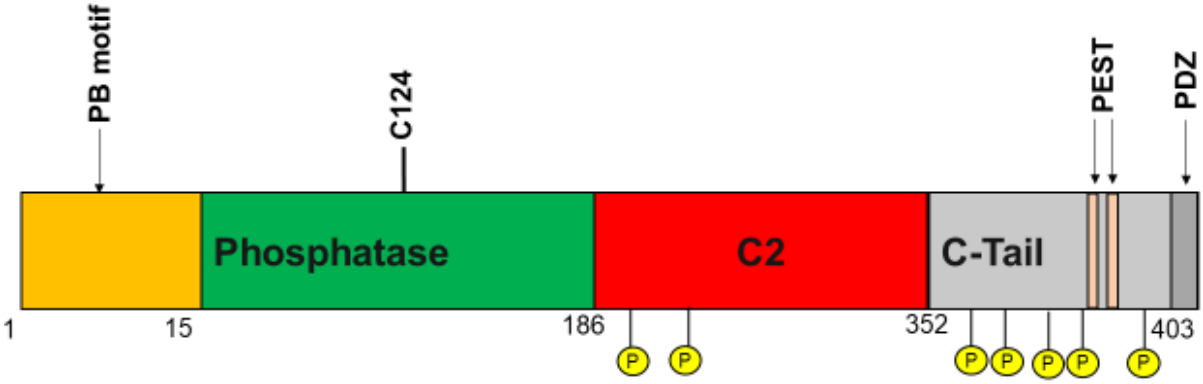

Figure 1.4 The Structure of human PTEN consists distinct domains that are modulated by post translation modifications.
The N terminus (residues 1-14) contains the PIP2 binding (PB) motif followed by the catalytically active phosphatase domain (residues 15-185), the C2 domain (residues 186-351) is involved in membrane localization and binding to phospholipid bilayer. The C tail (residues 352-403) contains the PEST sequence and PDZ domain (401-403) which are essential for stability and subcellular localization, respectively (Figure adapted from Hopkins et al, 2014).

The PTEN protein is conserved from yeast to mammals, although aspects of its structure differ. PTEN homologues in Drosophila and C. elegans are significantly larger (523 and 965 amino acids) than the 403-amino acid long human PTEN, because they contain longer C-terminal tails (Goberdhan & Wilson, 2003; Goberdhan et al., 1999). The Structure of human PTEN consists of five distinct domains including the phosphatase signature motif HCXXGXXRS/T that is found in all protein tyrosine phosphatases (Li & Sun, 1997; Steck et al., 1997).

1.6. PTEN Regulation

Post translational modifications of PTEN include phosphorylation, oxidation, acetylation, ubiquitination and SUMOs (Small ubiquitin like modifiers) known as SUMOylation (reviewed in (Naderali et al., 2018) (Fig. 1.4). Phosphorylation of multiple sites on the C-terminal region of PTEN affects protein stability, phosphatase activity and protein–protein interactions (Vazquez et al., 2000). Oxidation of PTEN at Cysteine-124 leads to the formation of a disulfide bond with Cysteine-71 resulting in decreased PTEN activity (Cho et al., 2004; Lee et al., 2002). PTEN is also acetylated at Lysine-125 and Lysine-128 by PCAF (p300/CREB-binding protein (CBP)-associated factor) and at Lys402 by CBP (CREB-binding protein) which reduces PTEN catalytic activity and enhances AKT phosphorylation (Ikenoue et al., 2008; Okumura et al., 2006).

Ubiquitination of PTEN at Lysine-13 and Lysine-289 by E3 ubiquitin ligases NEDD4-1 (neural precursor cell expressed developmentally downregulated protein 41), XIAP (X-linked inhibitor of apoptosis), and WWP2 (WW domain containing protein 2) regulates PTEN stability and sub-cellular localization (Fouladkou et al., 2008; Maddika et al., 2011; van Themsche et al., 2009). PTEN SUMOylation at Lysine-254 and Lysine-266 is critical for PTEN tumor suppressive functions and membrane affinity (Huang et al., 2012). Therefore, PTEN is highly modulated at the DNA (transcriptional), or RNA (post-transcriptional) and protein (post-translational) levels to regulate its protein levels and activity (reviewed in Naderali et al, 2018).

Although PTEN primarily associates with the plasma membrane to exert its phosphatase activity, it has also been shown to localize in the nucleus, in cytoplasmic organelles (Trotman et al., 2007) and extracellular space where it can be taken up by receiving cells (Hopkins et al., 2014; Putz et al., 2012). As described above (Chapter 1.4) PTEN has a critical role in regulating growth, the cell cycle progression, protein synthesis, survival and migration by regulating the PI3K/Akt signalling (Naderali et al., 2018). This suggest that PTEN sub-cellular localization is also important. Furthermore, loss of PTEN phosphatase activity resulted in enhanced cell survival, growth and proliferation due to activated PI3K/Akt signalling (Mirzoyan et al., 2019).

At the DNA level, PTEN can be lost or inactivated by complete allelic losses, point mutations or truncation mutations (Salmena et al., 2008). Epigenetic alteration can

also cause PTEN silencing through hypermethylation or mutation of PTEN promoter region (Waite & Eng, 2002).

I will be discussing my studies of the role of PTEN in regulating cell proliferation, growth, and proliferation in my results (Chapter 4) and Discussion (Chapter 6).

1.7. PTEN is highly mutated in multiple advanced cancers

PTEN is highly mutated in multiple advanced cancers and human diseases known as PTEN Hamartoma Tumor Syndromes or PHTS (Blumenthal and Dennis, 2008). PHTS is a genetic condition in which hamartomas or benign (non-cancerous) tumors develop in different parts of the body (Marsh et al., 1999) and an increased occurrence of cancer (Mirzoyan et al., 2019). PHTS is an autosomal dominant spectrum of hamartomatous overgrowth disorders with variable phenotypic manifestations characterized by germline mutations of the tumor suppressor gene PTEN (Blumenthal and Dennis, 2008). PHTS includes dominantly inherited human disorders like Cowden syndrome, Bannayan-Riley-Ruvalcaba syndrome (Cohen jr., 1990; Marsh et al., 1999), Proteus syndrome, Proteus-like syndrome, and PTEN-related Proteus syndrome (Wiedemann et al, 1983). People with *PTEN* hamartoma tumor syndromes are at higher risk of developing breast, thyroid, kidney, uterus, colorectal, and skin cancer (Eng, 2019). In somatic cancers, for example glioblastoma (GBM), endometrial, breast and prostate cancer, PTEN function can be compromised by a variety of mechanisms (Luongo et al., 2019). In addition, germline mutations of PTEN increase the risk of developing neurodevelopmental disorders, such as autism and mental retardation (Papa et al., 2014; Wang et al., 2010).

PTEN is a highly mutated across its primary amino acid sequence but the phosphatase domain is the most common site of germline or sporadic PTEN mutations (Myers et al., 1997). While many mutations have been identified, a thorough search of databases such as ClinVar and Catalogue of Somatic Mutations in Cancer (COSMIC) indicate that at present it is sometimes difficult to predict the phenotypic and functional outcome of a given PTEN mutation. ClinVar is an evidenced based, freely accessible public archive of reports of the relationships among human gene variations and associated phenotypes (Landrum et al., 2014).

PTEN has been shown, by previous studies, to be an “obligate haploinsufficient tumor-suppressor gene as the loss of 50% of its function compromises tumor suppression” (di Cristofano et al., 1999; Trotman et al., 2003). Haploinsufficiency of tumor suppressors describes a condition in which a single gene copy deletion in diploid cells results in a functional deficit due to a reduced amount of the gene product (Payne & Kemp, 2005; Santarosa & Ashworth, 2004). Obligate haploinsufficiency refers to the deleterious effects of homozygous PTEN deletion such that only a heterozygous deficient condition of PTEN leads to tumor formation (Berger et al., 2011). Furthermore, slight alterations of PTEN function can have dramatic effects on cancer predisposition and tumorigenesis, suggesting a dosage-dependent tumor suppression by PTEN (Berger et al., 2011). Kwabi-Addo et al. (2001) showed that haploinsufficiency of the *PTEN* gene and protein promotes the progression of prostate cancer in a well characterized transgenic adenocarcinoma mouse model of prostate cancer. Genetic ablation of PTEN was shown leads to the development of different tumor types in mice (di Cristofano et al., 1998; Podsypanina et al., 1999; Suzuki et al., 1998). In fact, complete ablation of PTEN, in the absence of other mutations, can perpetuate tumor growth due to the activation of p53-dependent senescence that counteracts tumor progression, an indication of “obligate haploinsufficiency” (Chen et al., 2005). Therefore, PTEN can also be dysregulated through monoallelic loss and thus is somewhat of an atypical tumor suppressor gene.

1.8. Human PTEN and Drosophila PTEN share high sequence similarity

Previous studies done by Huang et al (1999) showed that both Drosophila and human PTEN showed similar phenotypes during Drosophila eye development. Using the Gal4-UAS system the researchers expressed either fly or human PTEN in the developing eye and studied the consequences. They also found that PI3K expression could rescue PTEN induced eye and wing phenotypes, highlighting their antagonism (Huang et al, 1999). The primary structure of Drosophila PTEN (dPTEN) and human PTEN (isoforms 1- 3) are already known and available on UniProtKB database. Crude sequence alignment using ClustalW software revealed that the key domains are conserved between human and Drosophila despite the difference in the size of the protein (Fig. 1.5). Most of the residues are conserved (green), with large number also

showing conserved properties (blue) while other residues did not share similar properties (red) between human and Drosophila PTEN (Fig. 1.5). The significance of conserved and non conserved residues was not the focus of my study, but it is worth noting most of them are conserved.

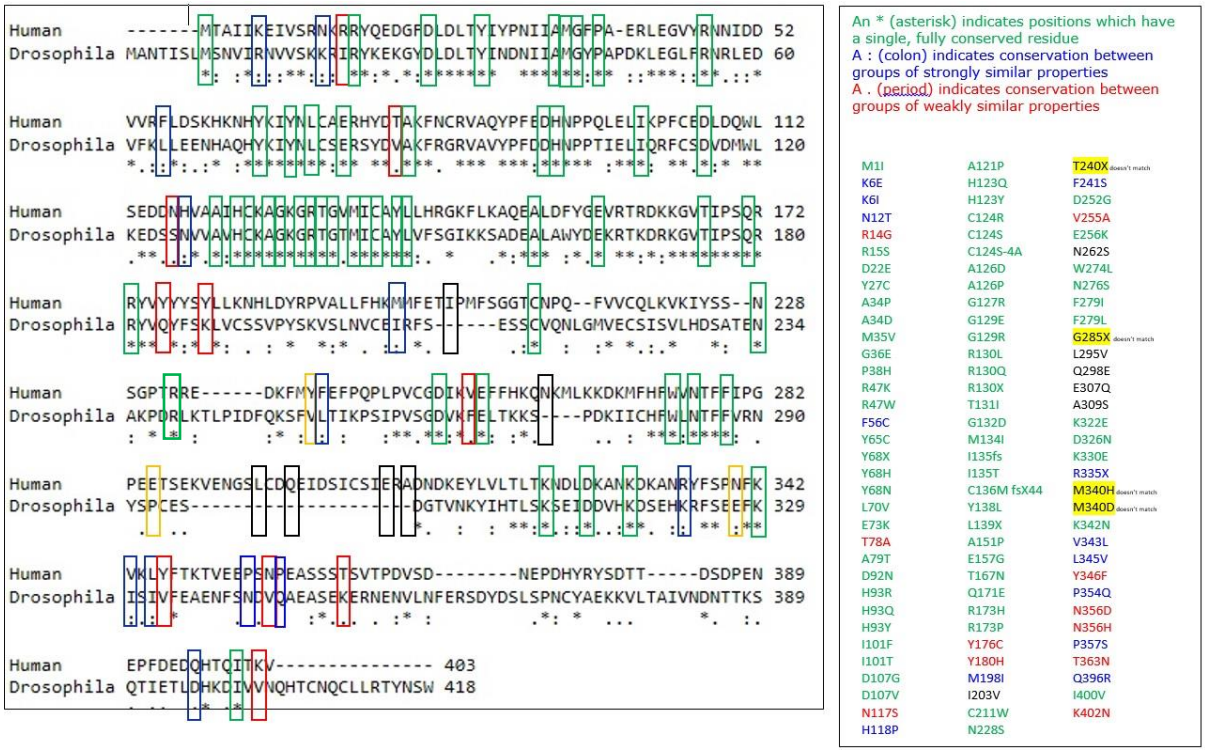

Figure 1.5 Sequence alignment for human and Drosophila PTEN show conservation of critical domains.

The human PTEN (403 amino acid length) shows conserved structural domain with the 418-amio acid long Drosophila PTEN. Sequence alignment done using Clustal W software and annotation of amino acid residues performed by Katja MacCharles.

1.9. Objectives of the study

Large-scale sequencing projects and sequencing of patient samples can reveal mutations or polymorphisms in many genes, but the functional consequences are not always apparent especially for single amino acid substitutions. However, the development of methods to determine whether these variants are function-altering, and therefore clinically relevant, still lags far behind. Consequently, it is still very difficult to predict the phenotypic outcome of a given single amino acid substitution in a gene, like the tumor suppressor PTEN which is the focus of my study. In ClinVar, 131 of 241 missense variants (~54%) are considered variants of unknown significance (VUS). In

COSMIC, a database for somatic mutations in cancer, 1994 out of the 4778 unique PTEN samples are missense variants. So, there is an urgent need to find a systematic way to test and test the relative function of these missense variants.

In collaboration with Dr. Doug Allan and Dr. Tim O'Connor at the University of British Columbia we are working on developing a robust assay that will enable us to functionally test human PTEN variants of unknown significance (VUS) in a variety of Drosophila assays. This "functionalization" will allow us to determine activity of PTEN VUS in selected assays, relative to wild type PTEN. This will entail large scale screening of ~100 variants, as well as more in-depth analysis of selected representative candidates that act as loss-of-function (LOF), gain-of-function (GOF) or wild type human PTEN in Drosophila, when expressed in $PI3K^{[act]}$ background. I will be using genetic interaction studies and tissue staining to characterize effects of PTEN VUS strains. I will also use quantitative methods to characterize adult phenotypes. Our colleagues at UBC will be simultaneously studying the same PTEN variants using different fly assays to monitor PIP3 levels, fly eclosion and phospho-Akt (p-Akt levels). However, in my thesis I will primarily be reporting data generated by myself in the Verheyen Lab (SFU, Burnaby).

Initially, I hypothesized that the amino acid mutations will either be conservative (retain function) or radical (loss of function). So, I proposed that (i) most PTEN variants with mutations in the phosphatase and C2 domain will result in PTEN loss of function phenotypes when compared to wild type human PTEN while most mutations outside the functional domains (N-terminus and C-tail) will result in wild type human PTEN phenotype (i.e. functional).

In addition to screening all available VUS strains, I also selected a few PTEN variants to further characterize at both larval and adult Drosophila wing stage. Confocal microscopy imaging was used to see how expression of human PTEN variants affected cell proliferation, growth and/or apoptosis in imaginal wing discs from third instar larva. The results from the anti-PH3 immunofluorescence (IF) staining will be compared and combined with the adult wing hair count data to determine if human PTEN variants regulate cell growth or proliferation, or both.

Chapter 2. Materials and Methods

2.1. Genetics

2.1.1. Drosophila stocks and culture conditions for testing human PTEN variants

Drosophila melanogaster flies were raised on standard cornmeal-molasses food and kept at room temperature (~22 °C). The *bifid/omb-Gal4* line (Bloomington Drosophila Stock Centre (BDSC), #58815) was used to express human PTEN variants. It is located on the X chromosome (chromosome I). A UAS strain expressing activated Drosophila PI3K was also obtained from BDSC, stock #25908. This line expresses myc-tagged PI3K92E (or Dp110) with the polybasic region and CAAX box of mammalian K-Ras fused to the C-terminus for membrane targeting under UAS control, inserted on the X chromosome. This fly strain is also referred to as *UAS-Dp110-CAAX*, but for the purpose of this thesis I will use the term UAS-dPI3K$^{[act]}$ or simply dPI3K$^{[act]}$

2.1.2. Drosophila stocks and culture conditions for investigating roles of PTEN in other signalling pathways

Drosophila fly stocks were grown at room temperature and crosses were performed at 29 °C unless otherwise noted. Genetic strains used in the experiments include; *omb-Gal4, UAS-GFP* which express GAL4 in the wing pouch and in abdominal segments as stripes spanning compartment boundaries, *arm[XP33]/FM7a;; MKRS/TM6B* fly strain created by Jessica Blaquiere in 2014 and used for balancing first and third chromosome, *Sco; MKRS/ Cyo~TM6B* fly line with the second fused to third chromosome balancer strain, *UAS-myr-RFP (III)* expressing red fluorescent protein with a myristoylation signal expressed under the control of UAS, *UAS-Arm S10 wt attP40* expressing Myc tagged Arm S10 inserted at the attP40 site on chromosome II, *UAS-Yki.S168A:GFP* on chromosome II, *UAS-Stat92E* on chromosome II and *UAS-N[nucl*] on chromosome III. The crosses were set up at 29 °C and the schematic of the workflow is shown on Fig. 5.1.

2.1.3. **Generation of flies expressing dPI3K[act] (Verheyen lab, SFU)**

Flies expressing the constitutively active form of Drosophila PI3K (dPI3K [act]) were generated using the GAL4/UAS system at 25 °C. *omb-GAL4* females were crossed with males expressing UAS-dPI3K[act]. Flies carrying both transgenes display a wing overgrowth and mild patterning defect. To generate recombinant flies that carry both transgenes on the same chromosome, *omb-GAL4/UAS-dPI3K[act]* females were mated to FM7 balancer males to identify progeny that showed the phenotype observed in the female parents and these were selected as putative recombinants since the two elements would otherwise segregate in the offspring. The larger wing phenotype was used to select candidate female flies expressing the transgene. These females were individually crossed with *FM7/Y* males, from which the desired F1 generation of females were selected and then backcrossed with *FM7/Y* males to select balanced flies displaying the desired wing phenotype. Two recombinant lines were recovered and are referred to as *omb-GAL4>UAS-dPI3K[act]/FM7c*. While we do not know the position of the recombination event, we know that two unique recombinant chromosomes carry both the UAS and Gal4 element and display equivalent phenotypes.

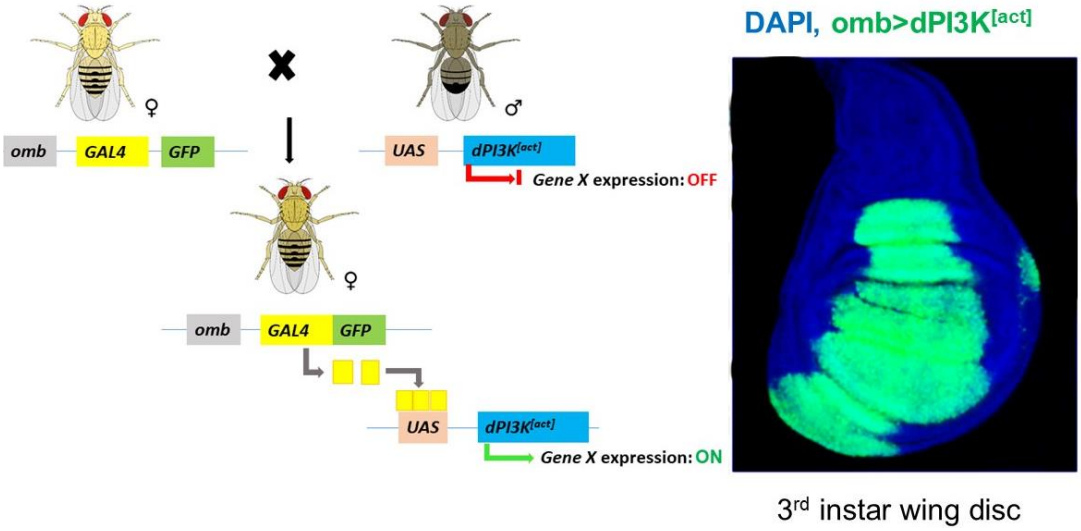

Figure 2.1 Targeted ectopic gene expression using the GAL4-UAS system.
The GAL4 gene, a transcriptional activator introduced into the Drosophila genome under the control of a specific endogenous promoter; optomotor-blind or omb. Drosophila expressing the GAL4 protein in the wing discs (and eye discs) are crossed to fly lines carrying a human PTEN^{VUS} (Variant of Unknown Significance) denoted by gene X in the figure subcloned downstream of the GAL4 binding site (the UAS) and inserted at the attp2 site (Chromosome III). The desired progeny will be expressing both UAS-transgenes (*UAS-dPI3K*[act] and *UAS-PTEN^{VUS}* (Brand and Perrimon 1993). The expression domain of *omb-Gal4* in the wing imaginal discs is shown in the inset using UAS-GFP as a reporter.

2.1.4. **Expression of activated Drosophila PI3-Kinase and human PTEN variants**

To determine whether PTEN transgenes retained wildtype function, or whether they displayed loss or gain function, we carried out crosses with the omb-GAL4>UAS-dPI3K[act]/FM7c flies. Each human PTEN fly strain (wildtype and VUS), as well as a negative control called ‘no PTEN’ which consisted of the strain into which the UAS-transgenes were injected, were crossed to omb-GAL4>UAS-dPI3K[act]/FM7c females and the phenotypes of the offspring in which the omb-Gal4 driver drove expression of both dPI3K[act] and UAS-PTEN variant lines was determined, as described below.

Flies expressing both activated Drosophila PI3K and human PTEN variants of known or variants unknown significance (VUS) were selected (females only) and stored in 70% Ethanol at room temperature. Adult wings were mounted using aqueous mounting agent for microscopy (Millipore Sigma, Cat#108562). Wings were imaged using the Zeiss Axioplan 2 attached to episcope (Verheyen Laboratory, SFU) at 5X magnification for whole wing area calculation for all the tested PTEN variants. and 20X magnification (for hair counting). Wing areas were calculated using Adobe Photoshop CS3 (2007) and hair counts performed using ImageJ software, respectively. Graphs were created using Graphad (Prism 5 software).

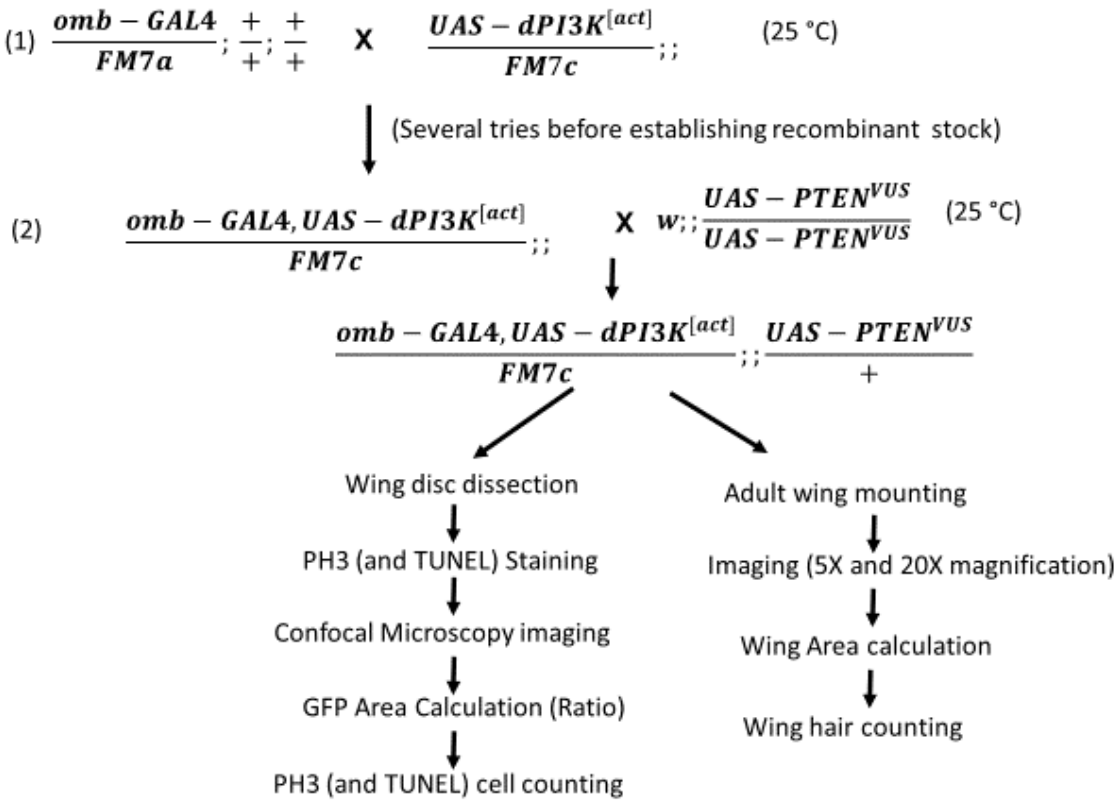

Figure 2.2 Schematic showing how PTEN Variants of unknown significance were tested.

Each PTEN variant of unknown significance will be tested in the context of activated Drosophila PI3-Kinase or dPI3K [act]. The effect of PTEN variants was studied the larval (3rd instar) and adult stage of Drosophila development.

2.2. Molecular and Cellular Biology

2.2.1. Generation of transgenic fly strains expressing human PTEN variants (Allan group, UBC)

All human PTEN (PTEN) variants were integrated into the attP2 locus of the Drosophila genome, on chromosome III by phiC31-integrase (performed by Rainbow Transgenics Inc, CA). The Allan lab at UBC first generated a series of transgenic flies with PTEN variants with established function to calibrate the assays. These include PTEN C124S (catalytically inactive), G129E (no lipid phosphatase activity), Y138L (no protein phosphatase activity) and a constitutively activated PTEN (PTEN 4A). These were all shuttled into the pGW-HA.attB destination vector (PMID: 23637332), and then

integrated into the attP2 locus of Drosophila by phiC31-integrase-based transgenesis (PMID: 17360644).

The Allan lab then generated another 103 transgenic flies each carrying a different PTEN variant, each encoding a single amino acid substitution in the primary structure of 403-amino acid long PTEN protein. The other (103+) PTEN variants were grouped into the following classes: ASD only, cancer only, ASD and cancer, EXaC variants, computationally predicted as high or low impact variants. This generated a panel of fly strains with UAS-PTEN variants (abbreviated as UAS-PTEN-VUS), where VUS stands for variant of unknown significance. Integration into the same site ensures reproducible expression of all variants to allow for direct comparison of PTEN-VUS function in Drosophila tissues.

2.2.2. **Isolation of RNA and cDNA synthesis**

Larval heads from third instar larvae were dissected in PBS and total RNA was extracted using RNeasy Mini Kits (Qiagen, 74101). First strand cDNA was synthesized using OneScript Plus cDNA Synthesis Kit (Applied Biological Materials, G236). The amount of starting total RNA used for CDNA synthesis was 1 - 1.5 µg when using whole larva or third instar (L3) larvae heads. The amount of starting total RNA was 250 ng when total RNA was extracted from wing imaginal discs from L3 larva. The PCR machine used for cDNA synthesis was PCR#2 machine in the Verheyen Laboratory at SFU.

2.2.3. **Quantitative Real-Time Polymerase Chain reaction (qRT-PCR)**

Quantitative real-time PCR (qRT-PCR) was performed on RNA extracted from third instar larval heads using the RNEasy mini Kit protocol form Qiagen (above). The qRT-PCR was performed using SensiFast SYBR Lo-ROX Kit (Bioline, 92005) on Applied Biosystems's StepOne Real-time PCR System (initially) and QuantStudio 3 Real Time PCR systems (later). The qPCR thermocycler was as follows; 90 °C for 3 min, [90 °C for 15s, 60 °C for 30s, 90 °C for 15 s] x 40 cycles. The melting (hold step was) done continuously at 60 °C for 1 minute. Fold change in mRNA levels (thus gene expression) was computed using the comparative Delta-Delta Ct ($2^{-\Delta\Delta Ct}$) method as previously described in (Pogmore et al., 2016).

2.2.4. **Immunofluorescence (IF) staining and confocal microscopy imaging**

Third instar larval (L3) imaginal discs were dissected and stained using standard protocols larval imaginal discs were dissected in PBS and fixed in 4% paraformaldehyde (PFA) for 15 min at room temperature. Samples were then washed with PBS with 0.1% Triton X-100 (PBST) two times (10 min/wash). After blocking with 2% BSA in PBST for 1 hr at room temperature, samples were incubated with primary rabbit PH3 antibody (1:1000; Cell Signaling Technology #9701S) overnight at 4°C in the shaker. After primary antibody solution was removed, samples washed with PBST (as before) and then incubated with Alexa Fluor 647-conjugated secondary antibody (1:500, Jackson ImmunoResearch Laboratories, Inc), DAPI (4',6-Diamidino-2-Phenylindole, Dihydrochloride) (final concentration: 0.2 mg per mL, Invitrogen D1306). Samples were washed with PBST and mounted in 70% Glycerol/PBS.

Images were taken on a Nikon Air laser-scanning confocal microscope (Nikon, Tokyo, Japan) and processed by Image J (FIJI). PH3 cell counting was performed on max-projection images created using ImageJ software. To compare PH3-positive cell counts per genotype, counts were converted as a ratio of PH3 cells/area, then analyzed as experimental condition over control tissue. Significance between groups was assessed by one-way analysis of variance (ANOVA) and $P<0.025$ was considered significant unless stated otherwise

2.2.5. **Detecting Cell Death in Drosophila wing discs**

TUNEL (Terminal deoxynucleotidyl transferase-mediated dUTP nick-end labeling) was used detect cell death in larval discs of third instar larvae (females only). TUNEL staining detects fragmented DNA ends, which are characteristic of apoptotic cells (Leevers et al., 1996). Larval heads (3rd instar) were dissected and co-stained with anti PH3 (described in Chapter 2.3.1) followed by TUNEL staining. Basically, after dissection samples were fixed in 4% PFA, washed 3 x 5m PBS, add rabbit anti-PH3 (1:1000 Cell Signaling PH3, #9701S) in blocking solution (400 µL of 2% BSA in PBT) and incubated overnight at 4 °C on a rocker. Sample were washed samples four times (10 min/wash) in 600ul PBT on a rocker at room temp. Then, I combined 90 µL Labelling solution (Red tube) with 10 µL Enzyme solution (Blue tube) per sample. The TUNEL

reagent was incubated with Alexa Fluor 647-conjugated secondary antibody and incubated samples on rocker at 4 degrees overnight. After discarding TUNEL+ secondary antibody solution, samples were washed two times (10 min per wash) in PBT, incubated at room temperature for 1 hour with DAPI (1:500) in fresh PBT. Samples were when washed four times (10 min per wash) in PBT, removed last PBT wash and stored samples in cold 1X PBS in fridge (4 °C) for 1 day, before mounting discs using standard protocols and confocal imaging of discs as described above (Chapter 2.3.1).

2.3. Adult wing mounting, wing area calculation and wing hair counting

Adult wings were dissected in 70% ethanol followed by mounting in Aquatex (EMD Chemicals, Gibbstown, USA). A minimum of 10 wings were mounted per genotype for analysis. Adult wings were imaged with an Axioplan-2 microscope (Zeiss, Oberkochen, Germany). Adult wing areas and GFP area (ratio) of wing disc were quantified using Adobe Photoshop CS3 and ImageJ (https://imagej.nih.gov/ij/), respectively. Adult wings for area calculation were taken at 5X magnification and wing images for hair counting were take 20X magnification. The area of the adult wing blade was calculated using Photoshop CS3 and selected area was kept consistent for each wing when PTEN variants were expressed in an activated PIK background. Wing hairs were counted in the 2nd posterior cell (2P) near the posterior cross vein or p-cv but also in the 1st posterior cell (1P) above the posterior cross vein.

2.4. Estimating the total number of cells between the third and fifth longitudinal veins (L3 and L5, respectively)

The total number of cells within the area between the L3 and L5 veins was estimated using the images taken for wing area calculation and images used for performing hair counts. The images for hair counts were taken at higher magnification (20X) to get better resolution of wing hairs while images taken for wing area were taken at lower magnification (5X) using the Zeiss Axioplan-2 microscope. The total number of cells with the L3 and L5 boundary was computed as follows; (i) calculate the area of specific part of the wing taken at both 5X and 20X magnification. Then the area between the a-cv and p-cv was used as reference. Then, Find the average Ratio = $(\frac{Area\ (20X)}{Area\ (5X)})$.

Calculate the average ratio as n = 5 wings per variant. Area where hairs were counted was 432000 pixels^2 (720 pixels x 600 pixels). Next, divide the Area (Step 4) by the Ratio (Step 3) to get the mean area corrected to the size of the selected area at 5X. Lastly, Calculate total number of cell using the wing area data for the L3 to L5 are using the formula shown below;

$$\frac{No.\ of\ hairs}{Corrected\ Area} = \frac{Total\ No.\ of\ hairs}{Total\ wing\ Area}$$

2.5. Percentage of GFP area calculation in larval wing discs

The ratio of GFP area over the total wing disc area was calculated using confocal images and/or images taken using the Zeiss Axioplan-2 microscope. The DAPI channel image was used to outline and calculate the area of the whole discs. The GFP channel image was used to calculate the area of the GFP (and hence *omb* > *PI3K*$^{[act]}$) expression. The GFP area was calculated as percentage or ratio of the whole disc area for all genotypes to normalize for differences in disc size.

2.6. Generating graphs and statistical analysis

Scatter graphs were generated using GraphPad prism to represent the distribution of wing area, wing hair and PH3 cell count data. Statistical analysis on datasets were performed using both GraphPad and/or Excel. The data were represented by mean ± SD. The p values were determined by two-tailed Student's *t* tests. $P < 0.05$ was considered statistically significant. A one factor ANOVA followed by the Turkey-Kramer honest significance (Microsoft Excel) test or Dunnett's post hoc tests (using GraphPad Prism) were performed using Microsoft Excel to determine if means were significantly different form the negative (attP2 or no PTEN) and positive (wildtype human PTEN or PTEN).

Chapter 3. Results

3.1. Expression of activated Drosophila PI3-Kinase results in adult wing over-growth

Most of the work shown in the next two chapters will be incorporated in a manuscript that we are currently writing with our collaborators from UBC. In these chapters I am only presenting work done by me and my undergraduate assistants at SFU. The authors and title of the manuscript in preparation is as follows.

Payel Ganguly[1], **Landiso Madonsela**[5], Barry P. Young[1], Kathryn Post, Jesse Chao[1], Fabian Meili, Manuel Belmadani[3,5], Sanja Rogic[3,5], Paul Pavlidis[3,5], Kurt Haas[1,2], Timothy P. O'Connor[1,2], Christopher J. Loewen[1,2], Esther M. Verheyen [5], Douglas W. Allan[1,2]. "*High-volume functionalization of human PTEN disease variants in Drosophila and yeast*." In preparation.

[1-4]University of British Columbia, Vancouver, Canada.[1]Department of Cellular and Physiological Sciences, [2]Djavad Mowafaghian Centre for Brain Health, [3]Department of Psychiatry, [4]Michael Smith Laboratories. [5]Department of Molecular Biology and Biochemistry, Centre for Cell Biology, Development and Disease, Simon Fraser University, Burnaby, B.C Canada

In order to study PTEN variants of unknown significance, we needed to develop a robust, fast and inexpensive assay that would allow us to study their function. It was already known that the PI3-Kinase and PTEN antagonistic relationship is conserved in Drosophila. Therefore, we chose to express activated Drosophila PI3-Kinase in the Drosophila wing disc (specifically the pouch, Fig 1.1 B). Previous reports had shown that expression of dPI3K$^{[act]}$ increase Drosophila wing size by increasing both cell size and cell number (Leevers et al., 1996; MacDougall et al., 2004). The increased wing size was important so that we could see significant changes in wing sizes when wild type human PTEN was co-expressed with dPI3K$^{[act]}$. The work presented in this chapter was performed primarily by Landiso Madonsela, with assistance from SFU undergraduate research student Katja MacCharles and summer volunteer Eszter Pal, a McGill student living in Surrey.

In this study we first created transgenic fly strains using the GAL4/UAS system to express *UAS-dPI3K*$^{[act]}$ (on the X chromosome) in the wing imaginal disc using the *bifid/omb-GAL4 driver* (wing disc pouch specific GAL4 driver). We chose the omb-GAL4 driver because of its expression in the wing disc which eventually gives rise to the adult wing blade (Fig.1.1, A). *omb-GAL4* is also expressed in eye discs and adult flies expressing *omb-GAL4* have a striated eye colour phenotype, which was used to select the desired female offspring for subsequent studies (Fig. 3.1). The FM7c balancer also results in bean shaped eyes phenotype due to the dominant mutation of the gene *Bar*. The Bar-eye was used as extra selection criterion for scoring and mounting wings from the desired female offspring.

In this research project we generated a recombinant fly strain expressing activated Drosophila PI3-kinase (UAS-dPI3K$^{[act]}$ or UAS-Dp110-CAAX (the former genotype name will be used throughout my thesis) using the *optomotor-blind* (*omb*) Gal4 strain on the X chromosome in Drosophila. The expression domain of the GAL4 driver that was used in this study was visualized with the UAS-GFP reporter protein. The advantage of using *omb-GAL4* with GFP was that it allowed for efficient selection of the desired offspring at the larval stage (only females expressing GFP were selected) and adult stage (only females with the *omb* eye color variation phenotype were selected) for functionalization of the tested PTEN variants.

First, we wanted to see the wing phenotype when we expressed activated Drosophila PI3-Kinase or *dPI3K*$^{[act]}$ in the wing disc. We characterized the adult wing phenotype seen in the *omb-Gal4>dPI3K*$^{[act]}$ (after outcrossing to w^{1118} control flies) stock by measuring wing area.

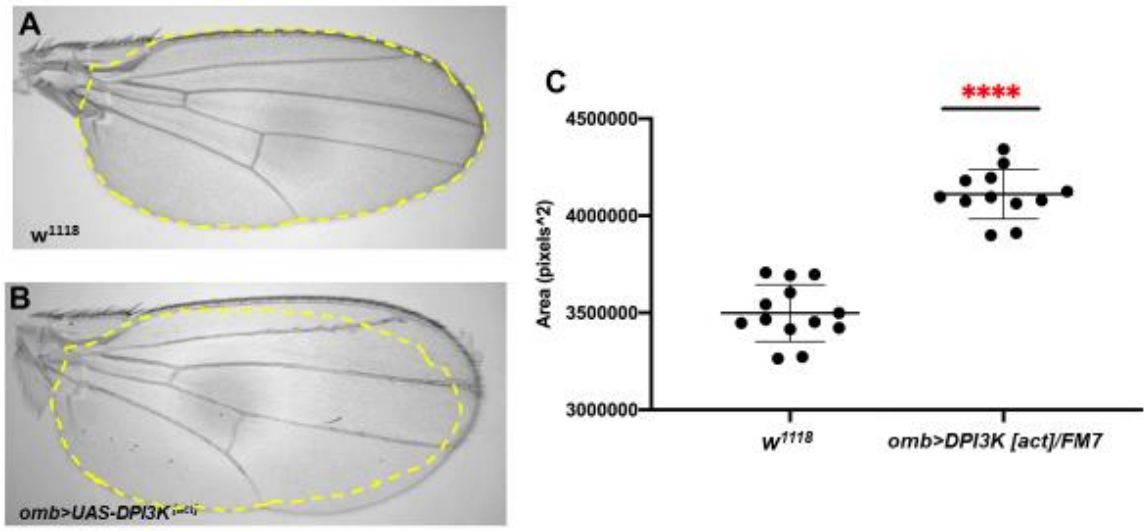

Figure 3.1. Activated Drosophila PI3K or dPI3K[act] increases adult wing size. A) Adult wing from control ^{w1118} female flies. B) Adult wing from *omb>dPI3K [act]* female flies. (d) Quantification of wing size (area) shown with selection (yellow dashed outline shows size of wildtype and superimposed over *omb>dPI3K [act]*). n = 10 or more wings were mounted per genotype. Area calculated using Adobe Photoshop CS3. Graphs created with and statistics performed using GraphPad (one-way ANOVA followed Dunnett's post hoc test. ****p < 0.0001.

The results from our experiment showed that the expression of dPI3K[act] resulted in enlarged wings. The average area of the wing blade was increased by 17.5 % ± 4 % when activated dPI3K was expressed compared to the w^{1118} flies, which carry only an eye colour mutation and are effectively wildtype for wing size (Fig. 3.1, A and C). Our results were consistent with previous studies that showed that hyper-activated insulin signalling pathway or ectopic expression of dPI3K[act] results in increased wing and eye size by increasing the size of cells without affecting pattering (Stumpf & den Hertog, 2016).

Dysregulation of the PI3K signalling pathway has been shown to lead to a multitude of diseases including cancer. Cancer is a multistep disease that is often driven by the concomitant activation of oncogenic pathways (e.g. PI3-Kinase signalling) and loss of tumor suppressor genes (like PTEN), resulting in uncontrolled division of abnormal cells in a part of the body (Dillon et al., 2007; Paes & Ringel, 2008). Shimizu et al (2008) agrees that defective regulation in diverse cellular activities such as cell cycle, apoptosis, and signal transduction, maintenance of cell polarity, and cell adhesion results in tumors. So, we had successfully mimicked a PI3-kinase induced overgrowth in

the Drosophila wing in our assay, since it has been previously shown that this PI3K[act] transgene behaves like an activated oncogene (Walker et al., 2004). Next, we wanted to see if the expression of wild type human PTEN would results is reduced wing size. This would tell us if the assay we designed revealed functional conservation of human PTEN in its antagonistic relationship to PI3-kinasee.

3.2. Human PTEN suppresses PI3K induced phenotypes in the developing Drosophila wing

Human PTEN has been shown to be negative regulator of PI3K-dependent Akt activation and its downstream signalling that is important for many cellular processes. Huang et al (1999) showed that human PTEN, similar to dPTEN, was able to suppress enlarged PI3K dependent eye phenotypes in Drosophila. We had already established that the expression of dPI3K[act] resulted in larger wings (Fig. 3.1). Next, we wanted to test if human PTEN-WT was able to suppress or rescue the PI3K[act] adult wing phenotype. We obtained transgenic flies from Doug Allan from the University of British Columbia (UBC) that were expressing human PTEN variants (i.e. including wildtype, validated mutant PTEN and UAS-PTEN^{VUS}). All human PTEN (PTEN) variants, including wild type PTEN, were integrated into the attP2 locus of the Drosophila genome, on chromosome III, by phiC31-integrase (performed by Rainbow Transgenics Inc, CA). A negative control for all crosses were flies from the attP2 strain without an inserted UAS transgene (called 'no PTEN (attP2)'). This strain controlled for any genetic background effects seen with the transgenes. The hard work from our UBC colleagues in generating and validating the transgenic flies expressing the desired PTEN variants made my research project possible. The PTEN variants provided to us for this research project were selected because they were associated with Autism spectrum disorder (ASD), PTEN Hamartoma Syndromes (PHTS) and somatic cancer (Table A.2, appendix). (The table in appendix was not made by me, it was adapted from a data table prepared and shared by our collaborators at UBC).

The *omb-GAL4>UAS-dPI3K[act]* females, with enlarged wings were then crossed to *UAS-PTEN-WT* flies to determine if wild type human PTEN rescues activated PI3-kinase phenotype in the Drosophila wing. All wing sizes are compared to the starting *omb>PI3K[act]* strain and compared to the effect of expressing wildtype PTEN in that assay.

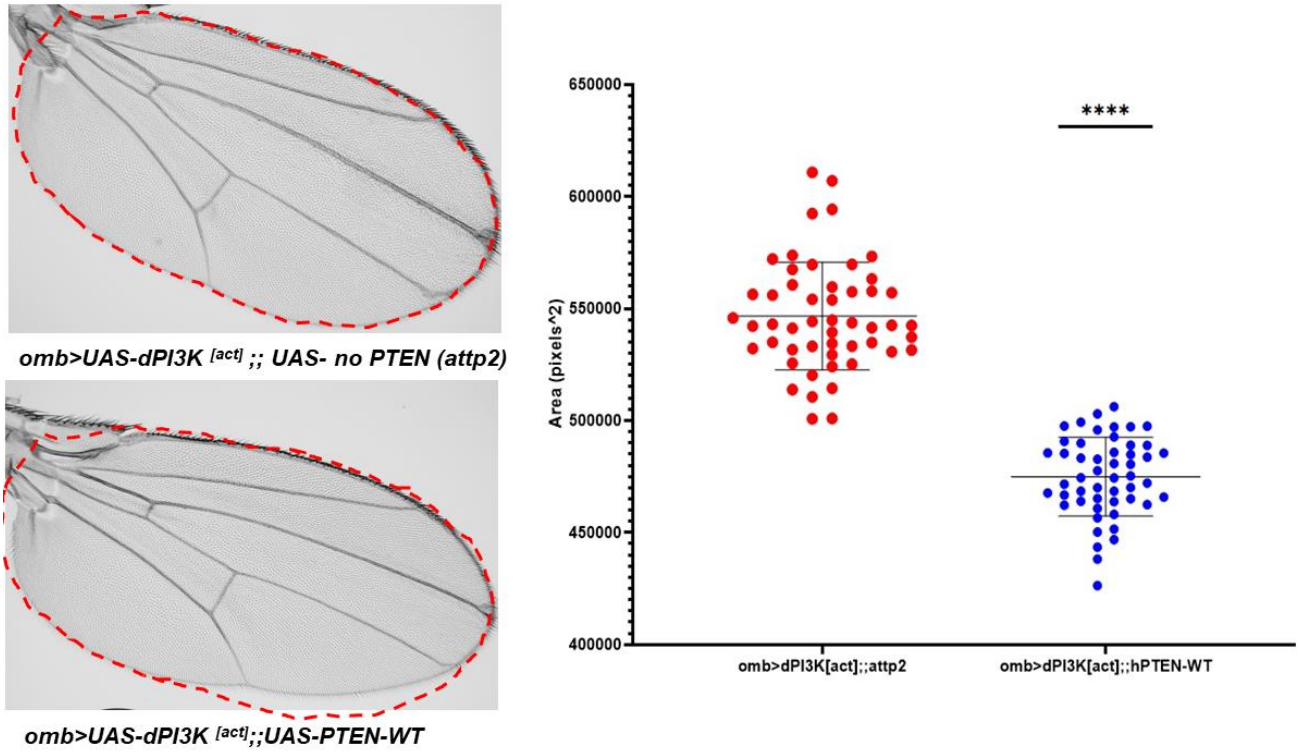

Figure 3.2. Human PTEN suppresses DPI3K induced phenotypes in the developing Drosophila wing.

The total area of the wing blade was measured for when dPI3K[act] was expressed alone (top left panel) or when co-expressed with wild type PTEN (bottom left panel). Red dashed outline shows size of *omb>dPI3K [act]* and superimposed over *omb>dPI3K [act]*+PTEN-WT.Quantification of wing area was performed using Adobe Photoshop CS3. Mean ± SD, n = 6 independent crosses, 7 - 10 wings per genotype for each cross. Statistical analysis performed using GraphPad, unpaired t-test with Welch's correction, ****p<0.0001.

The human PTEN consistently rescued the dPI3K[act]-dependent adult enlarged wing phenotype. The average wing size of dPI3K[act] flies (females only) was 17.5% larger than w^{1118} control flies (females only). On the other hand, the average size of adult wings from flies expressing wild type PTEN were only 4.5 % larger than w^{1118} wings and 13.1% smaller than dPI3K[act] wings (Fig. 3.2). In order to make characterization of more than 100 PTEN variants efficient in our assay, genetic crosses were set up in batches of around 15 variants at a time at 25 °C. Furthermore, 'no PTEN' and PTEN-WT controls were set up with every batch and the pooled wing size data is shown in Fig. 3.2. These results suggested that human PTEN consistently suppressed the dPI3K[act] wing overgrowth phenotypes across all assays. Statistical analysis (Unpaired t-test with Welch's correction) showed that the average sizes of the wings of each genotype (i.e. dPI3k[act] alone or dPI3k[act] plus PTEN) across batches were not statistically significant

(Fig. 3.2). In fact, our UBC collaborators also performed some normalization and statistical analysis on the adult wing area data and concluded that there was no difference between the means across batches.

3.3. Characterization of human PTEN variants of unknown significance (VUS) in an activated PI3-kisae background.

We had established that wildtype human PTEN consistently suppresses the dPI3K$^{[act]}$ wing overgrowth phenotype (see above). We then proceeded to test more than 100 PTEN variants including some previously studied and characterized PTEN mutants in the same assay. Testing and analysis of the previously characterized variants was used to validate our Drosophila wing assay. In order to make the work more manageable, genetic crosses were set up in batches of around 15 variants at a time at 25 °C. Furthermore, the negative control (no PTEN- attP2) and positive controls (PTEN-WT) were set up with every batch and it was determined that wild type human PTEN was behaving consistently over time (Fig. 3.2). PTEN mutants were tested in the same assay, to ensure that we could observe the range of suppression effects that we expected to see in our variants of unknown significance.

The tested human PTEN variants included previously characterized PTEN variants namely PTEN-C124S (dual phosphatase dead), G129E (lipid phosphatase dead) , Y138L (protein phosphatase dead) and PTEN 4A (constitutively active). The wing size (area) data for all the tested PTEN variants is presented and described below.

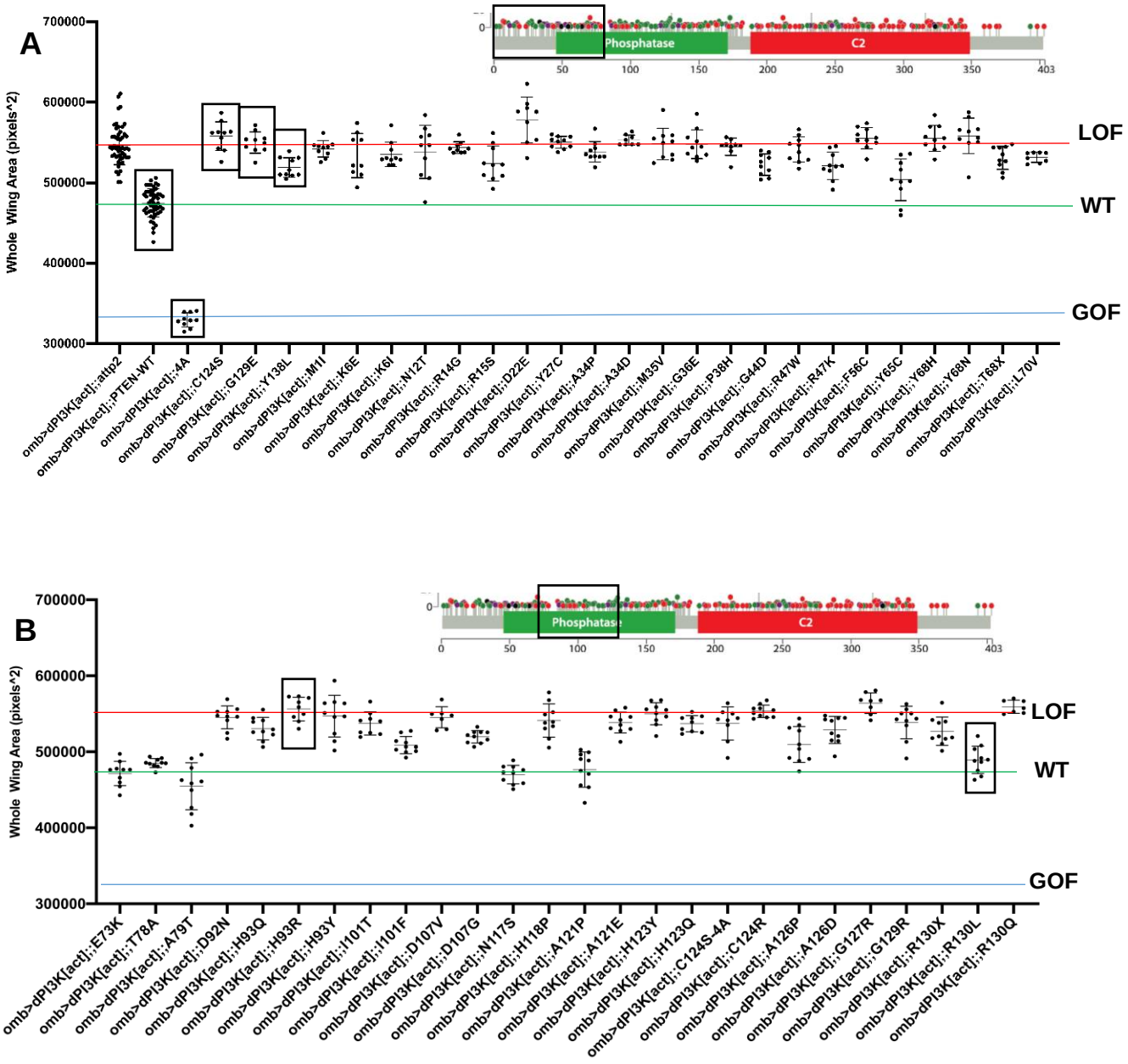
A
Whole Wing Area (pixels^2)
700000
600000
500000
400000
300000
Phosphatase
C2
0
50
100
150
200
250
300
350
403
LOF
WT
GOF
omb>dPI3K[act];;attp2
omb>dPI3K[act];;PTEN-WT
omb>dPI3K[act];;4A
omb>dPI3K[act];;C124S
omb>dPI3K[act];;G129E
omb>dPI3K[act];;Y138L
omb>dPI3K[act];;M1I
omb>dPI3K[act];;K6E
omb>dPI3K[act];;K6I
omb>dPI3K[act];;N12T
omb>dPI3K[act];;R14G
omb>dPI3K[act];;R15S
omb>dPI3K[act];;D22E
omb>dPI3K[act];;Y27C
omb>dPI3K[act];;A34P
omb>dPI3K[act];;A34D
omb>dPI3K[act];;M35V
omb>dPI3K[act];;G36E
omb>dPI3K[act];;P38H
omb>dPI3K[act];;G44D
omb>dPI3K[act];;R47W
omb>dPI3K[act];;R47K
omb>dPI3K[act];;F56C
omb>dPI3K[act];;Y65C
omb>dPI3K[act];;Y68H
omb>dPI3K[act];;Y68N
omb>dPI3K[act];;T68X
omb>dPI3K[act];;L70V

B
Whole Wing Area (pixels^2)
700000
600000
500000
400000
300000
Phosphatase
C2
0
50
100
150
200
250
300
350
403
LOF
WT
GOF
omb>dPI3K[act];;E73K
omb>dPI3K[act];;T78A
omb>dPI3K[act];;A79T
omb>dPI3K[act];;D92N
omb>dPI3K[act];;H93Q
omb>dPI3K[act];;H93R
omb>dPI3K[act];;H93Y
omb>dPI3K[act];;I101T
omb>dPI3K[act];;I101F
omb>dPI3K[act];;D107V
omb>dPI3K[act];;D107G
omb>dPI3K[act];;N117S
omb>dPI3K[act];;H118P
omb>dPI3K[act];;A121P
omb>dPI3K[act];;A121E
omb>dPI3K[act];;H123Y
omb>dPI3K[act];;H123Q
omb>dPI3K[act];;C124S-4A
omb>dPI3K[act];;C124R
omb>dPI3K[act];;A126P
omb>dPI3K[act];;A126D
omb>dPI3K[act];;G127R
omb>dPI3K[act];;G129R
omb>dPI3K[act];;R130X
omb>dPI3K[act];;R130L
omb>dPI3K[act];;R130Q

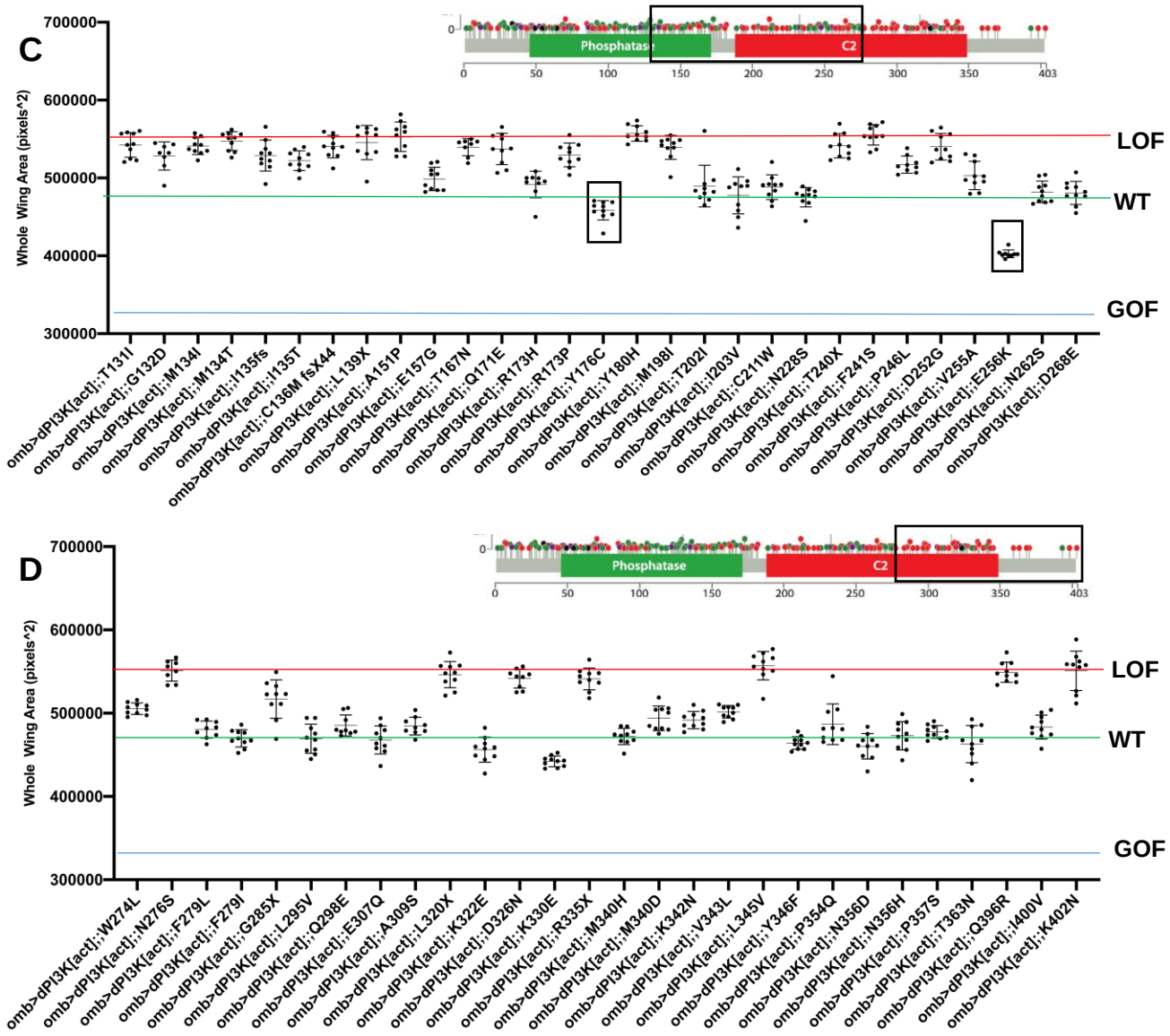

Figure 3.3 Functionalization of human PTEN variants of unknown significance. The distribution of the wing sizes (areas) of PTEN variants that have mutation in the PTEN amino acid structure. A) Wing area distribution for previously characterized PTEN variants and PTEN variants with a single amino acid substitution in amino acid residues 1 to 70 (boxed area in PTEN diagram). B) Wing area distribution for PTEN variants with a single amino acid substitution in amino acid residues 71 to 130. C) Wing area distribution for PTEN variants with a single amino acid substitution on amino acid residues 131 to 270. D) Wing area distribution for PTEN variants with a single amino acid substitution on amino acid residues 271 to 403. Lines were added to the figure to indicate PTEN variants that were loss of function or LOF (red), wild type (green) or gain of function (blue) when expressed in the dPI3K$^{[act]}$ background. Quantification of wing sizes (area) performed using Adobe Photoshop CS3. n = 10 wings per genotype analyzed for each tested PTEN variant. Wing area distribution data for each PTEN variant shown with Mean ± SD.

As mentioned in previous paragraph, the list of tested PTEN variants included previously characterized PTEN variants with distinct mutations targeting the lipid phosphatase and protein phosphatase domains. Among the tested variants was PTEN-

C124S which is a dual phosphatase dead PTEN variant, lacking both lipid and protein phosphatase activity. In the *omb>PI3K*$^{[act]}$ suppression assay PTEN-C124S was unable to suppress the PI3K large wing phenotype, while PTEN-WT suppressed PI3K-induced wing overgrowth (Fig. 3.3, A). The size of the wings from PTEN-C124S were similar in size to the negative control (no PTEN inserted attP2). Statistical comparison of the average wing size between the attP2 (no PTEN) and PTEN-C124S, revealed that there was not statistical difference between the two. Thus, as expected the PTEN phosphatase dead PTEN-C124S variant was unable to suppress the enlarged wing caused by *PI3K*$^{[act]}$ expression.

The constitutively active form of PTEN-4A showed a significantly smaller (40 ± 2.5 %) wing compared to the no PTEN control as expected in the *omb>PI3K*$^{[act]}$ suppression assay (Myers et al., 1997; Papa et al., 2015) (Fig. 3.3, A). PTEN-4A is a mutant PTEN with 4 alanine substitutions (S380A, T382A, T383A, and S385A) that eliminates the corresponding serine/threonine phosphorylation sites which are normally targeted to downregulate PTEN activity. This form of PTEN also shows enhanced membrane association (Rahdar et al., 2009). In addition, simultaneous co-expression of the PTEN cytoplasmic tail (residues 352–403) inhibited membrane association of non-phosphorylated full-length PTEN, suggesting that the C-terminal tail binds to PTEN (Rahdar et al, 2009). In addition, Ross and Gericke (2009) also demonstrated a phosphorylation-dependent specific interaction between residues 1–351 and 352–403 prevents membrane association of PTEN. Vazquez et al (2001) showed that phosphorylation of the PTEN tail negatively regulates its function as an antagonist of PI3K signaling. In summary, the PTEN-4A mutant cannot be phosphorylated in the C-tail and therefore its activity cannot be regulated. Our wing side data confirmed that PTEN-4A is gain of function mutation.

As was seen with the dual phosphatase dead PTEN variant, a lipid phosphatase dead PTEN-G129E failed to suppress the PI3K large compared to wild type PTEN in the *omb>PI3K*$^{[act]}$ suppression assay (Fig. 3.3, A). Statistical analysis showed no significance difference in the in the average wing size between PTEN-G129E and the no PTEN control, suggesting that our results are consistent with previous reports on the lack of phosphatase activity of PTEN-G129E (Brand & Perrimon, 1993; di Cristofano & Pandolfi, 2000; Gao et al., 2000). Another second variant targeting the same residue, termed PTEN-G129R, also failed to suppress the effects of PI3K with regards to

Drosophila awing size (Fig. 3.3, A). Thus, our results are consistent with previous studies that showed that PTEN-G129R is a loss of function mutation.

The last validated variant we tested in our assays was the protein phosphatase dead PTEN-Y138L. In the *omb>PI3K[act]* suppression assay this line partially rescued PI3-kinase dependent wing overgrowth. The average wing size of PTEN-Y138L was ~8.1 % larger than wild type PTEN wings when expressed in the dPI3K[act] (Fig. 3.3, A). The results suggested that PTEN-Y138L is a hypomorphic PTEN mutant and that the protein phosphatase activity is also important in rescuing the PI3K-depedent wing phenotype (i.e. larger wing).

The PTEN-C124S, PTEN-4A, PTEN-G129E and PTEN-Y138L variants displayed the expected phenotypes in the *omb>PI3K[act]* suppression assay and thus validated our assay in studying the tumor suppressor activity of other human PTEN variants of unknown significance. We then proceeded to test more than 100 PTEN variants of unknown significance and measure the wing size in the context of dPI3K[act] (Fig 3.3, A to D). In these figures, the variants are arranged in linear order corresponding to the position of the mutant amino acid within the protein sequence. Such a visualization allows us to correlate results obtained with the functional domains within the PTEN protein.

The results from our adult wing assay showed that most of the PTEN variants carrying mutations in the N-terminal tail (residues 1 – 14) (Leslie et al., 2009; Tibarewal et al., 2012) failed to rescue the enlarged *omb>PI3K[act]* wing phenotype compared to wild type PTEN (Fig. 3.3, A). This is consistent with previous results that showed that the N-terminal PIP2 binding domain play a critical role in both cellular and catalytic activity of PTEN and is required for “correct membrane orientation, cellular activity and tumour-suppressor function” Lee et al., 1999; Waite & Eng, 2002). Similarly, a majority of the PTEN variants with mutations within the phosphatase domain (residues 15 to 185) resulted in a failure to suppress the *omb>PI3K[act]* enlarged wing phenotype compared to wild type PTEN in the dPI3K[act] background, consistent with them acting as loss of function mutants (Fig. 3.3, A, B and C).

On the contrary, most of the PTEN variants with mutations in the C2 domain (residues 186 to 351) showed a similar ability to suppress the *omb>PI3K[act]* phenotype

compared to wild type PTEN, while a small number could not suppress and were functionalized as loss of function mutations (Fig 3.3, C and D). The C2 domain is found in a number of protein structures and known to be involved in membrane localization and binding to phospholipid bilayer (Stumpf & den Hertog, 2016).

Notably, expression of PTEN-E256K in the *omb>PI3K[act]* suppression assay caused the adult wings to be significantly smaller in size (~26 ± 1.2 %) compared no PTEN control (Fig. 3.3, C). In addition, PTEN-E256K wings were significantly ~13.2 % (± 1.2 %) smaller to the wild type PTEN rescued wings when expressed in the dPI3K[act] background. These results suggested that E256K might be a gain of function mutation. There are currently no studies to corroborate that PTEN-E256K increase the phosphatase activity of PTEN as seen in our assay, so this could be a novel finding worth exploring using different assays in other model organisms or human cell lines. Two PTEN variants in the C-terminal tail also carried a loss of function mutation (PTEN-Q396R and PTEN-K402N) while others remained functional similar to wild type PTEN (Fig. 3.3, D).

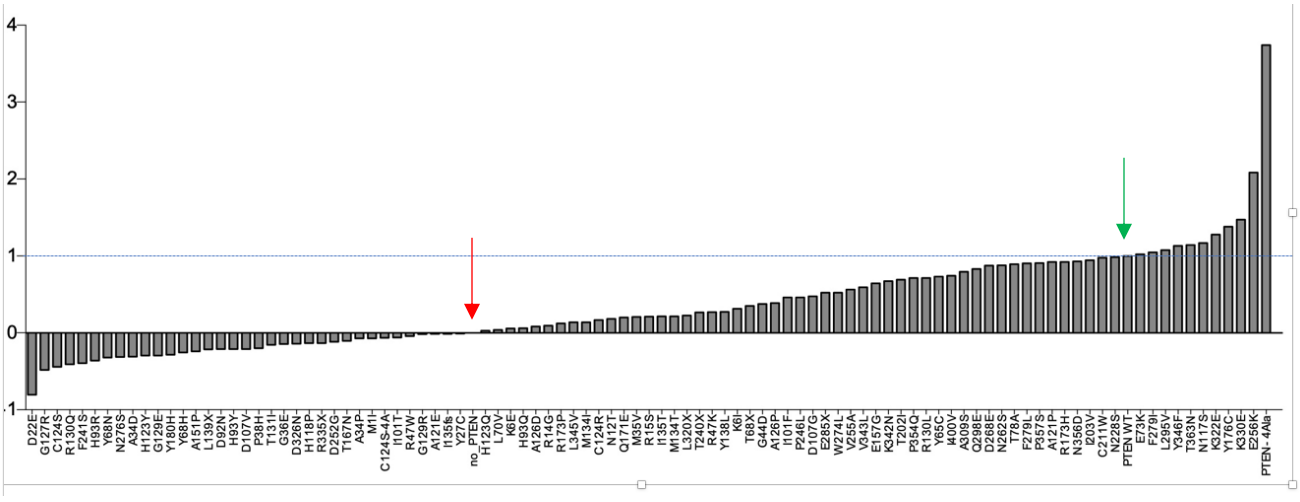

Figure 3.4 Activity based on normalized wing size data for the tested human PTEN variants expressed in the dPI3K[act] background.

The relative activity of variants compared to controls was plotted. The normalization was performed by our collaborators at UBC (see Materials and Methods). The negative control, DPI3K with no PTEN, was assigned an activity value of 0 (red arrow) and wild type human PTEN (green arrow) was assigned activity value of one.

The adult wing size data was sent to our collaborators at UBC, where they performed some data normalization and analysis to determine the activity of each PTEN variant based on wing size data (Fig. 3.4). In this assay the effects of the variants in the

omb>PI3K$^{[act]}$ phenotype were examined. The no PTEN control was assigned ‘lack of suppression’ as an activity value of 0, while wild type PTEN (suppression) was assigned an activity value of 1 (or 100% activity) based on the normalized adult wing size data in the dPI3K$^{[act]}$ background. As expected, the dual phosphatase dead PTEN-C124S showed no activity while the constitutively active PTEN-4A was more active (4X), compared to wild type PTEN (Fig. 3.4). PTEN was also more active than no PTEN control and 2x more active than wild type PTEN-WT further supporting that E256K mutation confers gain of function. Overall, the activity results are consistent with adult wing size data. PTEN variants that were assigned an activity value less than zero, had a slightly larger wing compared the dPI3K$^{[act]}$ wing alone. Therefore, this suggests LOF mutations in our assay (activated PI3K background) and activity based on the normalized wing data.

Chapter 4. Determining if PTEN controls wing growth by regulating cell growth, cell proliferation or apoptosis

The assays we developed show than genetic interaction between dPI3K and human PTEN can be used to functionalize human PTEN variants in Drosophila. Wild type human PTEN rescued PI3-kinase dependent wing overgrowth by reducing wing size. Previous studies have shown that dPTEN controls organ size by regulating cell size and cell number (Stumpf & den Hertog, 2016). Gao et al. (2000) showed that PI3K-depedent activation of Akt increases cell growth but not proliferation, yet loss of PTEN stimulates both cell growth and proliferation. This therefore suggest that PTEN might control wing size by regulating both cell growth and proliferation through PI3K/Akt -dependent and -independent manner.

The next objective of the study was to determine if the established dPI3K$^{[act]}$ and human PTEN antagonistic relationship controls wing size by regulating cell proliferation or cell size or both. Since, it be would time consuming and likely redundant study all tested human PTEN variants, only a few representative PTEN lines were selected for further analysis. The aim was to further characterize the selected PTEN variants at both the larval (third instar) and adult stages.

4.1. Further analysis of adult wing phenotypes using selected PTEN variants

In this section, I will describe the work done to further study the effect selected PTEN variants on cell size, cell number and cell death using cell biological and phenotypic analyses. The selected PTEN variants used in these follow up studies are shown in Table 4.1. These PTEN variants (PTEN-C124S, -4A, G129R and Y138L) were selected because in previous studies they were shown to carry mutations that alter the phosphatase activity of PTEN. In addition, three more PTEN variants (PTEN-H93R, -R130L and -Y176C) were selected for further analysis after discussions with our UBC collaborators. In short, the latter three PTEN-variants were chosen because they showed variability between our assays and assays done by Doug Allan's group at UBC, and we wished to characterize them further. I also included PTEN-E256K, in some of my

subsequent analysis, because it was identified as a gain of function variant in our adult wing area data. So, I wanted to further characterize of larval phenotypes was required in order to see if E256K is indeed a gain of function variant.

Table 4.1. PTEN variants selected for adult wing hair counts and imaginal wing disc PH3 staining.

PTEN Variant	Details (Reason Chosen)
attP2 – No PTEN	Negative control
PTEN – WT	Wild type Positive Control
PTEN-C124S	Dual phosphatase dead mutant
PTEN-4A	Constitutively active mutant
PTEN-G129R	Dual phosphatase dead (Initially presumed to be *only* lipid phosphatase dead similar to G129E)
PTEN-Y138L	Protein phosphatase dead
PTEN-H93R	Loss of function in wing assay
PTEN-R130L	Wild type in wing assay
PTEN-Y176C	Wild type in wing assay

The selected PTEN variants that were chosen for PH3 immunofluorescence staining and adult wing hair counting. The list comprises of previously studied variants that were used to validate our assay, plus three new variants that showed variability between the Drosophila wing assay (Verheyen Lab, SFU) compared to the Drosophila (Allen Lab, UBC) and yeast assays (Loewen lab, UBC) done by our collaborators at UBC.

The crosses between the *omb>dPI3K*$^{[act]}$ and the selected PTEN variants were repeated at 25 °C. Then adult wings were mounted, imaged and the wing area was re-calculated as described in materials and methods section of this thesis. Then, imaginal discs from third instar larva were dissected and immunofluorescence staining was done to asses proliferation (anti-PH3) and apoptosis (TUNEL).

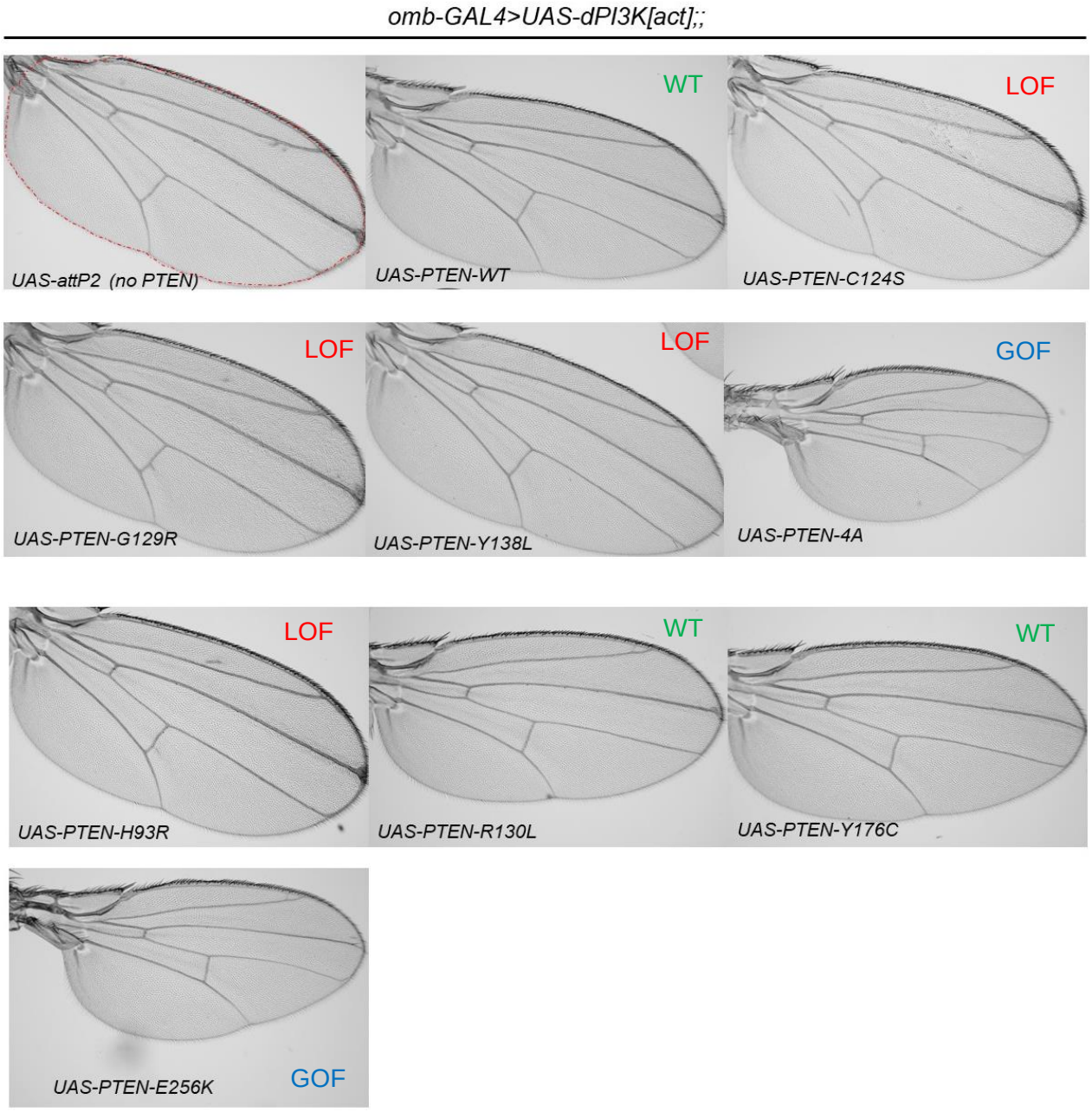

Figure 4.1 Adult wing phenotypes for selected PTEN variants.
Adult wing from females expressing dPI3K[act] with no PTEN showed enlarged wing, as previously observed. Representative adult wings from females expressing the selected PTEN variants in a dPI3K[act] background. From top left, no PTEN (attP2), PTEN-WT, PTEN-C124S, PTEN-G129R, PTEN-Y138L, PTEN-4A, PTEN-H93R, PTEN-R130L, PTEN-Y176C and PTEN-E256K. Wing phenotypes were as anticipated. Crosses were repeated at 25 °C, wings mounted and imaged as described in materials and methods.

While the quantification of the wing size for all PTEN strains was shown in the previous chapter, we now show the wing phenotypes of the selected variants (Fig 4.1).

While PTEN-E256K was not followed up on, its wings were tiny, and I wanted to show that its smaller wing area is reminiscent of a gain of function PTEN variant. In summary, the adult wing phenotypes for the selected variants were consistent with what was expected from the total wing area data presented before in this thesis.

In the previous analysis we measured the size of the whole adult wing to determine the effect of PTEN variants on the enlarged wing caused by omb-Gal4>PI3K[act]. However, according to Mao et al. (2011) *omb-GAL4* is expressed in a gradient manner perpendicular to the proximal – distal axis (Fig. 4.2, C). Given that the *omb* expression domain is highest in the center of the wing, we wanted to test whether measuring only that region of the wing might give more robust data. Thus, we sought to determine the area between the third and fifth longitudinal veins, L3 and L5, for the selected PTEN variants (Table 4.1).

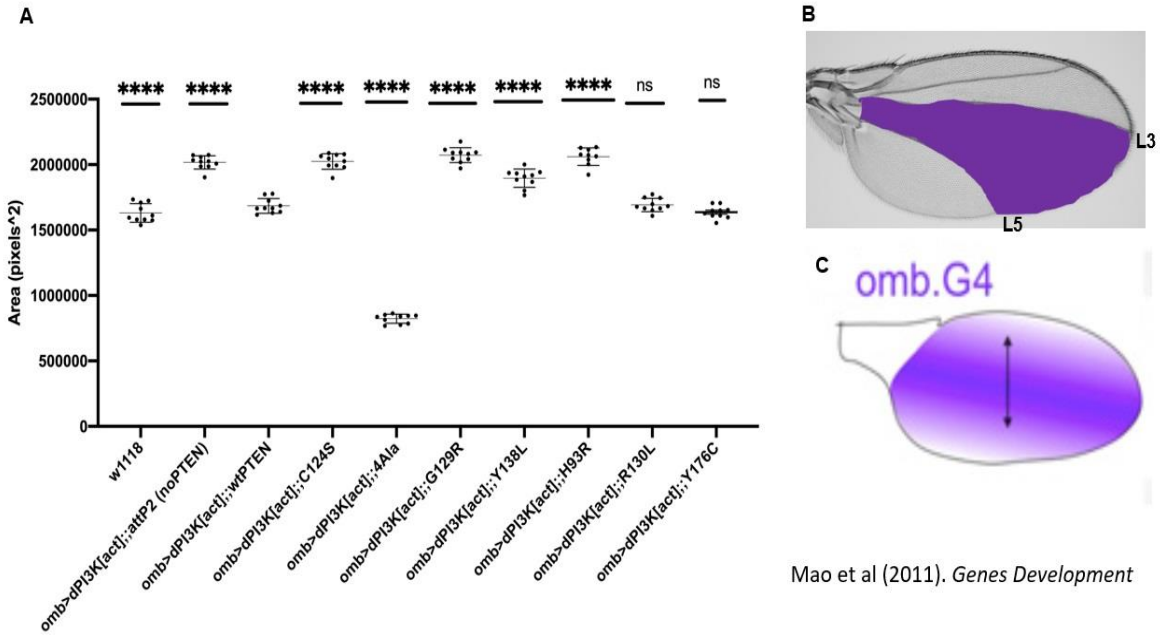

Figure 4.2 The area between the L3 and L5 of the adult wing for selected PTEN. The no PTEN control (*omb > dPI3K[act];;attP2*) showed larger area between the L3 and L5 wing veins. The area between L3 and L5 reduced when wild type PTEN is co-expressed with dPI3K[act]. As expected, loss of function mutations PTEN-C124S and PTEN-H93R increased wing area while the constitutively active PTEN-4A (or -4Ala) shown a significantly reduce area. (one-way ANOVA, Multiple Comparison: Dunnett test compared to the PTEN-WT mean)

Our results showed similar trends to the data we obtained measuring whole wings; thus, we can continue to use whole wing measurements as a readout of the PTEN activity in this assay (Fig. A.1, appendix). The negative control (no PTEN), PTEN-C124S, PTEN-G129R and H93R all failed to suppress *PI3K*$^{[act]}$- induced wing overgrowth while PTEN-WT rescued the overgrowth, compared to the no PTEN (attP2) control (Fig. 4.2, A). Among the VUS that we tested, we found that the average area between L3 and L5 for PTEN-R130L and PTEN-Y176C expression with dPI3K$^{[act]}$ was not significantly different from PTEN-WT with dPI3K$^{[act]}$. PTEN-4A had a significantly smaller wing area between L3 and L5, while PTEN-Y138L failed to suppress the enlarged wing (Fig. 4.2, A). (Stumpf & den Hertog, 2016) showed that both the lipid and protein phosphatase activity cooperate to suppress proliferation and invasion in cell-based assays. In vitro and in vivo studies on three phosphatase mutants of PTEN-C124S, -G129E and -Y138L, have been done to functionally dissect PTENs distinct phosphatase activities (Blochlinger et al., 1987; Brook & Cohen, 1996). Although rescue experiments in living organisms using all three phosphatase mutants of PTEN have not been done systematically so far, the necessity for lipid phosphatase activity of PTEN to suppress cell proliferation was confirmed definitively (Goto et al., 1999; Hendzel et al., 1997)

In zebrafish studies, Stumpf & den Hertog (2016) showed that the *Ptenb*^{Y138L} mutant decreased phosphorylated-Akt levels, similar to wild type *Pten*^{b} (zebrafish homolog of human PTEN), but did not fully “rescue” developmental effects (e.g. massive heart and abdominal edemas, craniofacial defects, aberrant pigmentation and reduced body axis extension) observed 4 days post fertilization but considerably alleviated the severity of these developmental defects. This therefore supports, that PTEN-Y138L can partially rescue phenotypes attributed to hyper-activated PI3K/Akt signalling but the protein phosphatase activity is also required for PTEN tumor suppression.

In order to determine if human wild type PTEN controls wing size by regulating cell growth or proliferation we determined the density of wing hairs on the surface of adult wings. In wildtype wings, each cell produces a single hair, and thus the number and density of hairs reflects the cell number and size. As a proxy for the whole wing, we selected a specific area of the adult wing and counted the number of hairs cells in that area to determine if larger wings are due to more cells (cell proliferation) or bigger cells (cell growth), or both.

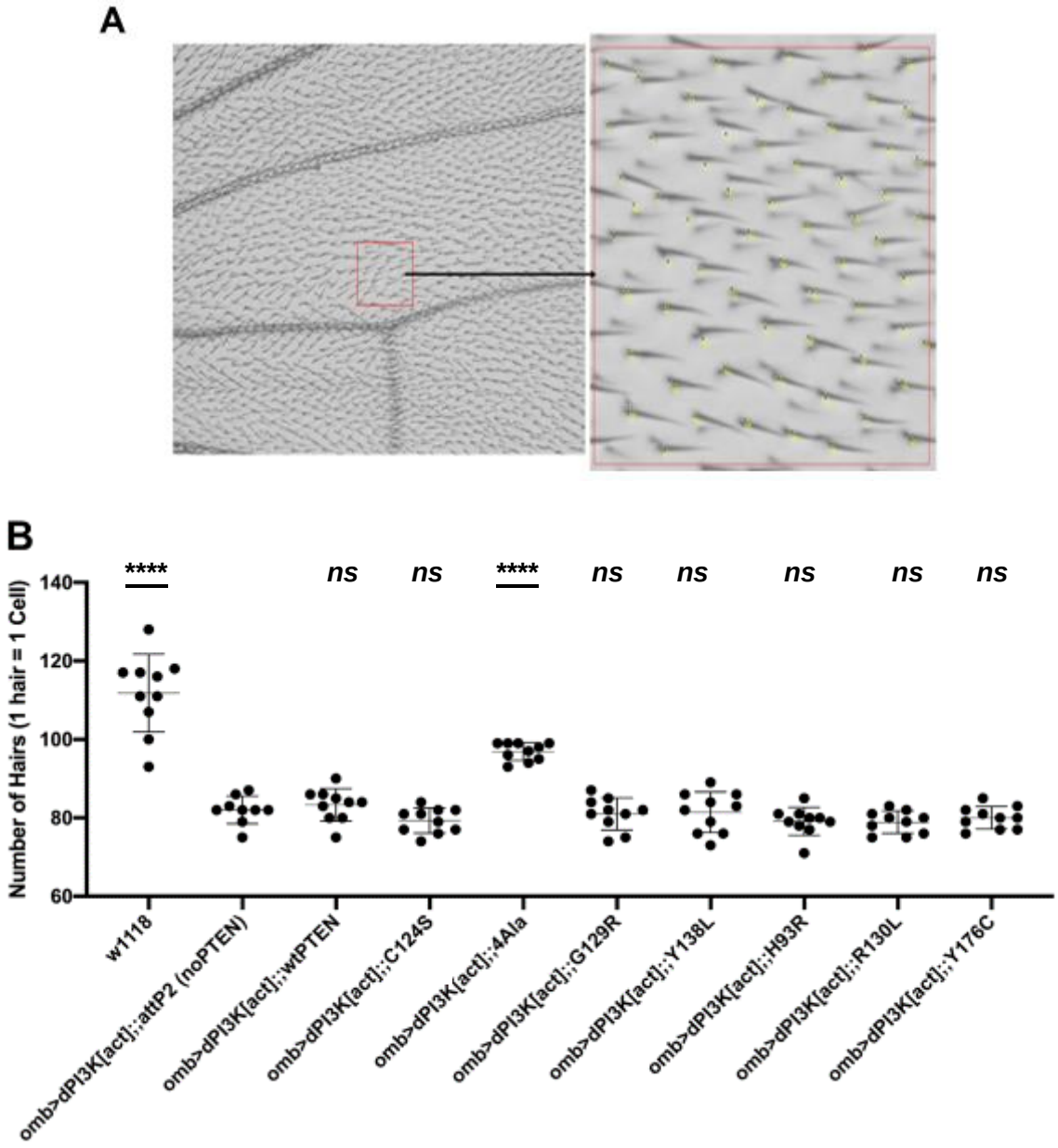

Figure 4.3 Wing hair count data for selected PTEN variants.
The number of hairs were counted in a fixed area on the adult wing to assess proliferation. (A) The selection area, inside first posterior cell above the posterior cross vein, where the hairs were counted shown in red box (left panel), and the when zoomed in for counting (right panel). (B) Number of hairs counted for the selected PTEN variants shown that there is so significant difference between the numbers of hairs between wild type and loss of function PTEN variants except for the constitutively active PTEN-4A. Hair count performed using ImageJ software. Mean ± SD, Statistical analysis computed using GraphPad Prism software (one-way ANOVA, Multiple Comparison: Dunnett test compared to the PTEN-WT mean) ****p<0.0001.

The results show that the number of hairs (and by extension, cells) when dPI3K[act] is expressed using the *omb-GAL4* driver, is significantly lower within the selected area (720 x 600 pixels^2) compared to the w^{1118} control wing. However, we previously showed that the overall dPI3K[act] wing size is significantly larger than the w^{1118} wing (see Fig. 3.1). Fewer hairs in the same size area suggested that dPI3K[act] expression increased cell size in the developing Drosophila wing (Fig. 4.3, B), while also leading to a larger adult wing overall. Therefore, this also suggests that over-expressing activated dPI3K resulted in increased wing overgrowth phenotype by increasing cell proliferation, which has been shown in previous studies (see Introduction of thesis). The average number of hairs counted for the selected PTEN variants for both loss of function and wild type variants in the *omb-Gal4>dPI3K[act]* background was not significantly different than *omb-Gal4>dPI3K[act]* (Fig. 4.3, B). The hair (cell) count data suggests equal number of cells within the selected area which means the average cell size for selected variants was similar. The only exception was PTEN-4A, which showed a significantly higher number of hairs within the selected area indicating that cells must be smaller compared to control dPI3K[act]. The average number of hairs (cells) for the constitutively active PTEN-4A is higher compared to PTEN-WT, suggesting that cell size and cell number is regulated when human PTEN is constitutively active (Fig. 4.3, B). Since the functional PTEN variants had no measurable effect on cell size in the *omb-Gal4>dPI3K[act]* background, yet did have effects on the overall size of the wing, we conclude that human PTEN likely does not control dPI3K[act] – induced wing overgrowth by regulating cell size.

Next, I wanted to characterize the selected PTEN variants at the larval stage (third instar) to determine if PTEN control wing size by regulating cell proliferation in the disc.

4.2. Characterizing larval phenotypes of selected PTEN variants

After establishing that human PTEN controls adult wing size induced by the overexpression of activated dPI3K[act] we sought to determine if this was through regulating proliferation or apoptosis. We studied late third instar larvae as this is the stage at which the wing disc morphology and proliferation is nearly complete. Larva were given colored food in order to make sure that larvae were selected at the same stage of

development for dissection and subsequent PH3 staining or GFP area calculation. As larvae begin to transition to the pre-pupal stage, they no longer ingest the colored food, so we selected larvae without colour in their abdomens. To study cell proliferation we used an antibody that detects phosphorylated Histone 3 (PH3) which is abundant in proliferating cells (Fig. 4.4). PH3 positive cells were counted using Image J (Fiji) software and statistical analyses were done, as shown below (Fig, 4.6).

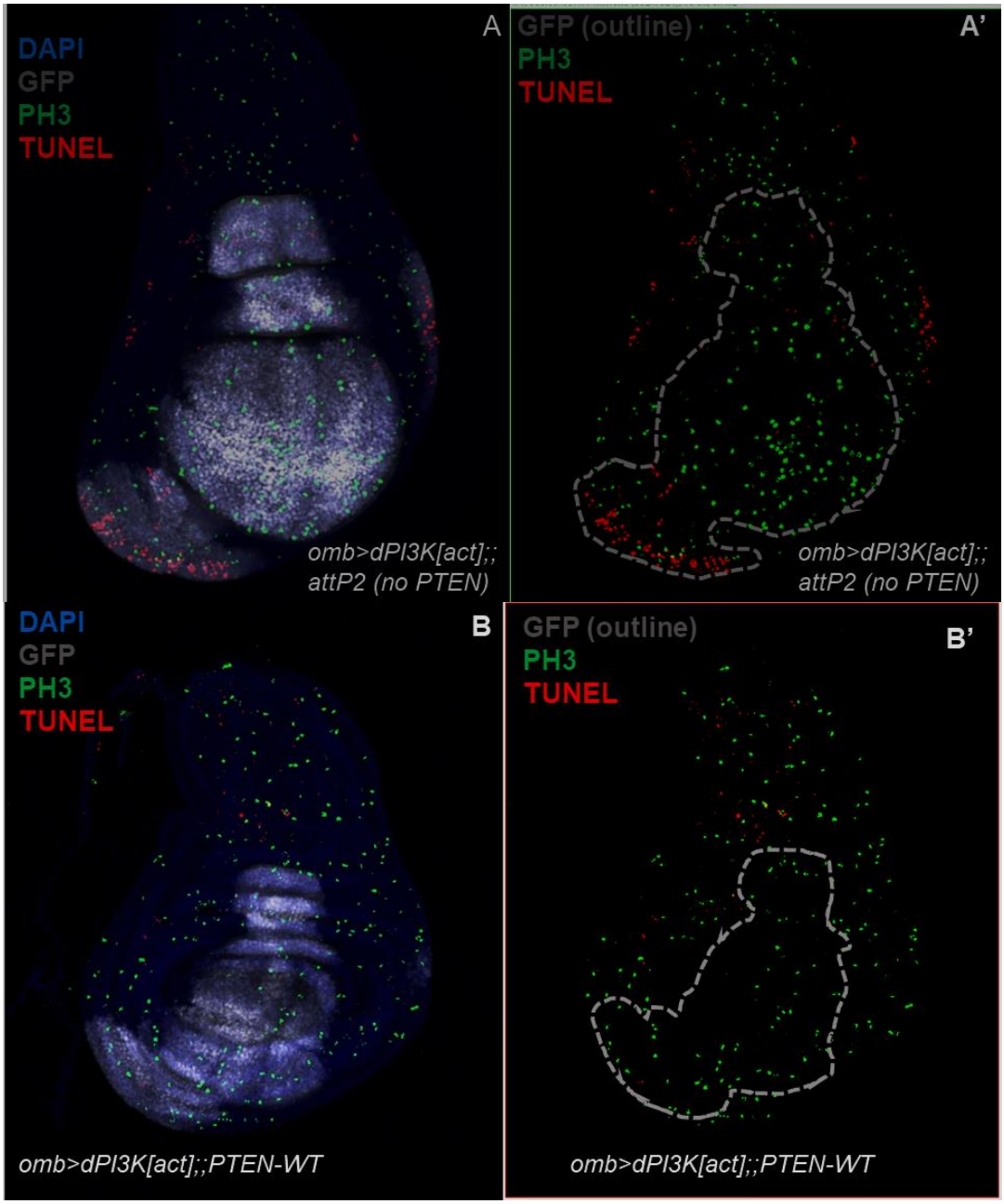
A
DAPI
GFP
PH3
TUNEL
omb>dPI3K[act];;
attP2 (no PTEN)
A'
GFP (outline)
PH3
TUNEL
omb>dPI3K[act];;
attP2 (no PTEN)
B
DAPI
GFP
PH3
TUNEL
omb>dPI3K[act];;PTEN-WT
B'
GFP (outline)
PH3
TUNEL
omb>dPI3K[act];;PTEN-WT

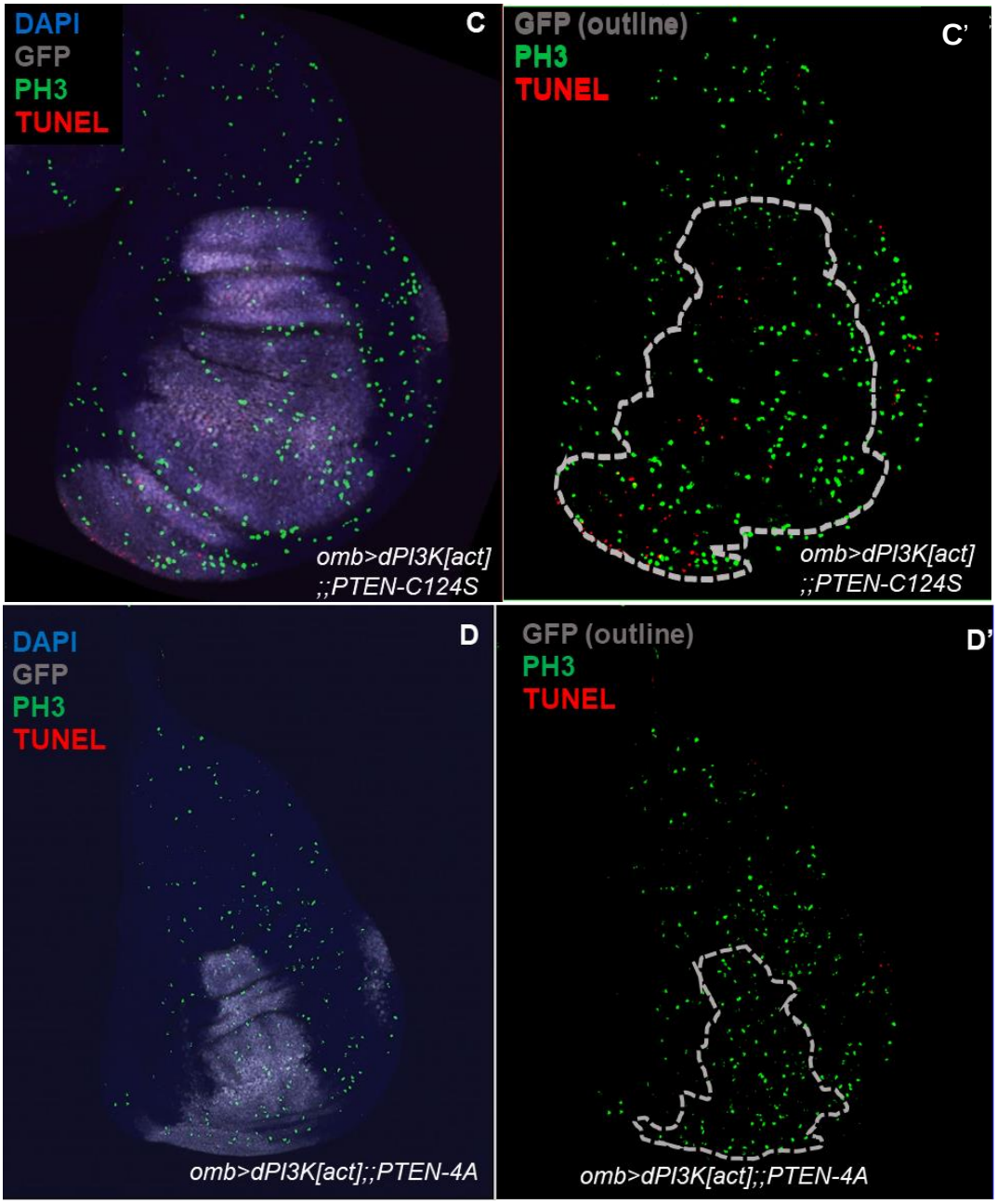

Figure 4.4 PH3 and TUNEL immunostaining results for PTEN controls expressed in the dPI3K[act] background.

Immunofluorescence staining to detect proliferation (PH3) and apoptosis (TUNEL) for the PTEN controls when expressed in a dPI3K[act] background. Representative imaginal discs dissected from larvae co-expressing dPI3K[act] and no PTEN control or attP2 (A, A'), wild type PTEN (B. B'), the dual phosphatase dead PTEN-C124S (C, C') and constitutively active PTEN-4A (D. D'). GFP reporter (grey) shows where dPI3K[act] and PTEN were expressed and DAPI (light blue) used to outline the size of the whole disc. Confocal microscopy (Nikon A1R) imaging and images processed using ImageJ. More than 10 discs were imaged per genotype.

The wing disc pouch develops into the adult wing blade as described by Aldaz et et al. (2010) (Fig. 1.1). It was observed that the GFP area, which shows all the cells expressing dPI3K$^{[act]}$ is larger with more proliferating (PH3+) cells of the wing disc when dPI3K$^{[act]}$ is expressed without human PTEN (Fig. 4.4, A). The GFP area and PH3+ cells were observed to be reduced when wild type PTEN was expressed with dPI3K$^{[act]}$ (Fig. 4.4, B). Similarly, the PI3K-induced enlarged GFP domain was not reduced or remained large when PTEN-C124S was expressed but was significantly reduced when PTEN-4A was co-expressed with dPI3K$^{[act]}$, compared to the no PTEN control (Fig. 4.4, C and D). These GFP area results were consistent with the adult wing area results shown above (Chapter 3). This suggested that PTEN likely regulates wing development at the larval stage. In order to further investigate, the number of proliferating cells were quantified within the *omb>GFP* area where dPI3K$^{[act]}$ and the selected PTEN variants (shown in Table 4.1) were expressed.

The confocal images of larval disc after PH3 immunofluorescence staining for the remaining selected PTEN variants (PTEN-G129R, PTEN-Y138L, PTEN-H93R, PTEN-R130L and PTEN-Y176C) and PTEN-E256K are shown below (Fig. 4.5). The latter was included because it was identified as a gain of function mutation in our adult wing area and so further characterization of larval phenotypes was required in order to see if E256K is indeed a gain of function mutant. Phosphorylation at Ser10 histone H3 has been tightly associated with chromosome condensation during both mitosis and meiosis (Goto et al., 1999; Hendzel et al., 1997). Therefore, immunofluorescence staining with an anti-pH3 (Ser10) antibody detects endogenous levels of phospho histone H3 from cells undergoing proliferation.

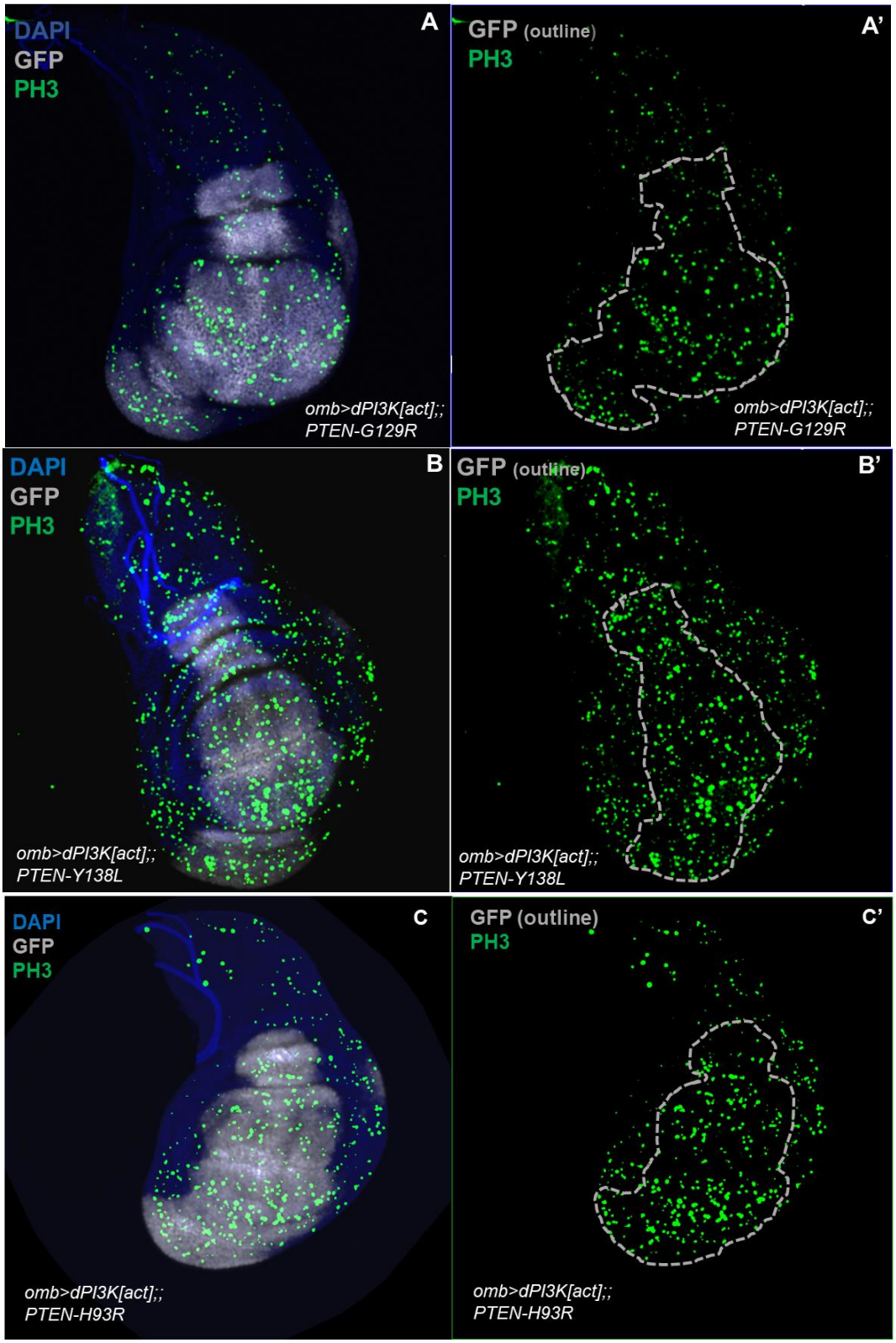
DAPI
GFP
PH3
A
omb>dPI3K[act];;
PTEN-G129R
GFP (outline)
PH3
A'
omb>dPI3K[act];;
PTEN-G129R
DAPI
GFP
PH3
B
omb>dPI3K[act];;
PTEN-Y138L
GFP (outline)
PH3
B'
omb>dPI3K[act];;
PTEN-Y138L
DAPI
GFP
PH3
C
omb>dPI3K[act];;
PTEN-H93R
GFP (outline)
PH3
C'
omb>dPI3K[act];;
PTEN-H93R

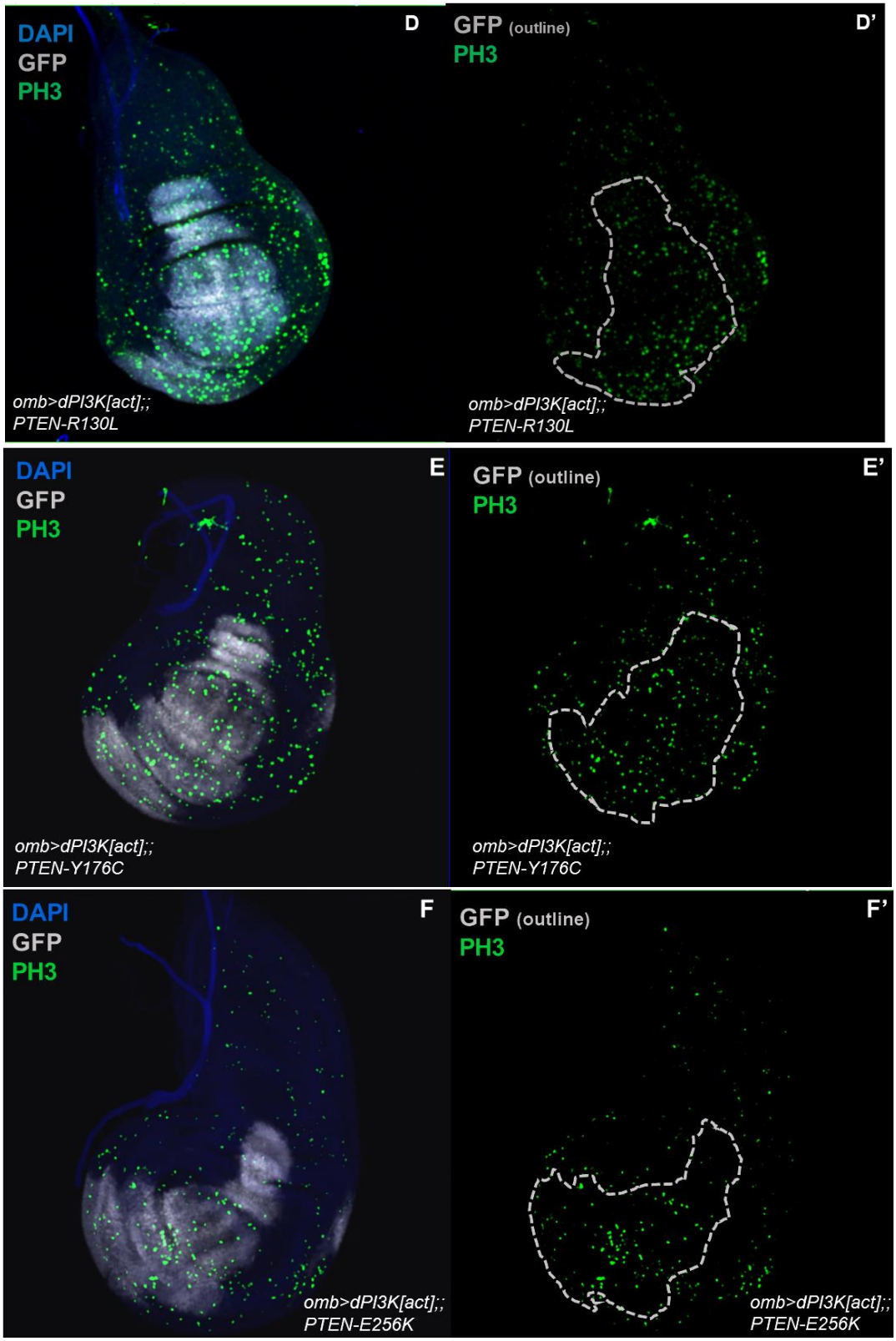
DAPI
GFP
PH3
D
omb>dPI3K[act];;
PTEN-R130L
GFP (outline)
PH3
D'
omb>dPI3K[act];;
PTEN-R130L
DAPI
GFP
PH3
E
omb>dPI3K[act];;
PTEN-Y176C
GFP (outline)
PH3
E'
omb>dPI3K[act];;
PTEN-Y176C
DAPI
GFP
PH3
F
omb>dPI3K[act];;
PTEN-E256K
GFP (outline)
PH3
F'
omb>dPI3K[act];;
PTEN-E256K

Figure 4.5 Immunoflourescence (PH3) Staining results for Selected PTEN Variants and putative gain of function PTEN variant (E256K).
PH3 staining results for previously characterized PTEN mutants that were used as extra controls to validate our assay. Immunofluorescence staining to detect proliferation (PH3) when dP13K$^{[act]}$ was co-expressed with PTEN-G129R (A, A'), PTEN-Y138L (B, B'), PTEN- PTEN-H93R (C, C'), PTEN-R130L (D, D'), PTEN-Y176C (E, E') and PTEN-E256K (F, F'). The GFP reporter (grey) shows where dPI3K$^{[act]}$ and PTEN were expressed and DAPI (light blue) used to outline the size of the whole disc. Confocal microscopy (Nikon A1R) imaging and images processed using ImageJ.

Consistently, it was observed that the GFP area, which reports cells expressing dPI3K$^{[act]}$, was not reduced when loss of function PTEN variants (PTEN-G129R, PTEN-Y138L and H93R) were co-expressed with dPI3K$^{[act]}$ (Fig. 4.5, A – C). However, the GFP area was noticeably smaller when wild type PTEN variants (PTEN-R130L and Y176C) were co-expressed with dPI3K$^{[act]}$ (Fig. 4.5, D and E). The GFP area was visibly much smaller when PTEN-E256K was co-expressed with dPI3K$^{[act]}$ compared to the dPI3K$^{[act]}$ control (Fig. 4.5, F).

After observing the differences in GFP area and PH3 staining results, we quantified both PH3+ positive cell and calculate the proportion of GFP area (%) out of the total wing disc area. The PH3+ cell count and GFP area (%) results are shown below.

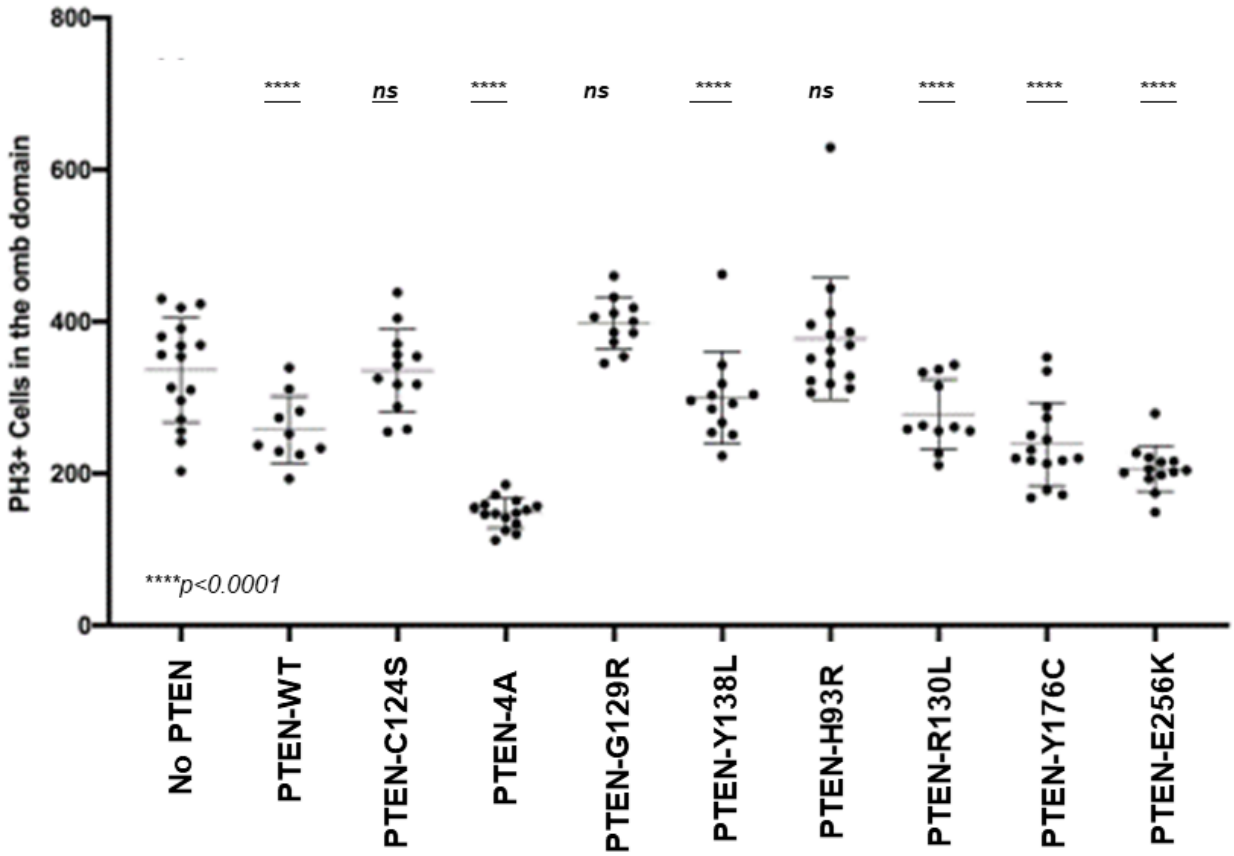

Figure 4.6 PH3 immunofluorescence staining results for selected PTEN Variants show that PTEN regulates cell proliferation in the dPI3K[act] background

Quantification of the PH3+ cells within the *omb>GFP+dPI3K[act]* region in the imaginal wing disc from the selected PTEN variants from Fig. 4.4 and 4.5. Anti-PH3 immunofluorescence staining was performed when activated Drosophila PI3K was co-expressed with selected PTEN variants. Mean ± SD, Statistical analysis computed using GraphPad Prism software (one-way ANOVA, Multiple Comparison: Dunnett test compared to the PTEN-WT mean) ** p<0.01, ****p<0.0001.

In order to see if the PTEN controls wing size by regulating proliferation, PH3+ were cells quantified within the *omb* domain in the wing disc pouch. The protocol for PH3 cell counting was developed with the assistance of Katja MacCharles (undergraduate researcher) and Stephen Kinsey (graduate student) in the Verheyen Laboratory (SFU). The number of proliferating cells in the *omb> dPI3K[act]* background was higher for the no PTEN (attP2) control, with the average number of PH3 cells approximately 336 (Fig. 4.6). The average number of PH3 cells was significantly reduced (average was approximately 257 cells) when wild type PTEN was co-expressed with dPI3K[act] (Fig. 4.6). Expression of the dual phosphatase dead PTEN-C124S and loss of function PTEN

variants (PTEN-G129R and PTEN-H93R) did not significantly reduce the number of proliferating cells in the dPI3K[act] background (Fig. 4.6). On the contrary, expression of wild type PTEN variants (PTEN-R130L and PTEN-Y176C) or the constitutively active PTEN-4A significantly reduced the number of proliferation cells within the specific omb>GFP region in the wing discs, compared to the dPI3K[act] control (Fig. 4.6). The protein phosphatase dead PTEN-Y138L significantly reduced the number of PH3+ cells compared to the *omb>dPI3K[act]*, but the number of PH3 cells was significantly higher compared to the effect of PTEN-WT on dPI3K[act] (Fig. 4.6). This was consistent with the adult wing size data which showed PTEN-Y138L to be a hypomorphic mutant. Overall, these results were consistent with our previous results that showed that human PTEN controls wing size by regulating cell proliferation.

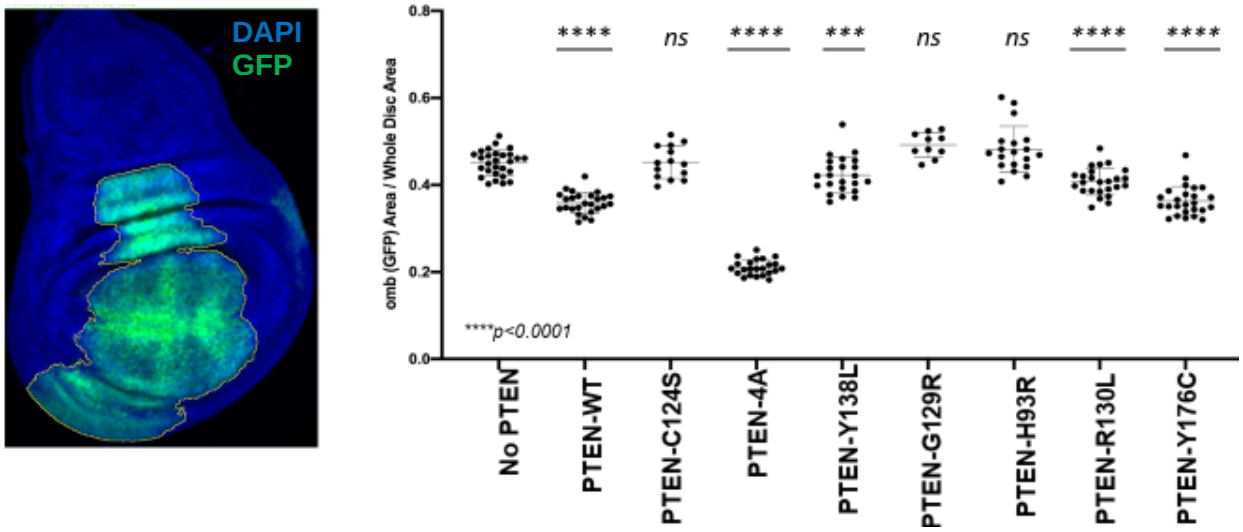

Figure 4.7 Ratio of GFP Area is larger when no PTEN or Loss of function PTEN variants are expressed with dPI3K[act].

The average proportion of omb>GFP+dPI3K[act] for selected PTEN variants compared to PTEN-WT. Mean ± SD, n = 10+ wing discs per genotype, Statistical analysis performed using GraphPad Prism (one-way ANOVA, Multiple Comparison: Dunnett test compared to the PTEN-WT mean) **0 p<0.001, ****p<0.0001.

Another way you can quantify proliferation is by measuring the size of the *omb* domain (reported by GFP) in which PI3K and PTEN are being expressed. In order to account for differences in imaginal discs size within and/or between genotypes, the size of the GFP area was reported as a proportion (%) of the whole disc area. That is

because even if third instar larvae were selected (using colored food as stated above) for the selected variants, one would expect different-sized discs to have slight differences in GFP area. If there is more proliferation (where PI3K[act] is expressed) you will expect to get a larger GFP area, while if that is suppressed (when PI3K[act] and by PTEN are co-expressed) the size of the GFP area will be suppressed.

Our results showed that the size (percentage) of the dPI3K-induced GFP area, which is a reporter for cells expressing dPI3K[act], was significantly suppressed when PTEN-WT was co-expressed with dPI3K[act] compared to the no PTEN control (Fig. 4.7). The average percentage of dPI3K-induced GFP area was not significantly different when PTEN-C124S, PTEN-G129R and PTEN-H93R were expressed compared to the no PTEN control (Fig. 4.7). The average size of GFP area is significantly smaller when PTEN-4A and PTEN-E256K were expressed in the dPI3K[act] background (Fig. 4.7). On the contrary, the percentage of dPI3K-induced GFP area per disc was significantly reduced when PTEN-Y138L, PTEN-R130L and PTEN-Y176C were expressed in a *dPI3K[act]* background compared to the no PTEN control (Fig. 4.7). Overall, these results suggest that wild type PTEN or wild type PTEN variants can suppress the proliferation of cells expressing *dPI3K[act]* in the imaginal wing disc. Previous studies showed that PTEN regulates cell proliferation during Drosophila wing (Gao et al, 2000) and eye (Huang et al, 1999) development. Huang et al (1999) proposed that PTEN regulates cell proliferation by causing cell cycle arrest at the G2 or G2/M phase of the cell cycle.

After showing that human PTEN controls wing development at the larval stage by regulating cell proliferation in a dPI3K[act] background, we wanted to see if PTEN has a role in apoptosis as suggested by previous studies(Khwaja, 1999; Morris et al., 2005). TUNEL staining was performed on the four PTEN controls i.e. no PTEN (attP2), PTEN-WT, PTEN-C124S and PTEN-4A for the same reasons stated above. Terminal deoxynucleotidyl transferase dUTP nick end labeling (TUNEL) staining highlights fragmented double-strand DNA breaks and detects cells undergoing cell death. TUNEL detects fragmented DNA by transferring a labelled terminal deoxynucleotide (dUTP) to the 3'-hydroxyl termini of DNA double strand breaks from cells undergoing cell death or apoptosis (Gorczyca et al., 1993; Negoescu et al., 1998). It was observed that there was more cell death (TUNEL+ cells) in a dPI3K[act] background in the no PTEN discs compare to the PTEN-WT imaginal discs suggesting that PTEN expression may regulate apoptosis (Fig. 4.8). PTEN-C124S also showed more TUNEL+ cells, similar to the no

PTEN control, whilst there were hardly any TUNEL+ cells observed when PTEN-4A was co-expressed with dPI3K[act] (Fig. 4.8). Quantification of the TUNEL+ cells is shown below.

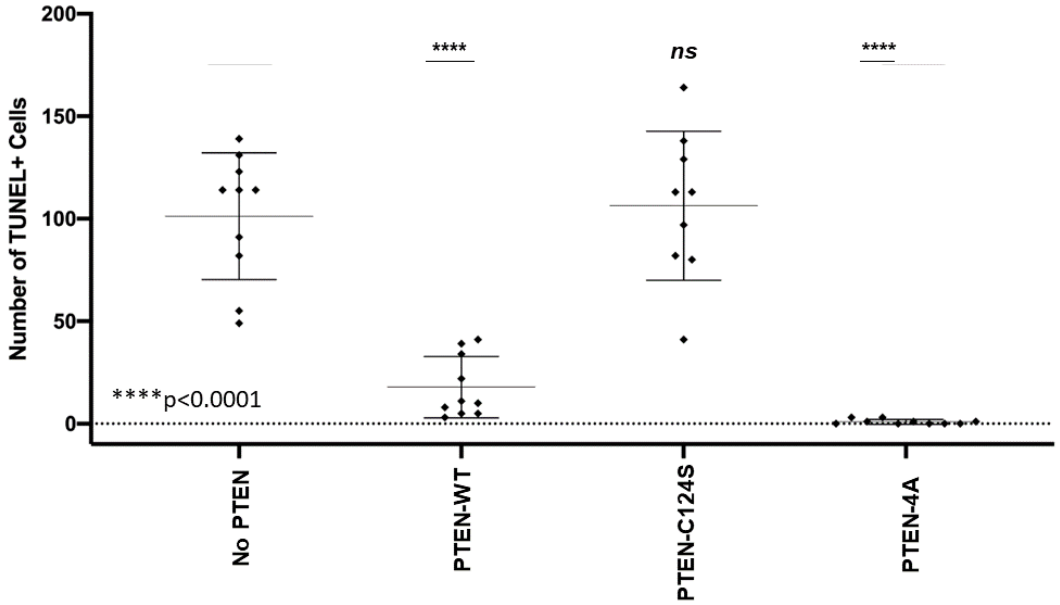

Figure 4.8 Quantification of TUNEL+ cells to assess apoptosis in the *omb-GAL4* expressing region in the dPI3K[act] background.

TUNEL staining was performed when activated PI3K was co-expressed with the PTEN-WT, -C124S and -4A and compared to the no PTEN control. Quantification of TUNEL+ cells performed using ImageJ software. There were 10 disc per genotype. ****p<0.0001.

TUNEL staining revealed that there was more cell death in the *omb* region of the wing disc (3rd instar larva) in the *omb>dPI3K[act]* background when there was no PTEN (negative control) (Fig. 4.8). Cell death was significantly decreased when PTEN-WT was expressed in the dPI3K[act] background, compared to the no PTEN control (Fig. 4.8). Expression of the phosphatase dead PTEN-C124S failed to suppress cell death when co-expressed with dPI3K[act], similar to the no PTEN control (Fig. 4.4, C' and 4.8). Interestingly, this cell death was mostly concentrated in the anterior side of the wing disc (near the bottom) for both the no PTEN and PTEN-C124S, with very little cell death observed in other parts of the omb region (Fig. 4.4, A' and C'). Lastly, cell death was almost undetected when PTEN-4A was expressed, in the PI3K[act] background, compared to the no PTEN control (Fig 4.4, D' and 4.8.). In fact, only four out of the ten quantified discs had 1 to 3 cells that were stained with TUNEL. These results suggest that PTEN may play role in regulating cell death through its antagonistic effect on activated PI3-kinase.

Chapter 5. Investigating possible PI3-kinase independent roles of PTEN in other signalling pathways.

The PIP3 lipid substrate for PTEN is well established but identification of the protein substrates for PTEN had so far lagged (Lento et al., 2012). There has been an increasing interest in studying PI3K/Akt-independent functions of PTEN. Protein levels and activities of PTEN have been shown to be regulated through binding with several PTEN-binding proteins (Naderali et al, 2018). The identity of the protein substrates of PTEN remains to be determined definitively. The underlying hypothesis is that while the human PTEN variants under study may have reduced activity relative to PI3K (show loss of function PTEN effects in our assays) it is possible that they may play a role in regulating other oncogenic pathways, such as those described below.

5.1. Wingless (Wnt) signaling

The Wingless/Integrated (Wnt) signaling pathway is evolutionary conserved and controls many events during the embryogenesis and adult homeostasis by regulating cell morphology, proliferation, motility and cell fate (Nelson & Nusse, 2004; Veeman et al., 2003). Our current knowledge of the canonical Wingless/Integrated (Wnt) signaling pathway emerges from studies of the Wingless (Wg) pathway in *Drosophila melanogaster* over the last three decades (Kikuchi, 1999). There are at least three distinct Wnt pathways: the canonical β-catenin pathway, planar cell polarity pathway, and Ca2+ pathway (Kikuchi, 1999).

In the canonical Wnt pathway, the absence of the Wnt/Wg ligand, levels of cytoplasmic β-catenin/Armadillo (Arm), the transcriptional effector of the pathway, are kept low through its constitutive degradation by a protein destruction complex composed of Axin, APC, GSK3/Zw3, and CK1 (Lento et al., 2012). As a result, Wnt/Wg-regulated genes are kept off by the DNA-binding transcription factor T-cell factor (Tcf) with the aid of other transcriptional corepressors (Kikuchi & Kishida, 2006). Binding of the Wnt/Wg ligand to its coreceptors, Frizzled2 (Fz2) and LRP/Arrow (Arr), initiates a sequence of cytoplasmic events that leads to the Dishevelled *(*Dsh)–mediated inactivation of the protein destruction complex, thereby allowing stabilized β-catenin/ Arm to translocate to

the nucleus, where it binds Tcf to direct the activation of Wnt/ Wg-target genes (Persad et al., 2016). Thus, in the canonical Wingless pathway, Wnt increases the stability of β-catenin, which stimulates Tcf/Lef mediated gene expression (Piddini & Vincent, 2009; Schneider et al., 2012). Wnt-regulated processes have been identified to be aberrantly regulated in a myriad of diseases, ranging from developmental disorders to cancers (Shimizu et al., 2008).

The PI3K/PTEN pathway has been shown to regulate subcellular localization of β-catenin (or Armadillo) in Wnt signaling (Huang et al., 2005; Range, 2012). The Wingless signalling pathway was tested using transcriptional target genes that were discussed in previous studies, namely *axin* and *distal-less* (Shimizu et al., 2008).

5.2. Notch signalling

The Notch signalling pathway is another highly conserved signalling pathway that plays a critical role in development and diseases (Shimizu et al., 2008). Notch receptors directly transduce extracellular signals at the cell surface into changes in gene expression that regulate differentiation, self-renewal, proliferation and apoptosis (Shimizu et al., 2008). Notch signaling was first identified in Drosophila and the pathway in Drosophila is relatively simple, which makes studying the fundamental principles of Notch regulation and function in in Drosophila very useful (Blochlinger et al., 1987; Brook & Cohen, 1996). In the canonical Notch pathway, activation of the Notch transmembrane receptor is initiated by the binding of Delta or Serrate (Jagged in mammals) to Notch resulting in two sequential proteolytic cleavage events (Shimizu et al., 2008). The cleaved Notch intracellular domain (NICD) is released into the nucleus where it interacts directly with the DNA-binding protein CSL [CBF-1/Su(H)/LAG-1] and the co-activator Mastermind to promote transcription(de Celis & Bray, 1997).

Previous immunofluorescence staining studies have shown that Cut and Wg are Notch pathway targets expressed at the dorsal/ventral boundary of the wing disc in response to pathway activation (Shimizu et al., 2008). Most studies have shown that *wg* and *cut* are upregulated when Notch signaling is activated, as detected with anti-Cut and anti-Wg antibody staining (Shimizu et al., 2008)(Komiya & Habas, 2008; Wodarz & Nusse, 1998)). However, in this study, I decided to measure the activity of Notch

signaling by measuring the mRNA levels of these two target genes, in the absence or presence of wild type human PTEN

According to (Lento et al., 2012) NOTCH1 regulates PTEN expression and the activity of the PI3K-AKT signaling pathway in normal and leukemic T cells. Notch signaling and the PI3K-AKT pathway synergize in vivo in a Drosophila model of Notch-induced tumorigenesis, and mutational loss of PTEN is associated with resistance to NOTCH1 inhibition in human lymphoblastic anemia (Tumaneng et al., 2012).

5.3. **Hippo Signaling**

The Hippo signaling pathway has been shown to be involved in regulating organ development and tumorigenesis in Drosophila and other mammalian species (Xu et al., 1995; Yu & Guan, 2013). The canonical Hippo pathway was originally discovered in a series of mosaic screens for genes in Drosophila whose removal augmented cell proliferation and cell growth (Blaquiere et al., 2018). Dysregulation of the Hippo signaling pathway has been shown to play an important role in tumorigenesis and organ development mainly though regulation or playing a part in the regulation of cell growth, proliferation and apoptosis (Huang et al., 2005).

Yorkie, the major downstream effector of the Hippo pathway, translocates into the nucleus to activate transcription of target genes e.g. Drosophila inhibitor of apoptosis protein 1 (*Diap1*) and is functionally inhibited by Hippo signaling (Harvey & Tapon, 2007; Pan, 2007). According to Shimizu et al (2008), loss of function of any of these genes (Mats and Wts/Lats) results in the upregulation of *cyclin E* and *Diap1* leading to cell over-proliferation and defective cell death in mosaic tissues. Thus, *Cyclin E* and *diap1* are considered to be two downstream targets of the Hpo/Wts pathway (Csibi & Blenis, 2012).

The Hippo and PI3K/Akt pathways were shown to cross talk to regulate cell proliferation and apoptosis. YAP (Yes associated protein), the main downstream target of the mammalian Hippo pathway may regulate organ growth by activating the mammalian target of rapamycin (mTOR)-a major regulator of cell growth (Blochlinger et al., 1987; Brook & Cohen, 1996). YAP (mammalian homolog of Yorkie) downregulates PTEN by inducing miR-29 to inhibit PTEN translation revealing a possible functional link

between Hippo and PI3-kinase signalling in regulating cell size, tissue growth and organ growth (Shimizu et al., 2008).

Since Hippo signaling has been shown to be involved in regulating organ development and tumorigenesis is conserved in Drosophila and other mammalian species (Shimizu et al., 2008). I wanted to test pathway activity using qRT-PCR to measure the mRNA levels of *Diap1* and *cyclin E* which had been shown to be transcriptional target genes of this pathway by previous studies (Shimizu et al., 2008).

5.4. JAK/STAT signaling

The Janus kinases (JAKs) and signal transducers and activators of transcription (STATs) signal transduction cascade, first identified in mammalian systems, is important in the transduction of a variety of cytokines and growth factor signals(Arbouzova & Zeidler, 2006; Binari & Perrimon, 1994; Hou et al., 1996). JAK/STAT signalling is an evolutionary conserved signal transduction pathway with characterized structural and functional homologues found in vertebrate and invertebrates (Zeidler et al., 2000). JAK/STAT signalling is required at different stages of Drosophila development and plays a role to control of proliferation during the early embryonic and larval development (Zeidler et al., 2000).

In the canonical JAK/STAT signalling pathway, binding of external ligand causes transmembrane receptors to dimerize bringing two JAK molecules into juxtaposition where they transphosphorylate one another (Zeidler et al., 2000). Phosphorylated (activated) JAKs then phosphorylate tyrosine residues (in the C-terminal region) their associated receptors causing normally cytosolic STAT molecules to bind to the receptor complex via their SRC homology 2 (SH2) domains (Hou et al., 1996). The STAT molecules activated by JAK-mediated phosphorylation then either homo- or hetero-dimerize and are translocated into the nucleus (Binari & Perrimon, 1994). Activated STAT dimers translocate to the nucleus where they bind DNA target sites and activate transcription (Hou et al., 1996). The JAK/STAT pathway is conserved activated similarly in Drosophila and cloning studies identified *unpaired (upd*) as a ligand for the Drosophila JAK/STAT pathway (Harrison et al., 1998). The Drosophila JAK homolog is *hopscotch (hop)* (Blochlinger et al., 1987; Brook & Cohen, 1996) and the *Drosophila* STAT homologue is Stat92E (Pai et al., 1997). Activity of the JAK/STAT signalling pathway

was tested by measuring the expression of transcriptional target genes that were discussed in previous studies*; soc36E* and pair rule gene *even-skipped* (Johansen et al., 2003).

JAKs can phosphorylate and recruit other receptor tyrosine kinases including PI3-kinase which is an antagonist of PTEN. For example, JAK phosphorylation of insulin receptor substrate (IRS) and p85 (PI3K regulatory subunit), results in the activation of the phosphoinositide 3-kinase (PI3K) pathway. While there have not been direct links between PTEN and JAK/STAT signaling, the JAK/STAT signaling pathway was included since because it is a key signaling pathway acting in development. Furthermore, Dysregulation of the JAK/STAT pathway is associated with multiple human malignancies including haematopoietically derived cancers (Arbouzova & Zeidler, 2006).

5.5. Purpose of the Study

We have a number of Drosophila tumor models in our lab (Verheyen Lab, SFU) carrying transgenes that result in the dysregulation of their respective cell signalling pathways (Blaquiere et al., 2018). I investigated whether expression of any of the selected PTEN variants impacted the activity of these signaling pathways. I introduced pathway transgenes into the omb>PI3K[act] genetic background and then I used quantitative reverse transcription followed by polymerase chain reaction (qRT-PCR) to measure the expression levels of the respective target genes (Table 5.1). Table 5.1 Investigating possible roles of PTEN independent of PI3-Kinase signaling.

Table 5.1 Investigating possible roles of PTTEN independent of PI3-Kinase signaling.

Signaling Pathway	Transgenes (Chromosome)	Target genes tested (RT-PCR)
Wingless/Integrated (Wnt)	*UAS-Arm-S10 (II)*	*Axin* and *distal less (dll)*
Notch	*UAS-N[nucl] (III)*	*Wingless (wg)* and *Cut*
Hippo	*UAS-Yki.S168A.GFP (II)*	*Diap1* and *Cyclin E*
JAK/STAT	*UAS-Stat92E.GFP (II)*	*Socs36E* and *eve-skipped (eve)*

Investigating the effect of expressing selected PTEN variants, independent of activated PI3-Kinase, on other signaling pathways (first column) in the presence of transgenes (second column) that have been shown (Blaquiere et al., 2018) to result in dysregulation their respective signaling pathways. Pathway activity, when PTEN variants are expressed with respective transgenes, will be determined by measuring expression (mRNA levels) of target genes (third column) via qRT-PCR.

The transgenes of interest were UAS-Arm^{S10} for Wingless signalling, UAS-N[nucl] for Notch signalling, UAS-Yki.S168A for Hippo signalling and UAS-Stat92E for JAK/STAT signalling. UAS-Arm^{S10} encodes a truncated Armadillo (Arm) protein, missing amino acid residues 34 to 87 (and tagged with Tag:MYC) expressed under the control of UAS regulatory sequences resulting in constitutively active Wg/Wnt signalling (Davidson et al., 2010; Johansen et al., 2003). Arm^{S10} is more stable than wild-type Armadillo, since it is less rapidly targeted for degradation (Ross & Gericke, 2009; Vazquez et al., 2001).

UAS-Yki.S168A is mutant form of the Drosophila homolog of mammalian Yes associated protein (YAP) called Yorkie (Yki). The Ser168 residue is critical for negative regulation of Yki by phosphorylation by Wts or Akt. This phosphorylation allows it to interact with cytoplasmic 14-3-3 proteins, which then prevents its nuclear localization (Basu et al., 2003). Therefore, Yki-S168A, where the serine 168 residue is changed to alanine does not get phosphorylated and thus localizes in the nucleus where it activates transcription of Hippo signalling pathway targets (Go et al., 1998).

UAS-N[nucl] or nuclear Notch contains a UAS regulatory sequences driving expression of a constitutively active form of Notch which lacks the extracellular domain including the signal peptide and transmembrane domain (Zacharioudaki & Bray, 2014).

Expression of N[nucl] therefore ensures that the Notch signalling pathway is always activated.

UAS-Stat92E (signal-transducer and activator of transcription protein at 92E) is a strain which has an UAS regulatory sequence driving expression of a wild type Drosophila STAT (Stat92E) gene also known as *marelle* (Sonoshita & Cagan, 2017). The Janus kinase-STAT pathway is vital to Drosophila early development.

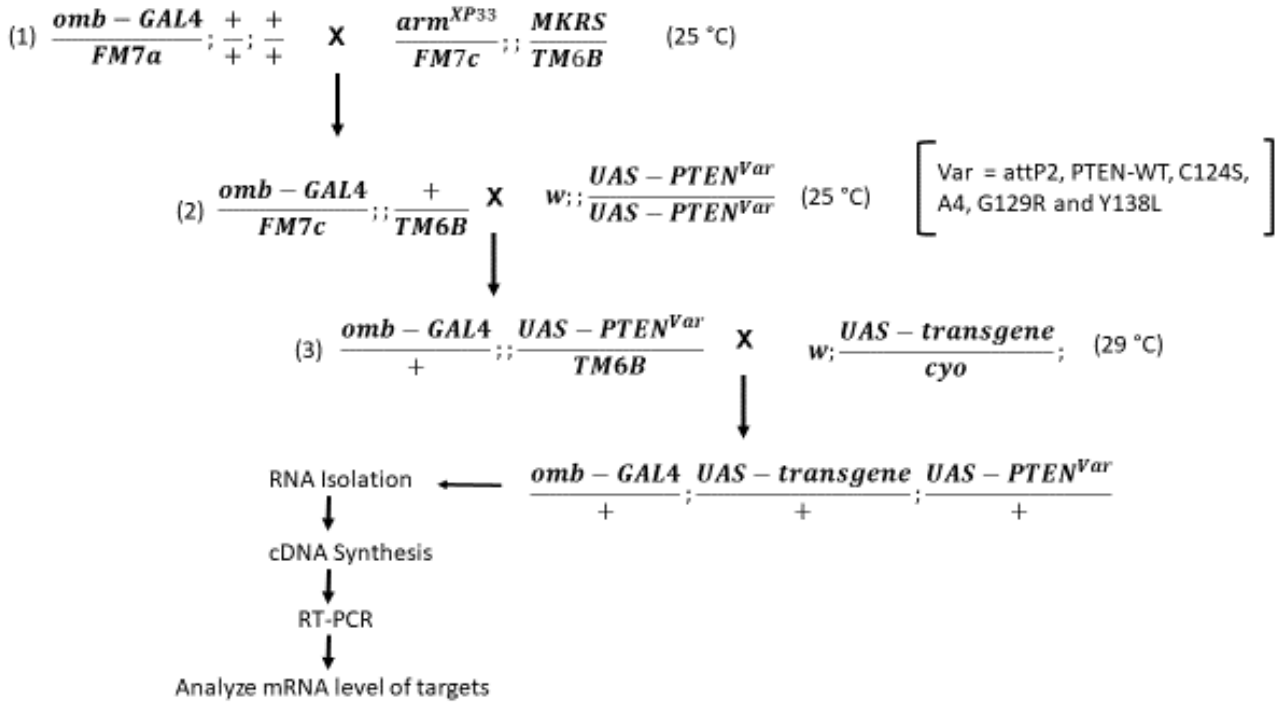

Figure 5.1 Summary of the strategy and workflow in order to generate fly stocks to investigate possible PI3-kinase independent roles of PTEN in other signalling pathways.

The first steps in this analysis involved generation of an *omb-Gal4* fly stock balanced on the first and third chromosome, which will allow me to track the chromosomes through the subsequent crosses (Fig. 5.1, step (1)). The *arm* loss of function mutation in the balancer strain is coincidentally present in this strain and I selected against it in subsequent generations. The balanced *omb-Gal4* stock was then crossed individually to UAS-PTEN transgenes as indicated in the figure (PTEN-WT,-C124S, -4A, -G129R and –Y138L) (Figure 5.1, step (2). The omb-Gal4; UAS-PTEN stocks were then crossed to stocks to activate the individual pathways, as described above (Figure 5.1, step (3)). This generated the desired genotypes in which both human

PTEN variants, as well as pathway activators were expressed in the *omb-Gal4* expression domain. Finally, RNA was isolated from female third instar larval heads (which contain the discs) using RNeasy kit (Qiagen) followed by cDNA synthesis and RT-PCR to measure the activity of the Wingless, Hippo, Notch and JAK/STAT signalling pathways. This was done so that the wing discs were included in RNA isolation without the rest of the larva, for example the gut. In future studies it would be more specific if wing disc were dissected and about 15 to 20 discs used to prepare the RNA samples.

To do this, quantitative qRT-PCR was used to measure pathway activity by determining the differences in gene expression when the transgenes (Table 5.1) were over-expressed. After establishing that the activity of the Wnt, Hippo, Notch and JAK/STAT, signalling pathways can be measured with RT-PCR we will over-express these oncogenes in the absence or presence of human PTEN-WT and selected variants (Fig. 5.1).

Next, I also measured these target genes when previously studied PTEN variants (WT, C124S, 4A, Y138L and G129R) were expressed using *omb-Gal4* in the absence of constitutively active *dPI3K*$^{[act]}$. Lastly, I looked at the activity of these pathways when the selected PTEN variants were expressed in the presence of constitutively activated *dPI3K* (since I had the RNA samples stored at -80 °C). Measuring the activity of these pathways in a PI3-kinase background allowed me to ask whether any observed results were due to changes in PI3-kinase signalling.

5.6. RT-PCR results

The Wnt, Hippo, Notch and JAK/STAT signaling pathways were chosen in my study because they (i) play a critical role in growth and development, (ii) we have shown in our lab that expressing these transgenes results in the tissue overgrowth compared to control sample (*omb>RFP*) and (iii) there have been some previous studies links with PI3K/Akt/PTEN signaling (Chapter 5.2 – 5.5). The fold change in mRNA levels (thus gene expression) was computed using the comparative Delta-Delta Ct ($2^{-\Delta\Delta Ct}$) method as previously described in Livak & Schmittgen (2001) and the housekeeping gene used was *drp49*. Significant change in fold mRNA levels was considered to be less than 0.5-

fold (suppression) or greater than 1.5-fold (more expression), as per the accepted standard (Morris et al., 2005).

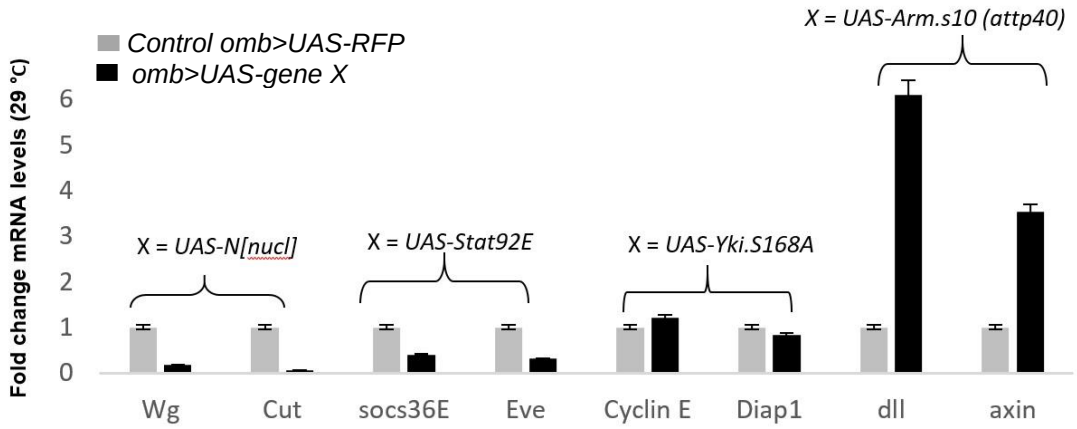

Figure 5.2 Over-expressing transgenes to determine activity of signalling pathways

Measuring the activity of the other signaling pathways when the respective transgene was over-expressed. Notch signaling activity was determined by measuring the mRNA levels of *Wg* and *Cut.* JAK/STAT signaling activity was determined by measuring the mRNA levels of *socs36E* and *Eve.* Hippo signaling activity was determined by measuring the mRNA levels of *cyclin E* and *Diap1.* Notch signaling activity was determined by measuring the mRNA levels of *Wg* and *Cut.* Wnt signaling activity was determined by measuring the mRNA levels of *dll* and *Axin.* Significance change in fold mRNA levels was considered to be less than 0.5-fold (suppression) or greater than 1.5-fold (more expression), as per the accepted standard (Sonoshita & Cagan, 2017). Drosophila *ribosomal protein 49* (*drp49)* was used s housekeeping gene. RT-PCR samples ran in duplicates and difference in Ct values < 0.3.

5.6.1. **Measuring activity of signaling when respective oncogenic transgenes were expressed in Drosophila**

The mRNA levels of *Wingless* (0.18-fold) and *Cut* (0.05-fold) were significantly lower when *UAS-N[nucl]* was expressed compared to control sample (*omb-GAL4>UAS-RFP*) (Fig. 5.2) suggesting that the assay conditions actually inhibited Notch signaling. The expression (mRNA levels) of *socs36E* (0.40-fold) and *Eve* (0.31-fold) were also significantly lower when UAS-Stat92E was over expressed compared to the control sample (Fig. 5.2), which was not expected. On the contrary, the expression of *Diap1* (1.22-fod) and *Cyclin E* (0.84-fold) were not significantly different when *UAS-Yki.S168A.GFP* was expressed compared to the control sample (Fig. 5.2), which was also unexpected. It is possible the larvae selected for RNA isolation for the Yki.S168A transgenes were not the correct genotype. That is because both the omb-Gal4 and UAS-

Yki.S168A have the GFP reporter and since, GFP expression was used a selected criterion for the correct genotype. Therefore, larvae that were dissected could have either *omb-GAL4* alone, UAS-Yki.S168A alone, which would result in incorrect RNA sample and hence very low mRNA levels observed for the target genes.

The expression of *dll* (6.11-fold) and *Axin* (3.53-fold) were significantly higher when *UAS-Arm-S10* was expressed compare to the control sample, *omb>UAS-RFP* (Fig. 5.2). These results suggested that activity of the Wnt signaling pathway was successfully measured using qRT-PCR, as expression of target genes was elevated as expected.

5.6.2. **Measuring activity of other signaling pathways when selected PTEN variants are expressed in the absence or presence of activated Drosophila PI3K**

I also measured these target genes when previously studied PTEN variants (WT, C124S, 4A, Y138L and G129R) were expressed alone, using the omb-Gal4 driver, or in the dPI3K$^{[act]}$ background. Measuring the activity of these pathways in a PI3-kinase background was to test if the observed results were possibly due to changes in PI3-kinase signaling. Hence comparing the qRT-PCR results of expressing the selected PTEN variants will shed some light on possible roles of PTEN that are PI3K-dependent or PI3K-independent. The fold change in mRNA levels (thus gene expression) was computed using the comparative Delta-Delta Ct ($2^{-\Delta\Delta Ct}$) method as previously described in Livak & Schmittgen (2001) and the housekeeping gene used was drp49. The qRT-PCR results are shown below.

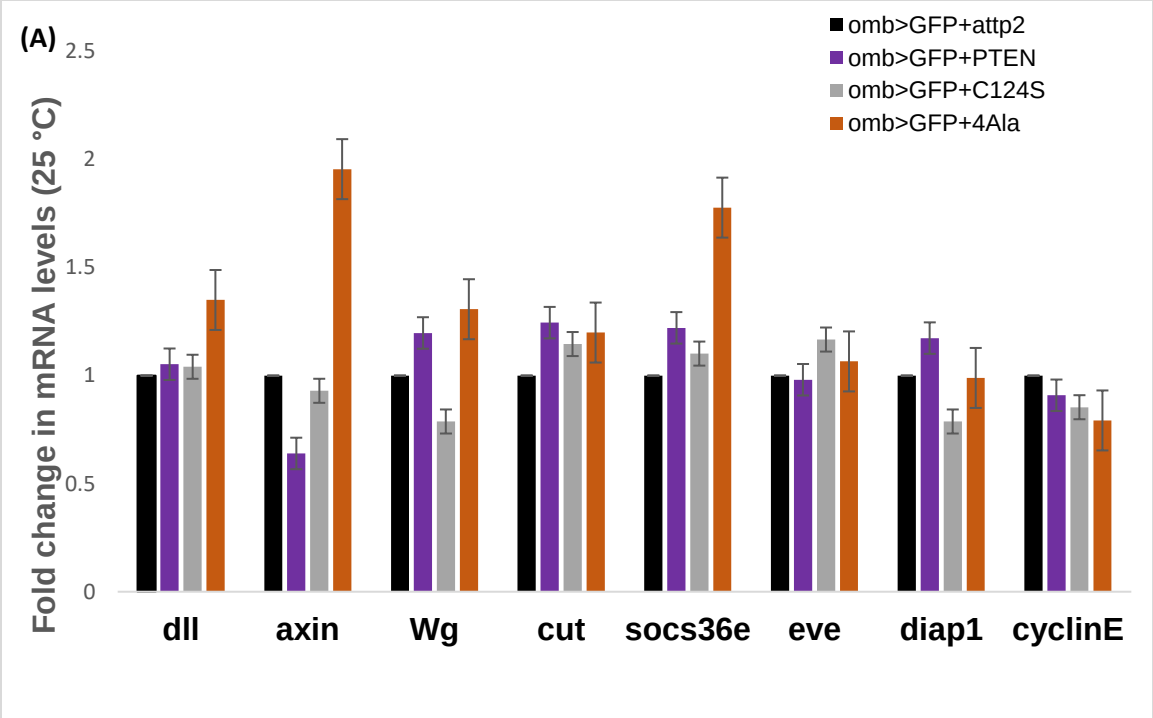

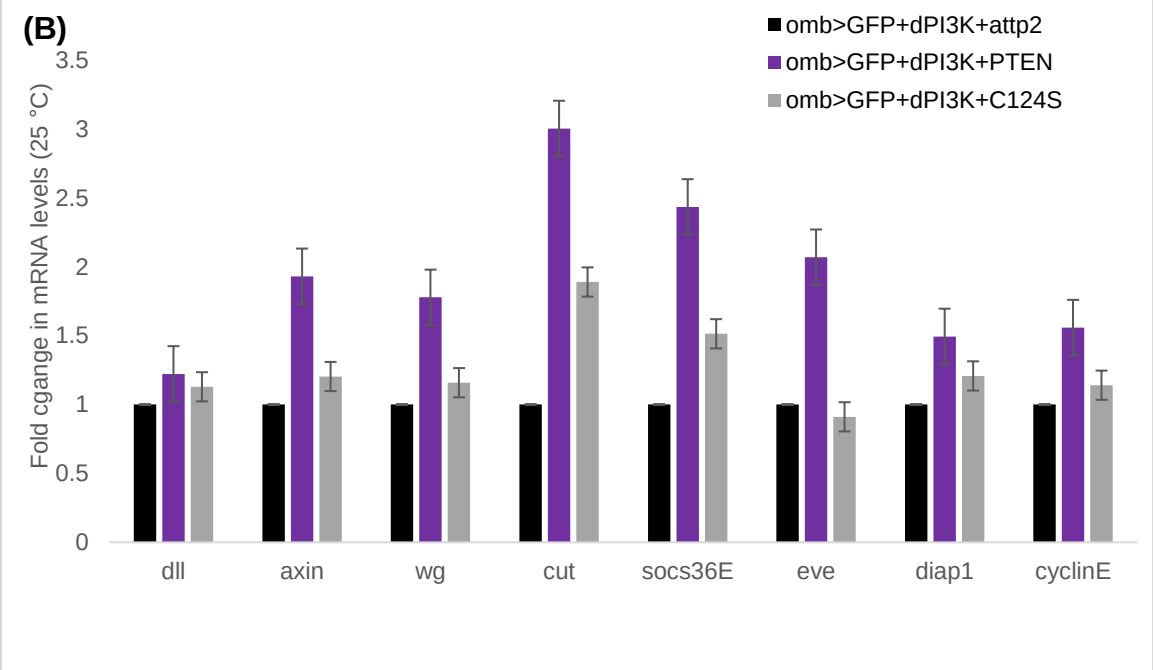

Figure 5.3 PCR results for targets of other signalling pathways when previously human PTEN variants are expressed in the absence (A) or presence of dPI3-Kinase (B).

Measuring the activity of the other signaling pathways (Wnt, Notch, JAK/STAT and Hippo signaling) using qRT-PCR experiments. (A) Measuring expression of target genes when wild type PTEN and two previously studied PTEN variants (PTEN-C124S, -4A) were expressed alone, using omb-Gal4 driver and compared to the control sample; no PTEN (attp2). (B) Measuring expression of target genes when wild type PTEN and PTEN-C124S were expressed in a dPI3K$^{[act]}$, using omb-Gal4 driver and compared to the control sample; no PTEN (attp2). The fold

change in mRNA levels was computed using the comparative $2^{-\Delta\Delta Ct}$ method. Significance change in fold mRNA levels was considered to be less than 0.5-fold (suppression) or greater than 1.5-fold (more expression), as per the accepted standard (Gao et al., 2000). Drosophila *ribosomal protein 49* (*drp49)* was used as housekeeping gene for both experiments. RT-PCR samples ran in duplicate and difference between in Ct values < 0.3.

Axin mRNA levels did not change significantly (0.64-fold change) when PTEN-WT was expressed alone compared to the control sample, no PTEN (attP2) (Fig. 5.3, A). However, the fold mRNA levels of *axin* significantly increased (1.93-fold) when dPI3K was co-expressed with wild type human PTEN (Fig. 5.2, B). On the other hand, the expression of *dll* did not change significantly when wild type PTEN was expressed alone or co-expressed with dPI3K since there was 1.22-fold and 1.05-fold change in mRNA levels (Fig. 5.3, A and B). These results suggest that PTEN might play a role in Wnt signaling but, in a PI3K-dependant manner.

The mRNA levels of wingless (*wg*) and *cut* were significantly increased, by 1.78-fold and 3.00-fold, when human PTEN wild type was co-expressed with dPI3K compared to the control sample (*omb>UAS-PTEN*), respectively (Fig. 5.3, B). However, both genes did not show a significant change when *UAS-PTEN* was expressed in the absence of dPI3K, with a 1.20-fold change for *wg* and 1.25-fold for *cut* (Fig. 5.3, A). These qPCR results also suggest that PTEN may play a role in Notch signaling but likely in a PI3K-dependant manner.

The expression (mRNA levels) of JAK/STAT target genes*, socs36E* (1.22-fold) and *eve* (0.98-fold), was not significantly different when PTEN was expressed compared to the no PTEN control sample (*omb>UAS-GFP;; UAS-attp2/*+) (Fig. 5.3, A). However, there was a significant increase in *socs36E* (3.00-fold) and *Eve* (2.43-fold) when wild type human PTEN was expressed compared to the control (*omb>dPI3K/+;; UAS-PTEN/*+) (Fig. 5.3, B). These results suggest that the PI3K/PTEN pathway may pay a role in JAK/STAT signaling. So again, PTEN's role in this signaling pathway is PI3K-dpendant.

Next, I wanted to measure pathway activity when PTEN-C124S (dual phosphatase dead) and PTEN-4A (constitutively active) variants to see if the phosphatase activity of PTEN was critical for this observed significant changes in activity of the four tested signaling pathways (Table 5.1) in the presence of $dPI3K^{[act]}$.

The expression of all eight target genes was not significantly different when PTEN-C124S was expressed in the absence of dPI3K[act] ; *dll* (1.04-fold), *axin* (0.93-fold), *wg* (0.79-fold), *cut* (1.15-fold), *socs36E* (1.10-fold), *eve* (1.07-fold), *Daip1* (0.75-fold), *cyclin E* (0.85-fold) (Fig. 5.3, A). However, co-expression of dPI3K[act] and PTEN-C124S saw an increase in the expression (mRNA levels) of *cut* (1.89-fold) and socs36E (1.51-fold) while expression of the other six target genes did not change significantly; *dll* (1.13-fold), *axin* (1.20-fold), *wg* (1.16-fold), *eve* (0.91-fold), *Diap1* (1.21-fold) and *cyclin E* (1.14-fold) (Fig. 5.3, B). At this point, it seems any significant changes in pathway activity is dependent on the increased PI3-Kinase pathway.

The expression of *axin* (1.97-fold) and *socs36E* (1.76-fold) were the only two of the eight target genes, of the four signaling pathways tested, that were significantly different when PTEN-4A was expressed while the other six did not change drastically; *dll* (1.35-fold), *wg* (1.31-fold), cut (1.20-fold), eve (1.07-fold), *Diap1* (0.99-fold) and *cyclin E* (0.79-fold) (Fig. 5.3, A).

In summary, the RT-PCR results showed a slight difference in pathway activity when PTEN is co-expressed with activated PI3-kinase, for the tested signaling pathways; Notch, JAK/STAT and Wnt signaling but not Hippo signalling pathway.

Chapter 6. Discussion and Conclusion

6.1. Studying the tumor suppressor activity human PTEN variants on activated PI3-kinase signalling pathways.

Currently, there are ~5,000 genes implicated in human diseases and this number continues to rise. Identifying genetic mutations in patients is a primary approach to understanding and tackling disease. Large-scale sequencing projects and sequencing of patient samples can reveal mutations or polymorphisms in many genes, but the functional consequences are not always apparent especially for single amino acid substitutions. The relative function of the majority of variants remains uncertain because the development of assays to characterize gene variants lags far behind. Here, together with our collaborators at UBC, we developed *Drosophila* genetic assays for rapid, inexpensive functionalization of human PTEN variants. Using this powerful genetic assay, we functionalized more than 100 PTEN variants. A majority of the tested PTEN variants were implicated in PTEN hamartoma tumor syndrome (PHTS), macrocephaly and autism spectrum disorders (ASD), but their functional significance is unknown.

The expression of dPI3K$^{[act]}$ using the *omb-GAL4* driver caused an increase in wing size (Fig. 3.1). The wing overgrowth was used as a tumor model, as tumors are often characterized by uncontrollable tissue or organ growth. We found that human PTEN *(PTEN)* can be functionally orthologous to the *Drosophila Pten (dPTEN)* gene which was consistent with data from previous studies done on Drosophila eye development (Huang et al, 1999). In this study, we established scalable Drosophila *in vivo* assays for screening of hundreds of human PTEN variants. For my part, I tested the ability of these human PTEN variants to supress or rescue the PI3-kinase dependent wing overgrowth. These assays are outlined in Fig. 2.2.

The tissue-specific human PTEN variants assay reports specifically on the tumor suppressor activity of PTEN variants, in a dPI3K$^{[act]}$ background, in the developing *Drosophila* wing. We characterized a few previously studied PTEN variants to validate

our assay and then determined if more than 100 human PTEN variants of unknown significance are functionally similar to wild type PTEN, loss of function (LOF) or gain of function (GOF) mutations, in the context of activated Drosophila PI3-kinase.

Our results showed that human wild type PTEN consistently supppresses dPI3K-induced wing ovegrowth phenotypes in the developing Drosophila wing (Fig. 3.2). The average wing size was reduced by ~13 % when wild type PTEN was co-expressed with dPI3K$^{[act]}$ in the Drosophila wing, compared to the no PTEN control wings. This observation was consistent with previous studies that showed that expression of Drosophila PI3K increases wing size (Haupt et al., 2003) and that human PTEN rescued PI3-kinase eye phenotypes, like Drosophila PTEN (Cheng et al., 2004).

Previously studied PTEN variants (PTEN-C124S, PTEN-4A, PTEN-G129E and PTEN-Y138L) resulted in expected phenotypes and thus validated our suppression assay in Drosophila. PTEN-C124S,a dual phosphatase dead mutant, did not rescue or reduce the size of enlarged dPI3K$^{[act]}$ adult wings (Fig. 3.3, A). PTEN-G129E (lipid phosphatase dead) and PTEN-Y138L (protein phosphatase dead) did not fully rescue dPI3K wing overgrowth, the latter rescuing it more than the former as expected (Fig. 3.3, A). In our assay, we were mainly measuring the lipid phosphatase activity and expected PTEN-Y138L to rescue adult wing phenotype similar to PTEN-WT control but only saw a partial rescue (hypomorph) suggesting that cooperation of the protein phosphatase activity and lipid phosphatase activity are both required for PTEN tumor suppression.

The constitutively active form of PTEN-4A, showed a significantly smaller wing compared to the no PTEN control and human PTEN-WT wings, as expected (Fig. 3.3, A). PTEN-4A is a well understood gain of function mutant lacking the serine/threonine phosphorylation sites (S380A, T382A, T383A, and S385A) which are normally targeted to downregulate PTEN activity (Cheng et al., 2004) showed that unphosphorylated PTEN remains in an active “open” conformation which strongly interacts with PDZ domain-containing proteins such as MAGI-1 and -2 which significantly downregulates Akt activity. Davidson et al. (2010) further adds that the phosphorylation of the PTEN tail regulates its activity by preventing it from participating in the PTEN Association Complex or PAC. Thus, the PTEN-4A, which cannot be phosphorylated to regulate phosphatase activity, is constitutively active form of PTEN resulting in significantly rescued wing phenotypes.

Characterization of PTEN variants of unknown significance revealed that most PTEN mutations result in loss of PTEN function or activity across all domains of PTEN (Fig. 1.4). Most of the PTEN variants carrying mutations in the N-terminal tail (residues 1 – 14) failed to suppress the effects of PI3K$^{[act]}$ compared to wild type PTEN (Fig. 3.3, A). This is consistent with previous results that showed that the N-terminal PIP2 binding domain (PBD) play a critical role in both cellular and catalytic activity of PTEN and is required for “correct membrane orientation and tumour-suppressor function” (Pogmore et al., 2016). Similarly, a majority of the PTEN variants with mutations within the phosphatase domain (residues 15 -185) failed to suppress the *omb>PI3K$^{[act]}$* enlarged wing phenotype (Fig. 3.3, A and B). Most of the PTEN variants with mutations in the C2 domain (residues 186 – 351) were able to rescue the *omb>PI3K$^{[act]}$* phenotype like wild type PTEN, while a few were non-functional (Fig. 3.3, B and C). The C2 domain is found in a few protein structures and known to be involved in membrane localization and binding to phospholipid bilayer (Morris et al., 2005). Variants that mapped within the C-tail domain (residues 352 – 402) and PDZ domain (residues 401 – 403) showed mostly wild type PTEN function except for two PTEN variants (PTEN-Q396R and PTEN-K402N), that acted like loss of function mutants in our wing assay (Fig. 3.3, C and D). The results suggest that mutations in the N-terminal region, phosphatase domain and C2 domain mostly results in PTEN loss of function while mutations in the c-tail region retain wild type PTEN function.

The next aim of the study was to determine if PI3K/PTEN controls Drosophila wing size by regulating cell growth, cell proliferation or apoptosis. As a proxy for the whole wing, we selected a specific area of the adult wing and counted the number of hairs cells in that selected area (Fig. 4.2, A) to determine if larger wings are due to more cells (cell proliferation) or bigger cells (cell growth), or both. We chose to count the number hairs in an area of the wing where omb effects were greatest as demonstrated by Mao et al. (2011). Each cell on the adult wing produces one hair, thus counting hairs indicates cell numbers.

Our results showed significantly decreased number of hairs (and by extension, cells) when dPI3K$^{[act]}$ is expressed using the *omb-GAL4* driver, within the selected area (720 x 600 pixels^2) compared to the w^{1118} normal wing (Fig. 4.3, B). Fewer number of hairs within the same selected area while also leading to a larger adult wing overall, suggested that dPI3K$^{[act]}$ expression increased cell size in the developing Drosophila.

First, the average number of hairs were not significantly different between no PTEN and PTEN-WT wings in the PI3K[act] genetic background (Fig. 4.3). However, PTEN-WT wings were smaller compared to the no PTEN control, in the dPI3K[act] background. This number of cells in the adult wing within the specified region was similar in the presence or absence of human PTEN-WT in the dPI3K background. Therefore, wild type PTEN likely controls wing size by regulating cell proliferation.

In addition, the average number of hairs counted for the selected PTEN variants, which included both loss of function and wild type variants, were not significantly different. One exception, PTEN-4A, showed a significantly higher number of hairs within the selected area but a significantly smaller wing overall, indicating that cells were smaller and fewer (Fig. 4.3). These results suggest that PTEN-4A and possibly other GOF variants (e.g. E256K) regulates both the size and the number of cell whereas other wild type PTEN variants (e.g. R130L, Y176C) regulate the number of cells (proliferation) rather than cell growth. Therefore, we can infer that the PTEN-WT and wild type PTEN variants that were tested in our genetic assay controls wing size (area) by regulating cell proliferation. In the future, it could be helpful to test this inferred assumption in order to see if some human PTEN variants control either cell growth, cell proliferation or both.

After observing that PTEN-WT controls adult wing size (area) by regulating cell proliferation, the next step was characterizing third instar larval tissues to see if that corroborates our preliminary adult wing assay findings. In order to determine if indeed PTEN-WT regulates proliferation, we performed immunofluorescence staining with anti-phospho-histone 3 (or anti-PH3) antibody to detect proliferating (PH3+) cells. Immunofluorescence (PH3) staining was first performed the four PTEN controls i.e. no PTEN , PTEN-WT, PTEN-C124S (dual phosphatase dead) and PTEN-4A (constitutively active) in the *PI3K[act]* genetic background (Fig. 4.4). PH3 positive (PH3+) were then counted using ImageJ software. Preliminary PH3+ cell counting data showed that expression of wild type PTEN significantly reduced the number of proliferating cells within the *omb* domain in larval discs of third instar larvae in the *PI3K[act]* background, compared to the no PTEN (attP2) control (Fig. 4.4 and 4.6). In addition, the dual phosphatase PTEN-C124S did not reduce the number of proliferating cells while the constitutively PTEN-4A reduced the number of proliferating cells, compared to the no PTEN control (Fig. 4.6). Thus, PTEN regulates proliferation at the larval stage of the developing Drosophila wing, in the dPi3K[act] background.

We also quantified the GFP area, which was a reporter for cells expressing dPI3K[act] (and the PTEN variants) larval discs. Increased GFP area represented enhanced cell proliferation and a suppression of dPI3K-dependent enlarged GFP area would reflect functional PTEN in our assays. We found that the percentage of GFP area relative to the whole disc was not rescued with loss of function variants (PTEN-C124S, PTEN-G129R and PTEN-H93R) and the no PTEN control (Fig. 4.7). Expression of wild type PTEN and other wildtype PTEN variants (R130L and Y176C) showed reduced GFP area, indicating a reduced number of cells expressing dPI3K[act] (Fig. 4.7). Therefore, we established that PTEN regulates the number of cells (proliferation) expressing dPI3K[act] within the *omb* region of the imaginal wing discs, which was consistent with adult wing hair count data.

TUNEL staining was performed on imaginal wing discs from third instar larvae to detect if PTEN controls wing size by regulating apoptosis. TUNEL staining results showed reduced cell death when PTEN-WT is expressed, compared to the no PTEN control in our dPI3K[act] background (Fig. 4.4 and 4.6). Cell death was not reduced when the when PTEN-C124S (dual phosphatase dead) was co-expressed with dPI3K [act], compared to the no PTEN control (Fig. 4.8). Cell death was nearly undetected when PTEN-4A was co-expressed with dPI3K[act] in our assay. These results suggested that PTEN may play a role in regulating apoptosis.

The role of PTEN in regulating cell growth, cell proliferation and apoptosis has been implicated in previous studies. PTEN has been shown to regulate proliferation by causing cause cell cycle arrest at the G1 phase (in glioma, endometrial cancer, and other tumors) (Lu et al, 2016). Huang et al (1999) proposed that PTEN regulates cell proliferation by causing cell cycle arrest at the G2 or G2/M phase during Drosophila eye development. According to Goberdhan et al. (1999) Drosophila PTEN controls cell size and number by antagonizing the Chico/PI3-kinase or Dp110 pathway and suppresses hyperplastic growth in flies.

Previous studies showed that phosphorylated Akt phosphorylates a number of substrates to inhibit apoptosis including the forkhead box (FOXO) family of transcription factors (Khwaja, 1999; Kurokawa & Kornbluth, 2009), caspase-9 (Haupt et al., 2003) and the E3 ubiquitin-protein ligase MDM2 (mouse double minute 2 homolog) thereby disabling p53-dependent apoptotic pathways (Zeng et al., 1997).

Therefore, it is suspected that suppression of dPI3K[act] signalling by PTEN prevents Akt phosphorylation and likely Akt-mediated apoptosis. This is possible since the phosphatase dead PTEN-C124S, which can not regulate PI3K activity has more cell death while PTEN-WT and PTEN-4A showed less cell death (Fig. 4.8). Therefore, PTEN may regulate death by inhibiting PI3-kinase dependent cell survival signals.

However, it would have been worthwhile to test the subcellular localization of PTEN in these PTEN variants. To this end, two antibodies against human PTEN (CPTC-PTEN-1 and -3, DHSB) were bought and tested (see section on testing human PTEN antibodies) but unfortunately did not yield any results. So, an antibody that works could shed some light in future studies on how these mutations affect PTEN activity and subcellular localization. Berger et al (2011) showed that PTEN function can have dramatic tumor suppression effects on cancer predisposition and tumorigenesis in a dosage-dependent. PTEN has been also been shown to be an obligate haploinsufficient tumor suppressor. Therefore, it would have been useful to measure the expression of PTEN protein levels for each PTEN variants, in our assay, to ensure that differences in wing size were not due to variation in the amount of PTEN proteins expressed.

6.2. Investigating possible PI3-kinase independent roles of PTEN in other signalling pathways.

The function of PTEN as an antagonist of activated PI3K signalling has been extensively studied in the past. However, recent research has been moving towards finding other possible PI3K-independent roles of PTEN. Since PTEN is a dual phosphatase with the ability to dephosphorylate and thus regulate the activity of both lipid and protein substrates as described in Chapter one (Introduction) of this thesis. I was interested in finding out if PTEN has any roles in other signalling pathways that have been shown to play a role in development and disease.

The qPCR results showed significant increases in expression of Wingless signalling pathway target gene, *axin*, when dPI3K was co-expressed with wild type human PTEN compared to the control, when PTEN was expressed alone (Fig. 5.3, B). *Axin* is a direct target gene and a negative regulator of Wnt signaling as its upregulation results in the phosphorylation and subsequent degradation of β-catenin thereby

negatively regulating the Wnt signalling pathway (Cheng et al., 2004). The levels of β-catenin were found to be higher in the melanoma cells deficient of PTEN (PTEN null cell lines) used to study melanoma progression and metastasis (Zeng et al., 1997). In addition, more studies revealed that the PI3K/PTEN pathway likely plays a role regulating levels of active β-catenin (cellular/nuclear) but dramatically regulates its subcellular localization(de Celis & Bray, 1997). The lack of significant changes in *dll* expression can't be explained at this point. It is therefore recommended that antibodies be used to test *dll* expression to get a better idea about the role of PTEN in the Wnt signalling pathway. These results suggest that there is a cross talk between wild type human PTEN is expressed in the presence of dPI3K, suggesting that PTEN might plays a PI3K-dependent role in Wnt signaling.

Similarly, the expression of Notch signalling transcriptional target genes, *wingless (wg)* and *cut,* were significantly increased when human PTEN wild type was co-overexpressed with dPI3K,compared to the control (Fig. 5.3, B). Previous studies have shown that Cut and Wg are upregulated in the dorsal/ventral boundary as has been detected with anti-Cut and anti-Wg antibody staining, to report Notch pathway activity(Sonoshita & Cagan, 2017). However, the activity of Notch signaling was determined by measuring the mRNA levels of these two target genes. The RT-PCR results also suggest that PTEN may play a role in Notch signaling but likely in a PI3K-dependant manner.

Likewise, the expression of JAK/STAT signalling transcriptional target genes s*ocs36E* and *eve were both* significantly increased when wild type human PTEN was co-expressed with *dPI3K*$^{[act]}$ compared to the control (PTEN expressed alone) (Fig. 5.3, B). These results suggest that the role of PTEN in the AK/STAT signaling pathway is PI3K-dpendant. Rawlings et al. (2004) showed that PI3K/Akt signalling was capable of activating JAK/STAT signalling pathway.

The expression of Hippo signalling pathway transcriptional target genes, *Diap1* and *cyclin E*, were not significantly changed when *UAS-Yki.S168A* was expressed or when wild type PTEN was co-expressed with *dPI3K*$^{[act]}$ (Fig. 5.2 and 5.3 A and B). This was surprising because the expression of *UAS-Yki.S168A* was expected to activate Hippo signalling.

Even though there were results obtained from the qRT-PCR experiments showed that the assay condition did not work, the approach to studying possible roles of PTEN can be used in the future. Crosses and qRT-PCR experiments could be repeated to determine if results are reproducible and to support preliminary findings.

6.3. Conclusion

In this research project we have developed an in vivo assay to study the tumor suppressor activity of the human PTEN variants, using Drosophila as a model organism. We created a tumor model by hyper-activating the oncogenic PI3K/Akt signalling pathway by over expressing *dPI3K*$^{[act]}$ in the Drosophila wing using the *bifid/omb-GAL4* driver. We have successfully functionalized over 100 PTEN variants of unknown significance and showed if they were loss of function or wild type and we identified PTEN-E256K as a gain of function mutant. In summary, our results suggest that PTEN regulates dPI3K-induced wing overgrowth in Drosophila by regulating proliferation. I have also shown that PTEN may regulate apoptosis in aPI3K/Akt-dependent manner. Here have presented an inexpensive, scalable and robust *in vivo* assay that can be used to study several genes involved in development and disease using Drosophila as a model organism.

The understanding of oncogenic phosphoinositide 3-kinase (PI3K) pathway has led to the discovery and development of PI3K inhibitors (e.g. Wortmannin) targeting cancer. It is important that when these therapeutics (PI3K inhibitors) are administered they significantly improve the quality of life for cancer patients. So, knowing which PTEN variants functional and which variants are non-functional will enable us to give certain therapeutics to patients based on their personal needs. Ultimately the results from this study will help identify mutations in PTEN primary sequence that likely contribute to the development and/or progression of PI3K-dependent diseases and cancers, heralding the long-anticipated era of personalized precision medicine.

References

Aldaz, S., Escudero, L. M., & Freeman, M. (2010). Live imaging of Drosophila imaginal disc development. *Proceedings of the National Academy of Sciences of the United States of America*, *107*(32), 14217–14222. https://doi.org/10.1073/pnas.1008623107

Arbouzova, N. I., & Zeidler, M. P. (2006). JAK/STAT signalling in Drosophila: Insights into conserved regulatory and cellular functions. *Development*, *133*(14), 2605–2616. https://doi.org/10.1242/dev.02411

Basu, S., Totty, N. F., Irwin, M. S., Sudol, M., & Downward, J. (2003). Akt phosphorylates the Yes-associated protein, YAP, to induce interaction with 14-3-3 and attenuation of p73-mediated apoptosis. *Molecular Cell*, *11*(1), 11–23. https://doi.org/10.1016/S1097-2765(02)00776-1

Beniston, M. (2011). Alps. *Encyclopedia of Earth Sciences Series*, *Part 3*, 35–38. https://doi.org/10.1007/978-90-481-2642-2_16

Berger, A. H., Knudson, A. G., & Pandolfi, P. P. (2011). A continuum model for tumour suppression. *Nature*, *476*(7359), 163–169. https://doi.org/10.1038/nature10275

Binari, R., & Perrimon, N. (1994). Stripe-specific regulation of pair-rule genes by hopscotch, a putative Jak family tyrosine kinase in Drosophila. *Genes and Development*, *8*(3), 300–312. https://doi.org/10.1101/gad.8.3.300

Blaquiere, J. A., Lam Wong, K. K., Kinsey, S. D., Wu, J., & Verheyen, E. M. (2018). Homeodomain-interacting protein kinase promotes tumorigenesis and metastatic cell behavior. *DMM Disease Models and Mechanisms*, *11*(1). https://doi.org/10.1242/dmm.031146

Blochlinger, K., Bodmer, R., Jack, J., Jan, L. Y., & Jan, Y. N. (1987). *sensory organ identity in Drosophila*. *298*(1986).

Brand, A. H., & Perrimon, N. (1993). Targeted gene expression as a means of altering cell fates and generating dominant phenotypes. *Development*, *118*(2), 401–415.

Brook, W. J., & Cohen, S. M. (1996). Antagonistic interactions between wingless and decapentaplegic responsible for dorsal-ventral pattern in the Drosophila leg. *Science*, *273*(5280), 1373–1377. https://doi.org/10.1126/science.273.5280.1373

Chan, H., Bartos, D. P., & Owen-Schaub, L. B. (1999). Activation-Dependent Transcriptional Regulation of the Human fas Promoter Requires NF-κB p50-p65 Recruitment . *Molecular and Cellular Biology*, *19*(3), 2098–2108. https://doi.org/10.1128/mcb.19.3.2098

Chen, Z., Trotman, L. C., Shaffer, D., Lin, H. K., Dotan, Z. A., Niki, M., Koutcher, J. A., Scher, H. I., Ludwig, T., Gerald, W., Cordon-Cardo, C., & Pandolfi, P. P. (2005). Crucial role of p53-dependent cellular senescence in suppression of Pten-deficient tumorigenesis. *Nature*, *436*(7051), 725–730. https://doi.org/10.1038/nature03918

Cheng, Y. C., Amoyel, M., Qiu, X., Jiang, Y. J., Xu, Q., & Wilkinson, D. G. (2004). Notch activation regulates the segregation and differentiation of rhombomere boundary cells in the zebrafish hindbrain. *Developmental Cell*. https://doi.org/10.1016/S1534-5807(04)00097-8

Cho, S., Lee, C., Ahn, Y., Kim, H., Kim, H., Ahn, C., Yang, K., & Lee, S. (2004). *Redox regulation of PTEN and protein tyrosine phosphatases in H 2 O 2 -mediated cell signaling*. *560*, 7–13. https://doi.org/10.1016/S0014-5793(04)00112-7

Cross, D. A. E., Alessi, D. R., Cohen, P., Andjelkovich, M., & Hemmings, B. A. (1995). Inhibition of glycogen synthase kinase-3 by insulin mediated by protein kinase B. *Nature*, *378*(6559), 785–789. https://doi.org/10.1038/378785a0

Csibi, A., & Blenis, J. (2012). Hippo-YAP and mTOR pathways collaborate to regulate organ size. *Nature Cell Biology*, *14*(12), 1244–1245. https://doi.org/10.1038/ncb2634

Davidson, L., MacCario, H., Perera, N. M., Yang, X., Spinelli, L., Tibarewal, P., Glancy, B., Gray, A., Weijer, C. J., Downes, C. P., & Leslie, N. R. (2010). Suppression of cellular proliferation and invasion by the concerted lipid and protein phosphatase activities of PTEN. *Oncogene*, *29*(5), 687–697. https://doi.org/10.1038/onc.2009.384

de Celis, J. F., & Bray, S. (1997). Feed-back mechanisms affecting Notch activation at the dorsoventral boundary in the Drosophila wing. *Development*, *124*(17), 3241–3251.

di Cristofano, A., Kotsi, P., Peng, Y. F., Cordon-Cardo, C., Elkon, K. B., & Pandolfi, P. P. (1999). Impaired Fas response and autoimmunity in Pten(+/-) mice. *Science*, *285*(5436), 2122–2125. https://doi.org/10.1126/science.285.5436.2122

di Cristofano, A., & Pandolfi, P. P. (2000). The multiple roles of PTEN in tumor suppression. *Cell*, *100*(4), 387–390. https://doi.org/10.1016/S0092-8674(00)80674-1

di Cristofano, A., Pesce, B., Cordon-Cardo, C., & Pandolfi, P. P. (1998). Pten is essential for embryonic development and tumour suppression. *Nature Genetics*, *19*(4), 348–355. https://doi.org/10.1038/1235

Diehl, J. A., Cheng, M., Roussel, M. F., & Sherr, C. J. (1998). *ciclyn D system*. *2*, 3499–3511.

Dillon, R. L., White, D. E., & Muller, W. J. (2007). The phosphatidyl inositol 3-kinase signaling network: Implications for human breast cancer. *Oncogene*, *26*(9), 1338–1345. https://doi.org/10.1038/sj.onc.1210202

Duffy, J. B. (2002). GAL4 system in Drosophila: A fly geneticist's Swiss army knife. *Genesis*, *34*(1–2), 1–15. https://doi.org/10.1002/gene.10150

Edoff, K., Dods, J. S., & Brand, A. H. (2007). Detection of GFP during nervous system development in Drosophila melanogaster. *Methods in Molecular Biology*, *411*, 81–98. https://doi.org/10.1385/1-59745-549-0:81

Eng, C. (2019). *PTEN Hamartoma Tumor Syndrome Summary Diagnosis Suggestive Findings*. 1–25. https://www.ncbi.nlm.nih.gov/books/NBK1488/pdf/Bookshelf_NBK1488.pdf

Fouladkou, F., Landry, T., Kawabe, H., Neeb, A., Lu, C., Brose, N., Stambolic, V., & Rotin, D. (2008). The ubiquitin ligase Nedd4-1 is dispensable for the regulation of PTEN stability and localization. *Proceedings of the National Academy of Sciences*

of the United States of America, *105*(25), 8585–8590. https://doi.org/10.1073/pnas.0803233105

Furnari, F. B., Su Huang, H. J., & Cavenee, W. K. (1998). The phosphoinositol phosphatase activity of PTEN mediates a serum- sensitive G1 growth arrest in glioma cells. *Cancer Research*, *58*(22), 5002–5008.

Gao, X., Neufeld, T. P., & Pan, D. (2000). Drosophila PTEN regulates cell growth and proliferation through PI3K- dependent and -independent pathways. *Developmental Biology*, *221*(2), 404–418. https://doi.org/10.1006/dbio.2000.9680

Gil, E. B., Link, E. M., Liu, L. X., Johnson, C. D., & Lees, J. A. (1999). Regulation of the insulin-like developmental pathway of Caenorhabditis elegans by a homolog of the PTEN tumor suppressor gene. *Proceedings of the National Academy of Sciences of the United States of America*, *96*(6), 2925–2930. https://doi.org/10.1073/pnas.96.6.2925

Go, M. J., Eastman, D. S., & Spyros, A. T. (1998). Cell proliferation control by Notch signaling in Drosophila development. *Development*, *125*(11), 2031–2040.

Goberdhan, D. C. I., & Wilson, C. (2003). PTEN: tumour suppressor, multifunctional growth regulator and more. *Human Molecular Genetics*, *12*(suppl 2), R239–R248. https://doi.org/10.1093/hmg/ddg288

Goberdhan, Deborah C.I., Paricio, N., Goodman, E. C., Mlodzik, M., & Wilson, C. (1999). Drosophila tumor suppressor PTEN controls cell size and number by antagonizing the Chico/PI3-kinase signaling pathway. *Genes and Development*, *13*(24), 3244–3258. https://doi.org/10.1101/gad.13.24.3244

Goto, H., Tomono, Y., Ajiro, K., Kosako, H., Fujita, M., Sakurai, M., Okawa, K., Iwamatsu, A., Okigaki, T., Takahashi, T., & Inagaki, M. (1999). Identification of a novel phosphorylation site on histone H3 coupled with mitotic chromosome condensation. *Journal of Biological Chemistry*, *274*(36), 25543–25549. https://doi.org/10.1074/jbc.274.36.25543

Guertin, D. A., & Sabatini, D. M. (2007). Defining the Role of mTOR in Cancer. *Cancer Cell*, *12*(1), 9–22. https://doi.org/10.1016/j.ccr.2007.05.008

Harvey, K., & Tapon, N. (2007). The Salvador-Warts-Hippo pathway - An emerging tumour-suppressor network. *Nature Reviews Cancer*, *7*(3), 182–191. https://doi.org/10.1038/nrc2070

Haupt, S., Berger, M., Goldberg, Z., & Haupt, Y. (2003). Apoptosis - The p53 network. *Journal of Cell Science*, *116*(20), 4077–4085. https://doi.org/10.1242/jcs.00739

Hendzel, M. J., Wei, Y., Mancini, M. A., van Hooser, A., Ranalli, T., Brinkley, B. R., Bazett-Jones, D. P., & Allis, C. D. (1997). Mitosis-specific phosphorylation of histone H3 initiates primarily within pericentromeric heterochromatin during G2 and spreads in an ordered fashion coincident with mitotic chromosome condensation. *Chromosoma*, *106*(6), 348–360. https://doi.org/10.1007/s004120050256

Hopkins, B. D., Fine, B., Steinbach, N., Dendy, M., Shaw, J., Pappas, K., Yu, J. S., Hodakoski, C., Klein, J., Pegno, S., Sulis, M., Goldstein, H., Amendolara, B., Lei, L., Maurer, M., Bruce, J., Canoll, P., Hibshoosh, H., & Parsons, R. (2014). *and survival*. *341*(6144), 399–402. https://doi.org/10.1126/science.1234907.A

Hopkins, B. D., Hodakoski, C., Barrows, D., Mense, S. M., & Parsons, R. E. (2014). PTEN function: The long and the short of it. *Trends in Biochemical Sciences*, *39*(4), 183–190. https://doi.org/10.1016/j.tibs.2014.02.006

Hou, X. S., Melnick, M. B., & Perrimon, N. (1996). marelle acts downstream of the Drosophila HOP/JAK kinase and encodes a protein similar to the mammalian STATs. *Cell*, *84*(3), 411–419. https://doi.org/10.1016/S0092-8674(00)81286-6

Huang, H., Potter, C. J., Tao, W., Li, D. M., Brogiolo, W., Hafen, E., Sun, H., & Xu, T. (1999). PTEN affects cell size, cell proliferation and apoptosis during Drosophila eye development. *Development*, *126*(23), 5365–5372. https://doi.org/10.5167/uzh-627

Huang, Jian, Yan, J., Zhang, J., Zhu, S., Wang, Y., Shi, T., Zhu, C., Chen, C., Liu, X., Cheng, J., Mustelin, T., Feng, G. S., Chen, G., & Yu, J. (2012). SUMO1 modification of PTEN regulates tumorigenesis by controlling its association with the plasma membrane. *Nature Communications*, *3*(May). https://doi.org/10.1038/ncomms1919

Huang, Jianbin, Wu, S., Barrera, J., Matthews, K., Pan, D., & Boulevard, H. H. (2005). *The Hippo Signaling Pathway Coordinately Regulates Cell Proliferation and Apoptosis by Inactivating Yorkie , the Drosophila Homolog of YAP at Dallas*. *122*, 421–434. https://doi.org/10.1016/j.cell.2005.06.007

Huang, W. C., & Hung, M. C. (2009). Induction of Akt activity by chemotherapy confers acquired resistance. *Journal of the Formosan Medical Association*, *108*(3), 180–194. https://doi.org/10.1016/S0929-6646(09)60051-6

Ikenoue, T., Inoki, K., Zhao, B., & Guan, K. L. (2008). PTEN acetylation modulates its interaction with PDZ domain. *Cancer Research*, *68*(17), 6908–6912. https://doi.org/10.1158/0008-5472.CAN-08-1107

Jennings, B. H. (2011). Drosophila-a versatile model in biology & medicine. *Materials Today*, *14*(5), 190–195. https://doi.org/10.1016/S1369-7021(11)70113-4

Johansen, K. A., Iwaki, D. D., & Lengyel, J. A. (2003). Localized JAK/STAT signaling is required for oriented cell rearrangement in a tubular epithelium. *Development*, *130*(1), 135–145. https://doi.org/10.1242/dev.00202

Kevin Range, and D. M. Y. A. M. (2012). 基因的改变NIH Public Access. *Bone*, *23*(1), 1–7. https://doi.org/10.1038/jid.2014.371

Khwaja, A. (1999). Apoptosis: Akt is more than just a bad kinase. *Nature*, *401*(6748), 33–34. https://doi.org/10.1038/43354

Kikuchi, A. (1999). Roles of axin in the Wnt signalling pathway. *Cellular Signalling*, *11*(11), 777–788. https://doi.org/10.1016/S0898-6568(99)00054-6

Kikuchi, A., & Kishida, S. (2006). *Kikuchi kishida Yamamoto 2010 Regulation of Wnt signaling by PPI and posttranslational modifications*. *38*(1), 1–10.

Komiya, Y., & Habas, R. (2008). *Wnt Secretion and Extra-Cellular Regulators*. *4*(2), 68–75. www.landesbioscience.com

Kurokawa, M., & Kornbluth, S. (2009). Caspases and Kinases in a Death Grip. *Cell*, *138*(5), 838–854. https://doi.org/10.1016/j.cell.2009.08.021

Kwabi-Addo, B., Giri, D., Schmidt, K., Podsypanina, K., Parsons, R., Greenberg, N., & Ittmann, M. (2001). Haploinsufficiency of the Pten tumor suppressor gene promotes prostate cancer progression. *Proceedings of the National Academy of Sciences of the United States of America*, *98*(20), 11563–11568. https://doi.org/10.1073/pnas.201167798

Landrum, M. J., Lee, J. M., Riley, G. R., Jang, W., Rubinstein, W. S., Church, D. M., & Maglott, D. R. (2014). ClinVar: Public archive of relationships among sequence variation and human phenotype. *Nucleic Acids Research*, *42*(D1), 980–985. https://doi.org/10.1093/nar/gkt1113

Lee, J., Yang, H., Georgescu, M., Cristofano, A. di, Maehama, T., Shi, Y., Dixon, J. E., Pandolfi, P., Pavletich, N. P., & Arbor, A. (1999). *Crystal Structure of the PTEN Tumor Suppressor : Implications for Its Phosphoinositide Phosphatase Activity and Membrane Association*. *99*, 323–334.

Lee, S., Yang, K., Kwon, J., Lee, C., Jeong, W., & Rhee, S. G. (2002). *Reversible Inactivation of the Tumor Suppressor PTEN by H 2 O 2 *. *277*(23), 20336–20342. https://doi.org/10.1074/jbc.M111899200

Leevers, S. J., Weinkove, D., MacDougall, L. K., Hafen, E., & Waterfield, M. D. (1996). The Drosophila phosphoinositide 3-kinase Dp110 promotes cell growth. *The EMBO Journal*, *15*(23), 6584–6594. https://doi.org/10.1002/j.1460-2075.1996.tb01049.x

Lento, W., Congdon, K., Voermans, C., Stamos, J. L., Weis, W. I., Whyte, J. L., Smith, A. a, Jill, A., & Chien, J. (2012). Wnt / Wingless Signaling in Drosophila Wnt / Wingless Signaling in Drosophila. *Cold Spring Harbor Perspectives in Biology*, *4*(a007930), 1–16. https://doi.org/10.1101/cshperspect.a007930

Leslie, N. R., Maccario, H., Spinelli, L., & Davidson, L. (2009). The significance of PTEN's protein phosphatase activity. *Advances in Enzyme Regulation*, *49*(1), 190–196. https://doi.org/10.1016/j.advenzreg.2008.12.002

Li, D. M., & Sun, H. (1997). TEP1, encoded by a candidate tumor suppressor locus, is a novel protein tyrosine phosphatase regulated by transforming growth factor β. *Cancer Research*, *57*(11), 2124–2129.

Li, D. M., & Sun, H. (1998). PTEN/MMAC1/TEP1 suppresses the tumorigenicity and induces G1 cell cycle arrest in human glioblastoma cells. *Proceedings of the National Academy of Sciences of the United States of America*, *95*(26), 15406–15411. https://doi.org/10.1073/pnas.95.26.15406

Li, J., Yen, C., Liaw, D., Podsypanina, K., Bose, S., Steven, I., Puc, J., Miliaresis, C., Rodgers, L., Mccombie, R., Bigner, S. H., Giovanella, B. C., Ittmann, M., Tycko, B., Hibshoosh, H., Wigler, M. H., Li, J., Yen, C., Liaw, D., … Parsonst, R. (1997). PTEN , a Putative Protein Tyrosine Phosphatase Gene Mutated in Human Brain , Breast , and Prostate Cancer and Ramon Parsons Published by : American Association for the Advancement of Science Stable URL : http://www.jstor.org/stable/2893082 JSTOR is a not-. *Science*, *275*(5308), 1943–1947.

Luo, J., Manning, B. D., & Cantley, L. C. (2003). Targeting the PI3K-Akt pathway in human cancer: Rationale and promise. *Cancer Cell*, *4*(4), 257–262. https://doi.org/10.1016/S1535-6108(03)00248-4

Luongo, F., Colonna, F., Calapà, F., Vitale, S., Fiori, M. E., & de Maria, R. (2019). Pten tumor-suppressor: The dam of stemness in cancer. *Cancers*, *11*(8), 1–26. https://doi.org/10.3390/cancers11081076

MacDougall, L. K., Gagou, M. E., Leevers, S. J., Hafen, E., & Waterfield, M. D. (2004). Targeted Expression of the Class II Phosphoinositide 3-Kinase in Drosophila melanogaster Reveals Lipid Kinase-Dependent Effects on Patterning and Interactions with Receptor Signaling Pathways. *Molecular and Cellular Biology*, *24*(2), 796–808. https://doi.org/10.1128/mcb.24.2.796-808.2004

Maddika, S., Kavela, S., Rani, N., Palicharla, V. R., Pokorny, J. L., Sarkaria, J. N., & Chen, J. (2011). WWP2 is an E3 ubiquitin ligase for PTEN. *Nature Cell Biology*, *13*(6), 728–733. https://doi.org/10.1038/ncb2240

Mirzoyan, Z., Sollazzo, M., Allocca, M., Valenza, A. M., Grifoni, D., & Bellosta, P. (2019). Drosophila melanogaster: A model organism to study cancer. *Frontiers in Genetics*, *10*(March), 1–16. https://doi.org/10.3389/fgene.2019.00051

Morris, J. B., Kenney, B., Huynh, H., & Woodcock, E. A. (2005). Regulation of the proapoptotic factor FOXO1 (FKHR) in cardiomyocytes by growth factors and α1-

adrenergic agonists. *Endocrinology*, *146*(10), 4370–4376. https://doi.org/10.1210/en.2005-0162

Myers, M. P., Stolarov, J. P., Eng, C., Li, J., Wang, S. I., Wigler, M. H., Parsons, R., & Tonks, N. K. (1997). P-TEN, the tumor suppressor from human chromosome 10q23, is a dual-specificity phosphatase. *Proceedings of the National Academy of Sciences of the United States of America*, *94*(17), 9052–9057. https://doi.org/10.1073/pnas.94.17.9052

Naderali, E., Khaki, A. A., Rad, J. S., Ali-Hemmati, A., Rahmati, M., & Charoudeh, H. N. (2018). Regulation and modulation of PTEN activity. *Molecular Biology Reports*, *45*(6), 2869–2881. https://doi.org/10.1007/s11033-018-4321-6

Nelson, W. J., & Nusse, R. (2004). Convergence of Wnt, β-Catenin, and Cadherin pathways. *Science*, *303*(5663), 1483–1487. https://doi.org/10.1126/science.1094291

Ogg, S., Ruvkun, G., & Morris, C. (1998). *<Mol Cell 1998 OggThe C-elegans PTEN homolog DAF-18.pdf>*. *2*, 887–893. https://doi.org/10.1016/S1097-2765(00)80303-2

Okumura, K., Mendoza, M., Bachoo, R. M., DePinho, R. A., Cavenee, W. K., & Furnari, F. B. (2006). PCAF modulates PTEN activity. *Journal of Biological Chemistry*, *281*(36), 26562–26568. https://doi.org/10.1074/jbc.M605391200

Paes, J. E., & Ringel, M. D. (2008). Dysregulation of the Phosphatidylinositol 3-Kinase Pathway in Thyroid Neoplasia. *Endocrinology and Metabolism Clinics of North America*, *37*(2), 375–387. https://doi.org/10.1016/j.ecl.2008.01.001

Pai, L. M., Orsulic, S., Bejsovec, A., & Peifer, M. (1997). Negative regulation of Armadillo, a Wingless effector in Drosophila. *Development*, *124*(11), 2255–2266.

Pan, D. (2007). Hippo signaling in organ size control. *Genes and Development*, *21*(8), 886–897. https://doi.org/10.1101/gad.1536007

Papa, A., Wan, L., Bonora, M., Salmena, L., Song, M. S., Hobbs, R. M., Lunardi, A., Webster, K., Ng, C., Newton, R. H., Knoblauch, N., Guarnerio, J., Ito, K., Turka, L. A., Beck, A. H., Pinton, P., Bronson, R. T., Wei, W., & Pandolfi, P. P. (2014).

Cancer-associated PTEN mutants act in a dominant-negative manner to suppress PTEN protein function. *Cell*, *157*(3), 595–610. https://doi.org/10.1016/j.cell.2014.03.027

Papa, A., Wan, L., Bonora, M., Salmena, L., Song, M. S., Hobbs, R. M., Lunardi, A., Webster, K., Ng, C., Ryan, H., Knoblauch, N., Guarnerio, J., Ito, K., Turka, L. A., Beck, A. H., Pinton, P., Bronson, R., Wei, W., & Pandolfi, P. P. (2015). *NIH Public Access*. *157*(3), 595–610. https://doi.org/10.1016/j.cell.2014.03.027.Cancer-associated

Payne, S. R., & Kemp, C. J. (2005). Tumor suppressor genetics. *Carcinogenesis*, *26*(12), 2031–2045. https://doi.org/10.1093/carcin/bgi223

Persad, A., Venkateswaran, G., Hao, L., Garcia, M. E., Yoon, J., Sidhu, J., & Persad, S. (2016). Active β-catenin is regulated by the PTEN/PI3 kinase pathway: A role for protein phosphatase PP2A. *Genes and Cancer*, *7*(11–12), 368–382. https://doi.org/10.18632/genesandcancer.128

Persad, S., Attwell, S., Gray, V., Mawji, N., Deng, J. T., Leung, D., Yan, J., Sanghera, J., Walsh, M. P., & Dedhar, S. (2001). Regulation of protein kinase B/Akt-serine 473 phosphorylation by integrin-linked kinase: Critical roles for kinase activity and amino acids arginine 211 and serine 343. *Journal of Biological Chemistry*, *276*(29), 27462–27469. https://doi.org/10.1074/jbc.M102940200

Piddini, E., & Vincent, J. P. (2009). Interpretation of the Wingless Gradient Requires Signaling-Induced Self-Inhibition. *Cell*, *136*(2), 296–307. https://doi.org/10.1016/j.cell.2008.11.036

Podsypanina, K., Ellenson, L. H., Nemes, A., Gu, J., Tamura, M., Yamada, K. M., Cordon-Cardo, C., Catoretti, G., Fisher, P. E., & Parsons, R. (1999). Mutation of Pten/Mmac1 in mice causes neoplasia in multiple organ systems. *Proceedings of the National Academy of Sciences of the United States of America*, *96*(4), 1563–1568. https://doi.org/10.1073/pnas.96.4.1563

Pogmore, Justin., Pemberton, James., Chi, Xiaoke., & Andrews, David. (2016). Using FRET to measure protein interactions between Bcl-2 family proteins on

mitochondrial membranes. *Program Cell Death: Methods and Protocols in Molecular Biology*, *1419*, 197–212. https://doi.org/10.1007/978-1-4939-3581-9

Porta, C., Paglino, C., & Mosca, A. (2014). Targeting PI3K/Akt/mTOR signaling in cancer. *Frontiers in Oncology*, *4 APR*(April), 1–11. https://doi.org/10.3389/fonc.2014.00064

Putz, U., Howitt, J., Doan, A., Goh, C. P., Low, L. H., Silke, J., & Tan, S. S. (2012). The tumor suppressor PTEN is exported in exosomes and has phosphatase activity in recipient cells. *Science Signaling*, *5*(243). https://doi.org/10.1126/scisignal.2003084

Reiter, L. T., Potocki, L., Chien, S., Gribskov, M., & Bier, E. (2001). A systematic analysis of human disease-associated gene sequences in Drosophila melanogaster. *Genome Research*, *11*(6), 1114–1125. https://doi.org/10.1101/gr.169101

Rezával, C., Werbajh, S., & Ceriani, M. F. (2007). Neuronal death in Drosophila triggered by GAL4 accumulation. *European Journal of Neuroscience*, *25*(3), 683–694. https://doi.org/10.1111/j.1460-9568.2007.05317.x

Roberts, D. B. (2006). Drosophila melanogaster: The model organism. *Entomologia Experimentalis et Applicata*, *121*(2), 93–103. https://doi.org/10.1111/j.1570-8703.2006.00474.x

Ross, A. H., & Gericke, A. (2009). Phosphorylation keeps PTEN phosphatase closed for business. *Proceedings of the National Academy of Sciences of the United States of America*, *106*(5), 1297–1298. https://doi.org/10.1073/pnas.0812473106

Rouault, J. P., Kuwabara, P. E., Sinilnikova, O. M., Duret, L., Thierry-Mieg, D., & Billaud, M. (1999). Regulation of dauer larva development in Caenorhabditis elegans by daf-18, a homologue of the tumour suppressor PTEN. *Current Biology*, *9*(6), 329–334. https://doi.org/10.1016/S0960-9822(99)80143-2

Salmena, L., Carracedo, A., & Pandolfi, P. P. (2008). Tenets of PTEN Tumor Suppression. *Cell*, *133*(3), 403–414. https://doi.org/10.1016/j.cell.2008.04.013

Santarosa, M., & Ashworth, A. (2004). Haploinsufficiency for tumour suppressor genes: When you don't need to go all the way. *Biochimica et Biophysica Acta - Reviews on Cancer*, *1654*(2), 105–122. https://doi.org/10.1016/j.bbcan.2004.01.001

Schneider, P. N., Slusarski, D. C., & Houston, D. W. (2012). Differential Role of Axin RGS Domain Function in Wnt Signaling during Anteroposterior Patterning and Maternal Axis Formation. *PLoS ONE*, *7*(9). https://doi.org/10.1371/journal.pone.0044096

Sears, R., Nuckolls, F., Haura, E., Taya, Y., Tamai, K., & Nevins, J. R. (2000). Multiple Ras-dependent phosphorylation pathways regulate Myc protein stability. *Genes and Development*, *14*(19), 2501–2514. https://doi.org/10.1101/gad.836800

Shimizu, T., Ho, L. L., & Lai, Z. C. (2008). The mob as tumor suppressor gene is essential for early development and regulates tissue growth in Drosophila. *Genetics*, *178*(2), 957–965. https://doi.org/10.1534/genetics.107.081570

Sonoshita, M., & Cagan, R. L. (2017). Modeling Human Cancers in Drosophila. In *Current Topics in Developmental Biology* (1st ed., Vol. 121). Elsevier Inc. https://doi.org/10.1016/bs.ctdb.2016.07.008

Southall, T. D., Elliott, D. A., & Brand, A. H. (2008). The GAL4 system: A versatile toolkit for gene expression in Drosophila. *Cold Spring Harbor Protocols*, *3*(7), 1–10. https://doi.org/10.1101/pdb.top49

Steck, P. A., Pershouse, M. A., Jasser, S. A., Yung, W. K. A., Lin, H., Ligon, A. H., Langford, A., Baumgard, M. L., Hattier, T., Davis, T., Frye, C., Hu, R., Teng, D. H. F., & Tavtigian, S. v. (1997). *Identification of a candidate tumour advanced cancers*. *15*(april).

Stumpf, M., & den Hertog, J. (2016). Differential requirement for pten lipid and protein phosphatase activity during zebrafish embryonic development. *PLoS ONE*, *11*(2), 1–16. https://doi.org/10.1371/journal.pone.0148508

Suzuki, A., de La Pompa, J. L., Stambolic, V., Elia, A. J., Sasaki, T., del Barco Barrantes, I., Ho, A., Wakeham, A., Itie, A., Khoo, W., Fukumoto, M., & Mak, T. W. (1998). High cancer susceptibility and embryonic lethality associated with mutation

of the PTEN tumor suppressor gene in mice. *Current Biology*, *8*(21), 1169–1178. https://doi.org/10.1016/S0960-9822(07)00488-5

Tamura, M., Gu, J., Matsumoto, K., Aota, S. I., Parsons, R., & Yamada, K. M. (1998). Inhibition of cell migration, spreading, and focal adhesions by tumor suppressor PTEN. *Science*, *280*(5369), 1614–1617. https://doi.org/10.1126/science.280.5369.1614

Tibarewal, P., Zilidis, G., Spinelli, L., Schurch, N., Maccario, H., Gray, A., Perera, N. M., Davidson, L., Barton, G. J., & Leslie, N. R. (2012). PTEN protein phosphatase activity correlates with control of gene expression and invasion, a tumor-suppressing phenotype, but not with AKT activity. *Science Signaling*, *5*(213), 1–12. https://doi.org/10.1126/scisignal.2002138

Trotman, L. C., Niki, M., Dotan, Z. A., Koutcher, J. A., di Cristofano, A., Xiao, A., Khoo, A. S., Roy-Burman, P., Greenberg, N. M., van Dyke, T., Cordon-Cardo, C., & Pandolfi, P. P. (2003). Pten dose dictates cancer progression in the prostate. *PLoS Biology*, *1*(3), 385–396. https://doi.org/10.1371/journal.pbio.0000059

Trotman, L. C., Wang, X., Alimonti, A., Chen, Z., Teruya-Feldstein, J., Yang, H., Pavletich, N. P., Carver, B. S., Cordon-Cardo, C., Erdjument-Bromage, H., Tempst, P., Chi, S., Kim, H., Misteli, T., Jiang, X., & Pandolfi, P. P. (2007). Ubiquitination regulates PTEN nuclear import and tumor suppression of PTEN that target post-translational modification and demonstrate how a discrete molecular mechanism dictates tumor-progression by differentiating between degradation and protection of P. *Cell. January*, *12*(1281), 141–156.

Tumaneng, K., Schlegelmilch, K., Russell, R. C., Yimlamai, D., Basnet, H., Mahadevan, N., Fitamant, J., Bardeesy, N., Camargo, F. D., & Guan, K. L. (2012). YAP mediates crosstalk between the Hippo and PI(3)K-TOR pathways by suppressing PTEN via miR-29. *Nature Cell Biology*, *14*(12), 1322–1329. https://doi.org/10.1038/ncb2615

Ugur, B., Chen, K., & Bellen, H. J. (2016). Drosophila tools and assays for the study of human diseases. *DMM Disease Models and Mechanisms*, *9*(3), 235–244. https://doi.org/10.1242/dmm.023762

van Themsche, C., Leblanc, V., Parent, S., & Asselin, E. (2009). X-linked inhibitor of apoptosis protein (XIAP) regulates PTEN ubiquitination, content, and compartmentalization. *Journal of Biological Chemistry*, *284*(31), 20462–20466. https://doi.org/10.1074/jbc.C109.009522

Vazquez, F., Ramaswamy, S., Nakamura, N., & Sellers, W. R. (2000). Phosphorylation of the PTEN Tail Regulates Protein Stability and Function. *Molecular and Cellular Biology*, *20*(14), 5010–5018. https://doi.org/10.1128/mcb.20.14.5010-5018.2000

Vazquez, Francisca, Grossman, S. R., Takahashi, Y., Rokas, M. v., Nakamura, N., & Sellers, W. R. (2001). Phosphorylation of the PTEN Tail Acts as an Inhibitory Switch by Preventing Its Recruitment into a Protein Complex. *Journal of Biological Chemistry*, *276*(52), 48627–48630. https://doi.org/10.1074/jbc.C100556200

Veeman, M. T., Axelrod, J. D., & Moon, R. T. (2003). A second canon: Functions and mechanisms of β-catenin-independent Wnt signaling. *Developmental Cell*, *5*(3), 367–377. https://doi.org/10.1016/S1534-5807(03)00266-1

Waite, K. A., & Eng, C. (2002). Protean PTEN: Form and function. *American Journal of Human Genetics*, *70*(4), 829–844. https://doi.org/10.1086/340026

Walker, S. M., Leslie, N. R., Perera, N. M., Batty, I. H., & Downes, C. P. (2004). The tumour-suppressor function of PTEN requires an N-terminal lipid-binding motif. *Biochemical Journal*, *379*(2), 301–307. https://doi.org/10.1042/BJ20031839

Wang, H., Karikomi, M., Naidu, S., Rajmohan, R., Caserta, E., Chen, H. Z., Rawahneh, M., Moffitt, J., Stephens, J. A., Fernandez, S. A., Weinstein, M., Wang, D., Sadee, W., la Perle, K., Stromberg, P., Rosol, T. J., Eng, C., Ostrowsk, M. C., & Leone, G. (2010). Allele-specific tumor spectrum in Pten knockin mice. *Proceedings of the National Academy of Sciences of the United States of America*, *107*(11), 5142–5147. https://doi.org/10.1073/pnas.0912524107

Wodarz, A., & Nusse, R. (1998). Mechanisms of Wnt Signaling in Development. *Annual Review of Cell and Developmental Biology*, *14*(1), 59–88. https://doi.org/10.1146/annurev.cellbio.14.1.59

Xu, T., Wang, W., Zhang, S., Stewart, R. A., & Yu, W. (1995). Identifying tumor suppressors in genetic mosaics: The Drosophila lats gene encodes a putative protein kinase. *Development*, *121*(4), 1053–1063.

Yu, F. X., & Guan, K. L. (2013). The Hippo pathway: Regulators and regulations. *Genes and Development*, *27*(4), 355–371. https://doi.org/10.1101/gad.210773.112

Zacharioudaki, E., & Bray, S. J. (2014). Tools and methods for studying Notch signaling in Drosophila melanogaster. *Methods*, *68*(1), 173–182. https://doi.org/10.1016/j.ymeth.2014.03.029

Zeidler, M. P., Bach, E. A., & Perrimon, N. (2000). The roles of the Drosophila JAK/STAT pathway. *Oncogene*, *19*(21), 2598–2606. https://doi.org/10.1038/sj.onc.1203482

Zeng, L., Fagotto, F., Zhang, T., Hsu, W., Vasicek, T. J., Perry, W. L., Lee, J. J., Tilghman, S. M., Gumbiner, B. M., & Costantini, F. (1997). The mouse Fused locus encodes axin, an inhibitor of the Wnt signaling pathway that regulates embryonic axis formation. *Cell*, *90*(1), 181–192. https://doi.org/10.1016/S0092-8674(00)80324-4

Appendix Supplementary figures for Characterizing human PTEN variants in Drosophila

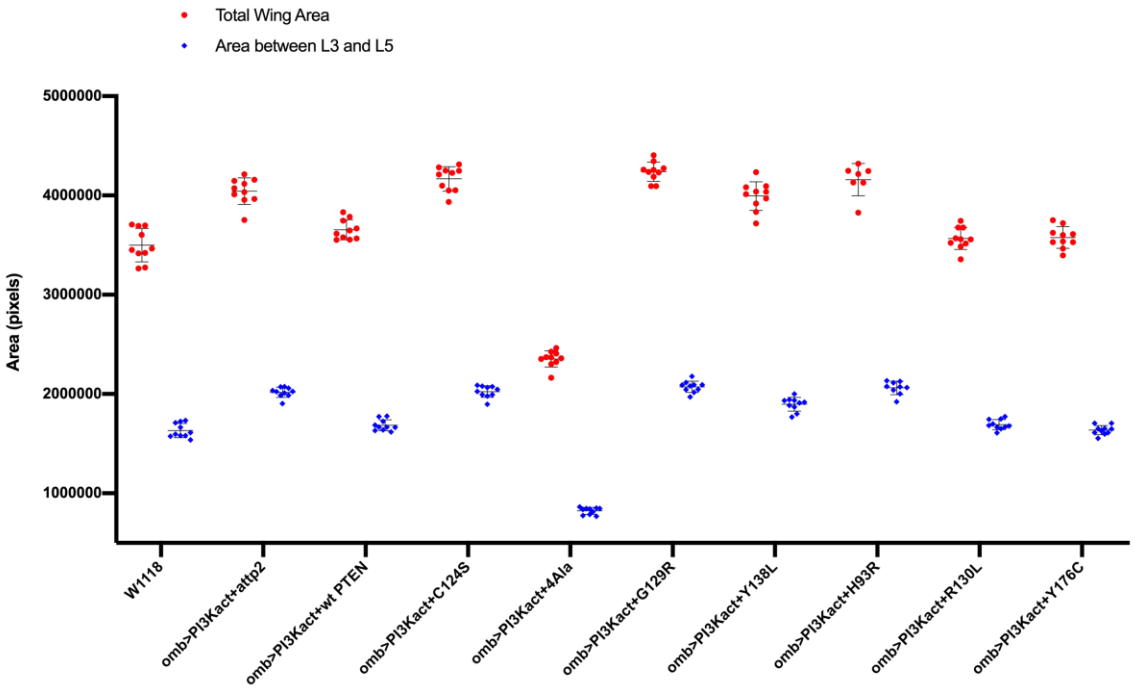

Figure A.1 Comparison of wing area distribution from the whole wing and the region between the L3 and L5 for selected variants. The total wing area and area between L3 and L5 show similar trends and are consistent for selected PTEN variants. Measuring the area between the L5 and L5 is more precise than total wing area, since data points are more clustered together.

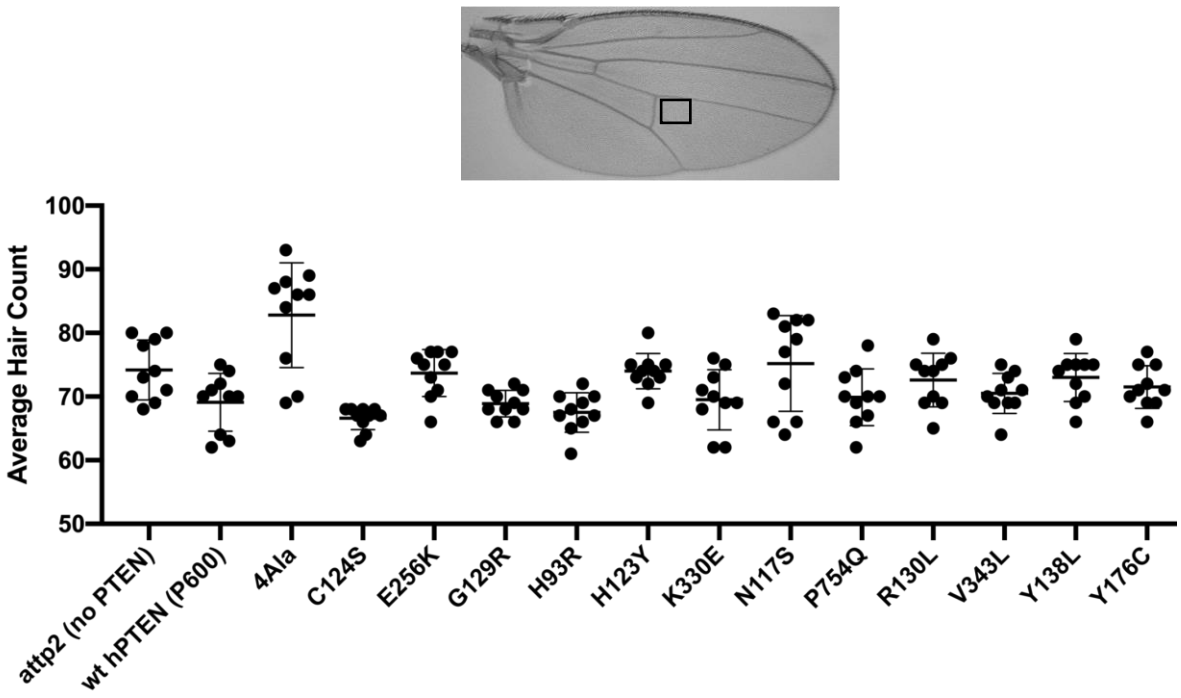

Figure A.2 Wing Hair count for selected PTEN variants. Hair count data for previously proposed selected PTEN variants in the *omb>PI3K[act]* genetic background. Ten adult wings were counted for each genotype and hair counting was done on specified area (720 x 600 pixels^2) selected in the second posterior cell on the distal side of the posterior cross vein (p-cv). Statistical analysis (one-way ANOVA followed by Dunnett's post hoc test) performed using GraphPad Prism software. ****p < 0.0001

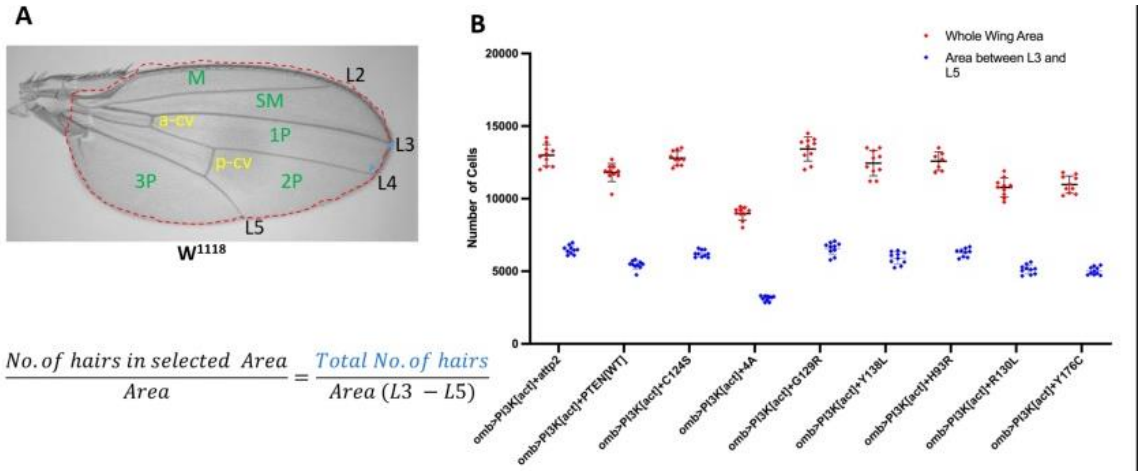

Figure A.3 Estimated total number of cells in the within the L3 and L5 region of the adult wing for selected PTEN variants.

The number of hairs were counted in the selected area (720 x 600 pixels^2) near the posterior cross vein or p-cv (Fig. 4.2). A) wild type (w1118) wing showing all the features (longitudinal veins (L2 - L5), marginal cell (M), sub marginal cell (SM)as well as the first (1P), second (2P) and third (3P) posterior cells of the adult Drosophila wing. The formula used to estimate the number of cells within the wing blade is shown below the Adult wing (bottom left). B) Estimation of the total number of cells using values obtained for the total wing area vs values obtained for area between L3 and L5, as the *omb* effects are more prominent in the L3 0 L5 region of the wing (Mao et al, 2011). 10 adult wings were analyzed per genotype. ****Statistical analysis

In summary, loss of function variants (PTEN-C124S, -G19R, -Y138L and -H93R) had more cells in the wing blade since they did not suppress the *omb>PI3K*$^{[act]}$ overgrowth phenotype, while functional PTEN variants (PTEN-R130L and Y176C) have similar number of cells, when compared to PTEN-WT. The constitutively active PTEN-4A showed significantly larger number of hairs with the specified region but overall showed a significantly lower number of cells on the wing blade or area between L3 and L5, compared to PTEN-WT. These results further support that the human PTEN controls Drosophila wing size by regulating cell proliferation.

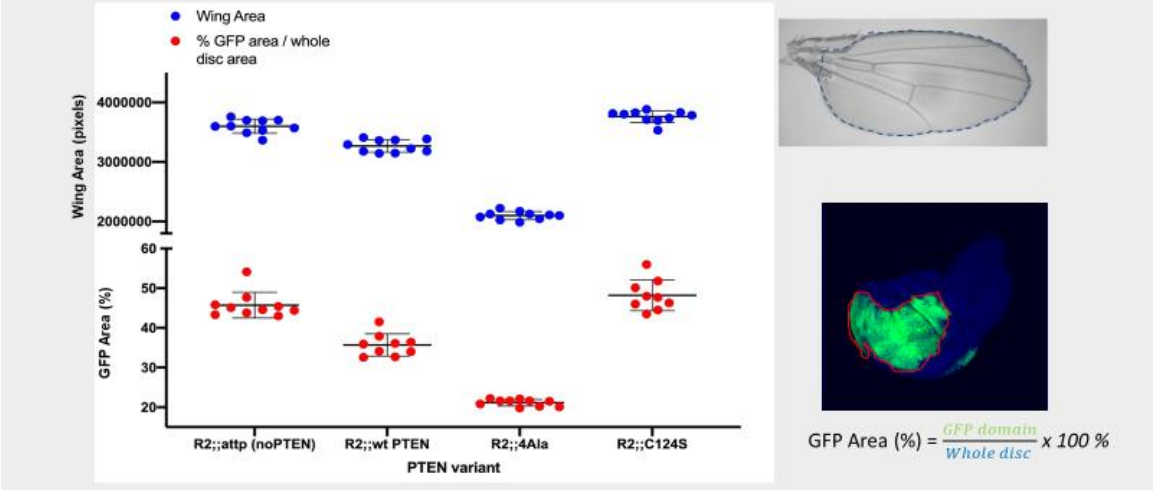

Figure A.4 Ratio of GFP area show similar trends to adult wing size (area) phenotypes. The *omb-GAL4>GFP* was used the visualize cells expressing activated *dPI3K* and human PTEN variants. Ten wings and ten discs were analyzed for each genotype.

The ratio of the GFP area was used to visualize cells expressing o*mb>dPI3K*$^{[act]}$ and PTEN variants using the GAL/UAS system. The averaged ratio of GFP area is significantly higher when no PTEN (~48 %) or the dual phosphatase dead PTEN-C124S

is expressed with dPI3K[act], compared to the PTEN-WT control. Expression of the constitutively active PTEN-4A significantly reduced the proportion of GFP area (~23 %), compared to PTEN-WT in the dPI3K[act] background. These results suggested that PTEN-WT significantly reduced the proportion of cell expressed dPI3K[act]. However, this data did reveal whether the observed differences of GFP Area were due the difference in the number or size of cells, within the domain of interest. This was the preliminary data, that prompted the investigation into cell proliferation as a way PTEN-WT regulated PI3-kinase dependent wing overgrowth.

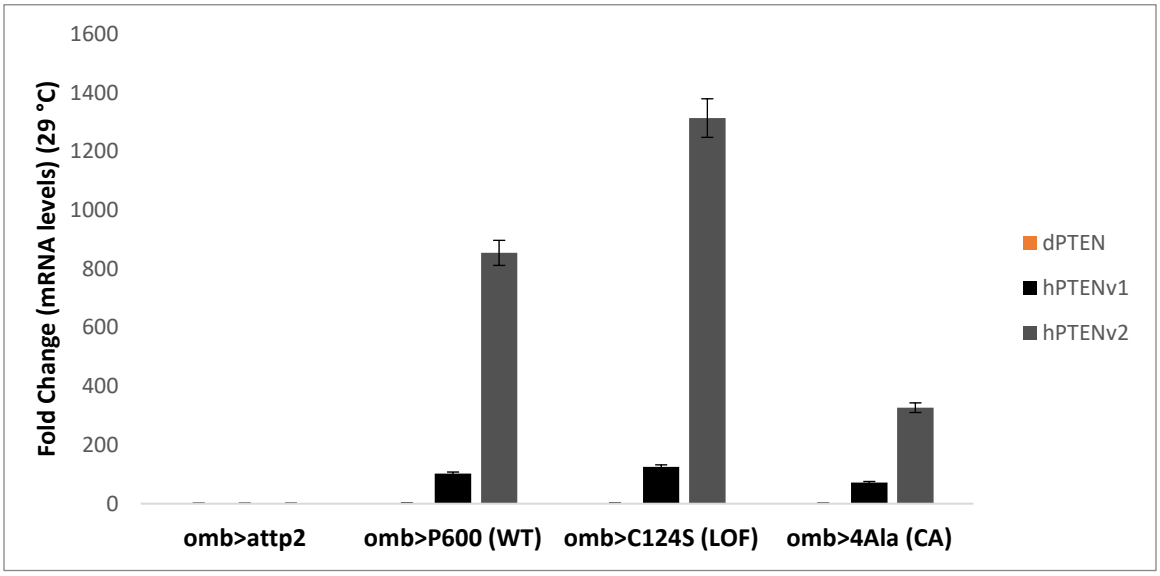

Figure A.4 RT-PCR result for the expression of Drosophila PTEN versus human PTEN for the selected PTEN variants.

RT-PCR experiment used to test the relative expression of drosophila PTEN and Human when these PTEN variants are expressed in the developing wing. Samples run in duplicates and RT-PCR experiment repeated twice. Significance change in fold mRNA levels was considered to be less than 0.5-fold (suppression) or greater than 1.5-fold (more expression), as per the accepted standard (Sonoshita & Cagan, 2017). RT-PCR samples ran in duplicate and difference in C_T values < 0.3.

Table A.1 List of Primers used RT-PCR experiments to test the role of PTEN in other signalling pathways.

Primer	Organism	Forward Sequence (5'-3')	Tm (°C)	Length (bp)	GC %	Product length (bp)
axin F	Drosophila	AATGAGTGTAGTGGCCCACG	57.3	20	55	120
axin R		ATCTGCTACCCCTTCGGTCA	57.9	20	55	
cut F	Drosophila	AGCAATCACCACTCCATTCGC	65	21	52	134
cut R		GCTTTTGACGTTGCCAGTTG	62	20	50	
dll F	Drosophila	CGGCTCACCCTCACATTATCT	55	21	52	142
dll R		GATCCAGTGCGGTTTCTGGTC	57	21	57	
wg F	Drosophila	CCAAGTCGAGGGCAAACAGAA	57	21	52	95
wg R		TGGATCGCTGGGTCCATGTA	57	20	55	
socs36e F	Drosophila	TCTGCGGATTCGCTGAATG	63	19	52	92
socs36e R		GCAGTTCGATTTGTCACCACG	63	21	52	
eve F	Drosophila	CCTCTTGGCCACCCAGTA	60	18	61	70
eve R		CGGACTGGATAGGCATTCAT	60	20	50	
cyclin E F	Drosophila	AGCCTCCATCAGCTAAGCG	61	19	57	76
cyclin E R		GCAACCGATGACAGATTGCC	64	20	55	
Diap1 F	Drosophila	CCCCAGTATCCCGAATACGC	63	20	60	76
Diap1 R		TCTGTTTCAGGTTCCTCGGC	62	20	55	
Human PTEN 1 F	Drosophila	TTTGAAGACCATAACCCACCAC	60.2	22	45.5	134
Human PTEN 1 R		ATTACACCAGTTCGTCCCTTTC	60	22	45.5	
Human PTEN 2 F	Drosophila	AGGGACGAACTGGTGTAATGA	60	21	47	100
Human PTEN 2 R		CTGGTCCTTACTTCCCCATAGAA	60	23	47	
dPTEN F	Drosophila	TCAGAAACCGTCTGGAAGATGT	61	22	45	85
dPTEN R		CGCTCCGAGCATAGGTTATAGA	60	22	50	

The list of primers that were used to test the activity of the Wnt, Notch, JAK/STAT and Hippo signalling pathways. I also tested Drosophila PTEN and human PTEN in the samples to ensure that observed wing phenotypes were solely due to human PTEN variants while Drosophila PTEN remained uniformly expressed across all genotypes.

Table A.2 The List of PTEN variants that were tested and their annotation

PTEN variant	Amino acid position	Initial association	ClinVar call	ClinVar Function call	COSMIC
4A		Biochemically validated			
M1I	1	ASD	not clinvar - M1V Hereditary cancer-predisposing syndrome Uncertain significance(Last reviewed: Jun 8, 2017)		cosmic - 1 var and numerous other - carcinoma glioma
K6I	6	ASD	not clinvar		cosmic - 1 var - glioma - plus lots other vars in this position - carcinomas
K6E	6	ASD	not clinvar		cosmic - 2 vars - carcinoma - plus lots other vars in this position - carcinomas
N12T	12	ASD	PTEN hamartoma tumor syndrome	Pathogenic(Last reviewed: Mar 1, 2017)	
R14G	14	ASD	PTEN hamartoma tumor syndrome|not provided	Pathogenic(Last reviewed: Mar 1, 2017)	

R15S	15	ASD	Hereditary cancer-predisposing syndrome	Likely pathogenic(Last reviewed: Sep 7, 2016)	
D22E	22	ASD	Not clinvar - D22Y PTEN hamartoma tumor syndrome, D22H not specified|Hereditary cancer-predisposing syndrome, D22G Hereditary cancer-predisposing syndrome		not cosmic - 2 other vars in this amino acid - glioma carcinoma
Y27C	27	ASD	PTEN hamartoma tumor syndrome|Inborn genetic diseases	Conflicting interpretations of pathogenicity(Last reviewed: Apr 13, 2017)	
A34D	34	Predicted High Impact	not clinvar - A39V - not specified Uncertain significance		cosmic - carcinoma
A34P	34	Predicted High Impact	not clinvar - A39V - not specified Uncertain significance		not cosmic - numerous other vars in this amino acid - carcinoma
M35V	35	cancer	PTEN hamartoma tumor syndrome|not	Conflicting interpretations of pathogenicity(	cosmic - lots carcinoma, glioma - multiple other var in

			provided|Inborn genetic diseases	Last reviewed: Dec 20, 2017)	this position - multiple cancers
G36E	36	Predicted High Impact	Hereditary cancer-predisposing syndrome	Uncertain significance(Last reviewed: Mar 2, 2016)	
P38H	38	ASD	not clinvar. - P38T Hereditary cancer-predisposing syndrome Uncertain significance(Last reviewed: Jan 6, 2015), P38S not provided | Hereditary cancer-predisposing syndrome Conflicting interpretations of pathogenicity(Last reviewed: Mar 8, 2017), P3R not provided Likely pathogenic(Last reviewed: Mar 21, 2017)		cosmic - 2 melanoma and many other vars in this amino acid - glioma carcinoma

G44D	44	ASD	PTEN hamartoma tumor syndrome	Pathogenic(Last reviewed: Mar 1, 2017)	
R47W	47	Predicted High Impact	not clinvar - R47G - PTEN hamartoma tumor syndrome Uncertain significance(Last reviewed: Dec 8, 2017) R47W - not provided Likely pathogenic(Last reviewed: Nov 15, 2016)		not cosmic - numerous other vars in this amino acid - carcinoma
R47K	47	Predicted High Impact	not clinvar - R47G - PTEN hamartoma tumor syndrome Uncertain significance(Last reviewed: Dec 8, 2017) R47W - not provided Likely pathogenic(Last reviewed: Nov 15, 2016)"		not cosmic - numerous other vars in this amino acid - carcinoma
F56C	56	Population Control	not clinvar		Cosmic - carcinoma
Y65C	65	ASD	not clinvar		cosmic - carcinoma
T68X	68	cancer			

Y68H	68	ASD	PTEN hamartoma tumor syndrome|Cowden syndrome 1|not provided|Hereditary cancer-predisposing syndrome	Pathogenic/Likely pathogenic(Last reviewed: Jul 11, 2017)	
Y68N	68	ASD	not specified	Uncertain significance(Last reviewed: Apr 16, 2015)	not cosmic - 2 other vars in this amino acid - glioma carcinoma
L70V	70	ASD	not clinvar - L70F not specified Uncertain significance(Last reviewed: Feb 11, 2015), L70P Cowden syndrome 1 Pathogenic(Last reviewed: Nov 1, 1998)		not cosmic - multiple other vars in this amino acid - glioma carcinoma
E73K	73	Predicted High Impact	not clinvar		cosmic - 1 carcinoma plus one other in this amino acid

T78A	78	ASD	not clinvar		not cosmic - T78N - prostate carcinoma
A79T	79	Population Control	Endometrial carcinoma|Macrocephaly/autism syndrome|Meningioma, familial|Squamous cell carcinoma of the head and neck|Bannayan-Riley-Ruvalcaba syndrome|Malignant tumor of prostate|Follicular thyroid carcinoma|VACTERL association with	Uncertain significance(Last reviewed: Dec 28, 2017)	

			hydrocephalus|Glioma susceptibility 2|PTEN hamartoma tumor syndrome|Cowden syndrome 1|Cutaneous malignant melanoma 1|not provided|Hereditary cancer-predisposing syndrome		
D92N	92	Predicted High Impact	not clinvar - D92T PTEN hamartoma tumor syndrome Uncertain significance(Last reviewed: Jul 26, 2017) D92A - Hereditary cancer-predisposing syndrome Likely pathogenic(Last reviewed: May 15, 2017)		cosmic - 4 glioma and carcinoma and multiple other vars in this amino acid - glioma carcinoma
D92N	92	ASD	not clinvar - D92Y PTEN hamartoma tumor syndrome, D92A Hereditary cancer-predisposing syndrome		cosmic - 4 glioma and carcinoma and multiple other vars in this amino acid - glioma carcinoma

H93R	93	ASD	Macrocephaly/autism syndrome|PTEN hamartoma tumor syndrome	Uncertain significance(Last reviewed: Feb 7, 2018)	
H93Y	93	ASD	not clinvar - H93N Macrocephaly|Large for gestational age|Loss of consciousness, H93P PTEN hamartoma tumor syndrome, H93R Macrocephaly/autism syndrome|PTEN hamartoma tumor syndrome		cosmic - multiple glioma and carcinoma - other vars in this amino acid carcinoma
H93Q	93	Cancer Variant	not clinvar - H93N Macrocephaly|Large for gestational age|Loss of consciousness, H93P PTEN hamartoma tumor syndrome, H93R Macrocephaly/autism syndrome|PTEN hamartoma tumor syndrome		cosmic - 1 other vars in this amino acid - carcinoma
I101T	101	ASD	not clinvar		cosmic - lots cancer

I101F	101	ClinVar	not clinvar		not cosmic - other vars in this amino acid - cancer
D107V	107	ASD	PTEN hamartoma tumor syndrome|not provided	Pathogenic(Last reviewed: Feb 23, 2018)	
D107G	107	ASD	not clinvar - D107Y Hereditary cancer-predisposing syndrome, D107V PTEN hamartoma tumor syndrome|not provided		not cosmic - multiple other vars in this amino acid - glioma carcinoma
N117S	117	Population Control	PTEN hamartoma tumor syndrome|not specified|Hereditary cancer-predisposing syndrome Uncertain significance(Last reviewed: Oct 19, 2017)		
H118P	118	ASD	not clinvar - H118R Hereditary cancer-predisposing syndrome		not cosmic - multiple other vars in this amino acid - glioma carcinoma
A121P	121	Predicted High Impact	not clinvar - A121G - Squamous cell carcinoma of the head and neck Pathogenic(Last reviewed: Jan 1, 2002)		cosmic - 3 glioma carcinoma and numerous other vars in this amino acid - carcinoma

A121E	121	Predicted High Impact	not clinvar - A121G - Squamous cell carcinoma of the head and neck Pathogenic(Last reviewed: Jan 1, 2002)		cosmic - 2 glioma carcinoma and numerous other vars in this amino acid - carcinoma
H123Y	123	ClinVar	PTEN hamartoma tumor syndrome|not provided	Pathogenic/Likely pathogenic(Last reviewed: Jun 28, 2017)	cosmic - lots vars - carcinoma glioma
H123Q	123	ASD	PTEN hamartoma tumor syndrome	Pathogenic(Last reviewed: Mar 1, 2017)	
C124S	124	biochemically validated			
C124S 4A	124	biochemically validated			
C124R	124	cancer	Cowden syndrome 1|not provided Pathogenic(Last reviewed: Mar 7, 2018)	Pathogenic(Last reviewed: Mar 7, 2018)	not cosmic - 1 var in this amino acid - carcinoma

A126P	126	Predicted High Impact	not clinvar - A126S - Hereditary cancer-predisposing syndrome Uncertain significance(Last reviewed: Jun 21, 2017). A126T PTEN hamartoma tumor syndrome Uncertain significance(Last reviewed: Mar 1, 2017) A126V Hereditary cancer-predisposing syndrome Likely pathogenic(Last reviewed: Sep 15, 2016)		cosmic - 3 carcinoma and many other vars in this amino acid - carcinoma
A126D	126	Predicted High Impact	not clinvar - A126S - Hereditary cancer-predisposing syndrome Uncertain significance(Last reviewed: Jun 21, 2017). A126T PTEN hamartoma tumor syndrome Uncertain significance(Last reviewed: Mar 1, 2017) A126V Hereditary cancer-predisposing syndrome Likely pathogenic(Last reviewed: Sep 15, 2016)		cosmic - 5 carcinoma and many other vars in this amino acid - carcinoma

G127R	127	Predicted High Impact	PTEN hamartoma tumor syndrome|not provided	Likely pathogenic(Last reviewed: Nov 8, 2016)	
G129R	129	ClinVar	not provided|Hereditary cancer-predisposing syndrome|Inborn genetic diseases	Pathogenic(Last reviewed: May 20, 2017)	cosmic - lots vars - carcinoma glioma
G129E	129	biochemically validated	PTEN hamartoma tumor syndrome|Cowden syndrome 1|not provided	Pathogenic(Last reviewed: Mar 16, 2018)	

R130X	130	ASD-LGD			

R130L	130	ASD	Malignant melanoma of skin|Squamous cell carcinoma of the head and neck|Small cell lung cancer|Squamous cell lung carcinoma|Renal cell carcinoma, papillary, 1|not provided|Neoplasm of the breast|Glioblastoma|Hereditary cancer-predisposing syndrome|Neoplasm of the large intestine|Colorectal Neoplasms|Uterine cervical neoplasms|Adenocarcinoma of stomach|Malignant neoplasm of body of uterus|Adenocarcinoma of prostate|Uterine Carcinosarcoma	Pathogenic(Last reviewed: Sep 18, 2017)	
R130Q	130	Predicted High Impact	Malignant melanoma of skin|Squamous cell carcinoma of the head and neck|Small cell lung cancer|PTEN hamartoma tumor syndrome|Squamous cell lung carcinoma|Cowden syndrome 1|Renal cell	Pathogenic(Last reviewed: Nov 22, 2017)	

			carcinoma, papillary, 1|not provided|Neoplasm of the breast|Glioblastoma|Hereditary cancer-predisposing syndrome|Neoplasm of the large intestine|Neoplasm|Ovarian Neoplasms|Colorectal Neoplasms|Uterine cervical neoplasms|Adenocarcinoma of stomach|Malignant neoplasm of body of uterus|Adenocarcinoma of prostate|Uterine Carcinosarcoma		
T131I	131	ASD	Macrocephaly/autism syndrome	Pathogenic(Last reviewed: Dec 21, 2012)	cosmic - 2vars carcinoma and many other vars in this amino acid - glioma carcinoma
G132D	132	ASD	PTEN hamartoma tumor syndrome|not specified | not provided	Conflicting interpretations of pathogenicity(Last reviewed: Jul 21, 2017)	

M134I	134	ASD	Hereditary cancer-predisposing syndrome	Likely pathogenic(Last reviewed: Feb 29, 2016)	
M134T	134	ASD	PTEN hamartoma tumor syndrome	Pathogenic(Last reviewed: Mar 1, 2017)	
I135fs	135	ASD-LGD			
I135V	135	ClinVar	PTEN hamartoma tumor syndrome|not provided | Hereditary cancer-predisposing syndrome	Pathogenic/Likely pathogenic(Last reviewed: Oct 9, 2017)	cosmic - numerous vars - carcinoma
I135T	135	Population Control	not clinvar - I135L PTEN hamartoma tumor syndrome|not provided | Hereditary cancer-predisposing syndrome Pathogenic/Likely pathogenic(Last reviewed: Oct 9, 2017)		not cosmic - multiple other vars in this amino acid - glioma carcinoma
C136Mfs	136	ASD-LGD			

Y138L	138	biochemically validated	not clinvar Y138C Hereditary cancer-predisposing syndrome Uncertain significance(Last reviewed: May 15, 2017)		not cosmic - numerous other vars in this amino acid - carcinoma
L139X	139	ASD-LGD			
A151P	151	Predicted High Impact	not clinvar		not cosmic - numerous other vars - numerous carcinomas
E157G	157	ASD	Macrocephaly/autism syndrome | PTEN hamartoma tumor syndrome	Conflicting interpretations of pathogenicity(Last reviewed: Jul 13, 2017)	
T167N	167	ASD	Macrocephaly/autism syndrome	Pathogenic(Last reviewed: Dec 21, 2012)	not cosmic - multiple other Var - various cancers
Q171E	171	ASD	not clinvar - Q171R not specified Uncertain significance		cosmic - 3 var carcinoma glioma - multiple other var in this amino acid - carcinoma glioma
R173H	173	ASD	PTEN hamartoma tumor syndrome|not provided | Neoplasm of brain	Pathogenic/Likely pathogenic(Last reviewed: Dec 27, 2017)	

R173P	173	Predicted High Impact	PTEN hamartoma tumor syndrome | Hereditary cancer-predisposing syndrome	Conflicting interpretations of pathogenicity(Last reviewed: Jan 12, 2018)	
Y176C	176	ASD	PTEN hamartoma tumor syndrome | Tumor susceptibility linked to germline BAP1 mutations | not specified|Hereditary cancer-predisposing syndrome	Uncertain significance(Last reviewed: Oct 6, 2017)	
Y178X	178	ASD-LGD			
Y180H	180	Population Control	Hereditary cancer-predisposing syndrome	Uncertain significance(Last reviewed: Jan 31, 2017)	
M198I	198	Population Control	not clinvar - M198V + M198L - BOTH are PTEN hamartoma tumor syndrome Uncertain significance(Last reviewed: Mar 6, 2017)		not cosmic - numerous other vars in this amino acid - carcinoma
T202I	202	ASD	PTEN hamartoma tumor syndrome	Pathogenic(Last reviewed: Mar 1, 2017)	

I203V	203	Predicted Low Impact	not clinvar		cosmic - 1 carcinoma
C211W	211	ASD	not provided	Pathogenic(Last reviewed: Feb 14, 2017)	not cosmic - 2 other var in this amino acid - carcinoma
N228S	228	Population Control	PTEN hamartoma tumor syndrome|not specified|Hereditary cancer-predisposing syndrome	Uncertain significance(Last reviewed: Feb 23, 2017)	
F241S	241	ASD	Macrocephaly/autism syndrome | PTEN hamartoma tumor syndrome	Uncertain significance(Last reviewed: Dec 11, 2017)	
P246L	246	ASD	PTEN hamartoma tumor syndrome | Cowden syndrome 1|not provided | Hereditary cancer-predisposing syndrome	Pathogenic/Likely pathogenic(Last reviewed: Mar 7, 2018)	
D252G	252	ASD	Macrocephaly/autism syndrome	Pathogenic(Last reviewed: Apr 1, 2005)	cosmic - 4 vars glioma carcinoma and many other vars in this amino acid - glioma carcinoma
V255A	255	ASD	not clinvar		cosmic - 2 carcinomas

E256K	256	Predicted High Impact	not clinvar		cosmic - 2 vars - glioma and carcinoma
N356H	256	Population Control	not clinvar _ N356Y PTEN hamartoma tumor syndrome|not provided Uncertain significance(Last reviewed: Oct 18, 2017)		not cosmic
N262S	262	Population Control	not clinvar - N262T - PTEN hamartoma tumor syndrome Uncertain significance(Last reviewed: Mar 6, 2017)		not cosmic - numerous other vars in this amino acid - carcinoma
D268E	268	Population Control	not clinvar		cosmic - 2 carcinoma plus one other in this amino acid
W274L	274	ASD	PTEN hamartoma tumor syndrome	Pathogenic(Last reviewed: Mar 1, 2017)	
N276S	276	ASD	not clinvar		Cosmic - glioma
F279I	279	Predicted High Impact	not clinvar		not cosmic
F279L	279	Predicted High Impact	not clinvar		not cosmic
G285X	285	ASD-LGD			

L295V	295	Predicted Low Impact	not clinvar		not cosmic
Q298E	298	Population Control	Endometrial carcinoma|Macrocephaly/autism syndrome|Meningioma, familial|Squamous cell carcinoma of the head and neck|Bannayan-Riley-Ruvalcaba syndrome|Malignant tumor of prostate|Follicular thyroid carcinoma|VACTERL association with	Uncertain significance(Last reviewed: Dec 13, 2017)	

			hydrocephalus|Glioma susceptibility 2|PTEN hamartoma tumor syndrome|Cowden syndrome 1|Cutaneous malignant melanoma 1|not specified|not provided|Hereditary cancer-predisposing syndrome		
E307Q	307	Population Control	Hereditary cancer-predisposing syndrome	Uncertain significance(Last reviewed: Jun 11, 2015)	
A309S	309	Predicted Low Impact	not clinvar		not cosmic
L320X	320	ASD-LGD			
K322E	322	Predicted High Impact	not clinvar		cosmic - glioma
D326N	326	ASD	not clinvar		not cosmic - multiple other Var - various cancers
K330E	330	Predicted High Impact	not clinvar		not cosmic - other var in this amino acid - carcinoma
R335X	335	ASD-LGD			

N340H	340	cancer	PTEN hamartoma tumor syndrome|not provided	Uncertain significance(Last reviewed: Jun 9, 2017)	no cosmic
N340D	340	cancer	not specified|Hereditary cancer-predisposing syndrome	Uncertain significance(Last reviewed: Apr 17, 2015)	co cosmic
K342N	342	cancer	not specified - other clinvar vars in this amino acid with carcinoma	Uncertain significance(Last reviewed: Apr 17, 2015)	no cosmic
V343L	343	cancer	not clinvar - 1 clinvar var in this amino acid hamartoma		no cosmic
L345V	345	cancer	Hereditary cancer-predisposing syndrome	Uncertain significance(Last reviewed: Feb 16, 2016)	no cosmic
Y346F	346	Predicted Low Impact	not clinvar - Y346C - Hereditary cancer-predisposing syndrome Uncertain significance(Last reviewed: Jul 25, 2016)		not cosmic - 2 other vars in this amino acid - carcinoma

T348S	348	Predicted Low Impact	not clinvar		not cosmic
P354Q	354	Population Control	PTEN hamartoma tumor syndrome|Cowden syndrome 1|not specified|not provided|Hereditary cancer-predisposing syndrome|Inborn genetic diseases	Uncertain significance(Last reviewed: Dec 14, 2017)	
N356D	356	Population Control	PTEN hamartoma tumor syndrome|Hereditary cancer-predisposing syndrome	Uncertain significance(Last reviewed: Sep 29, 2017)	
P357S	357	Predicted Low Impact	not clinvar - P357T - PTEN hamartoma tumor syndrome|Cowden syndrome 1|not specified|Hereditary cancer-predisposing syndrome Uncertain significance(Last reviewed: Nov 13, 2017)		cosmic - 2 vars - carcinoma and a few other other vars in this amino acid - carconoma

T363N	363	Population Control	not clinvar - T363A - Hereditary cancer-predisposing syndrome Uncertain significance(Last reviewed: Oct 11, 2017)		not cosmic
Q396R	396	Population Control	not clinvar		not cosmic
I400V	400	cancer	PTEN hamartoma tumor syndrome	Uncertain significance(Last reviewed: Jan 26, 2015)	no cosmic
K402N	402	cancer	not provided	Uncertain significance(Last reviewed: Jan 16, 2018)	no cosmic

Note: This table was adapted from a data table created and then shared by our collaborators at UBC. Table shows annotation of the human PTEN variants that were tested in the activated $PI3K^{[act]}$ background.